

RADIATION INDUCED NUCLEATION
IN
WATER AND ORGANIC LIQUIDS

by

Nicholas P. Oberle

B.S.M.E., Polytechnic Institute of Brooklyn
(1970)

Submitted in Partial Fulfillment of
the Requirements for the Degree of
Master of Science

at the

Massachusetts Institute of Technology

March 1972

Signature of Author _____

Certified by ✓ _____ Thesis Supervisor, Date

Accepted by _____
Chairman, Departmental Committee
on Graduate Students

Archives



Radiation Induced Nucleation
in
Water and Organic Liquids

by
Nicholas P. Oberle

Submitted to the Department of Nuclear Engineering
on March 24, 1972 in partial fulfillment of the requirements
for the degree of Master of Science.

Abstract

Experimental data for the threshold superheat was obtained for the case of fission fragments in water and in propylene glycol. Analytical results, using Bell's (5) energy balance method, for the threshold superheat values were obtained for both fission fragments and fast neutrons in water, propylene glycol, benzene, acetone, and nitromethane.

Experimental and analytical results were compared with data obtained by other investigators. (3),(4),(5).

A detailed discussion of the liquid suspension method used in this work is given, along with a criteria for selecting a test fluid and its supporting fluids.

Physical properties vs. temperature plots for a number of possible test fluids are also given.

Thesis Supervisor
Title

Neil E. Todreas
Associate Professor

Acknowledgements

I wish to express my sincere gratitude to my thesis supervisor, Professor Neil E. Todreas, for his advice and assistance throughout this study. I would also like to express my appreciation to Dr. Norman C. Rasmussen for being kind enough to be my thesis reader.

Special thanks are also due to Dr. C.R.Bell for his helpful advice. I would like to take this opportunity to thank all members of the M.I.T. reactor machine shop and radiation protection office for their technical advice and assistance.

Last but not least, I would like to thank all those friends in the Nuclear Engineering Department and in the Chemistry Department who had in one way or another assisted me in the present work.

Table of Contents

Abstract		2
Acknowledgements		3
List of Figures		6
List of Tables		9
Chapter 1.	Introduction	
1.1	Radiation Induced Nucleation	10
1.2	Experimental Methods	12
1.2a	Expansion Method	12
1.2b	Constant Pressure Method	13
1.2c	Advantages and Disadvantages	13
1.3	Objectives of Present Work	14
Chapter 2.	Theory	
2.1	General Introduction	16
2.2	The Electrostatic Theory	16
2.3	Thermal Theory	19
2.4	Minimum Energy for Bubble Formation	20
2.5	Energy Balance Method of Bell	28
2.6	Fission Fragments and Fast Neutrons	41
Chapter 3.	Experimental Apparatus and Procedures	
3.1	Apparatus Modifications	43
3.2	Experimental Procedure	51
3.3	Experimental Difficulties	55
3.4	Indication of Nucleation	57
3.5	Fission Fragments in a Test Liquid	58

Chapter 4.	Fluid Selection	
4.1	Background Information	60
4.2	Test Liquid Properties	60
4.3	Compatibility Requirements	62
4.4	Difficulties in Fluid Selection	63
4.5	Discussion of Surface Tension	71
Chapter 5.	Results	
5.1	Analytical Results	76
5.2	Experimental Results	87
5.3	Sensitivity Study of Superheat Data	90
5.4	Comparison with other Results	96
Chapter 6.	Conclusions and Recommendations	
6.1	Conclusions	103
6.2	Rayleigh's Criteria	105
6.3	Recommendations	108
Appendix A.	Physical Properties	
A.1	Introduction	112
A.2	Physical Properties of Acetone	114
A.3	Physical Properties of Diethyl Ether	120
A.4	Physical Properties of Propylene Glycol	121
A.5	Physical Properties of Nitromethane	127
A.6	Discussion of Vapor Density Results	128
A.7	Physical Properties of Methyl Alcohol	130
A.8	Physical Properties of Ethyl Alcohol	136
Appendix B.	Sample Calculation	137
Appendix C.	Computer Programs	147
Appendix D.	References	168

List of Figures

Figure		Page
2.1	Thermodynamic systems for bubble formation.	22
2.2	Typical energy loss for a heavy charged particle interacting with matter.	29
2.3	P_g routine flowchart	38
2.4	Threshold superheat flowchart	40
3.1	Diagram of Experimental	44
3.2	Diagram of Convection Generator	47
3.3	Light Source	48
3.4	Mirror system	50
3.5	Source Holder and Shielding	52
3.6	Pressure Gauge calibration Curve	53
4.1	Three-Liquid configuration	62
4.2	Spreading Effect of Test Liquid	68
5.	Threshold Superheat vs Pressure for	
5.1	Fast neutrons in water	77
5.2	Fission fragments in water	78
5.3	Fast neutrons in Propylene Glycol	79
5.4	Fission Fragments in Propylene Glycol	80
5.5	Fast Neutrons in Benzene	81
5.6	Fission Fragments in Benzene	82
5.7	Fast Neutrons in Acetone	83
5.8	Fission Fragments in Acetone	84
5.9	Fast Neutrons in Nitromethane	85
5.10	Fission Fragments in Nitromethane	86
5.11	Fission Fragments in water with experimental results	88

5.12	Fission Fragments in Propylene Glycol with experimental results.	91
5.13	Fission Fragments in water with $\pm 7\%$ uncertainty in surface tension.	93
5.14	Fission Fragments in water with $\pm 20\%$ uncertainty in mean charge.	94
5.15	Fission fragments in water with a combined uncertainty of $+7\%$ in surface tension and $\pm 20\%$ in mean charge	95
5.16	Fission fragments in Propylene Glycol with a $\pm 5\%$ uncertainty in surface tension	97
5.17	Fission fragments in Propylene Glycol with a $\pm 20\%$ uncertainty in the mean charge.	98
5.18	Fission Fragments in Propylene Glycol with a combined uncertainty of $\pm 5\%$ in surface tension, and $\pm 20\%$ in mean charge.	99
5.19	Fission fragments in water-data from Deitrich and Oberle.	100
5.20	Fast neutrons in Benzene , with El-Nagdy data.	101
5.21	Fast neutrons in Acetone, with El-Nagdy data.	102
6.1	Liquid-Vapor jet configurations.	106
6.2	Proposed experimental apparatus.	110
A.1	Vapor Pressure vs. Temperature plot for Acetone and Diethyl Ether.	115
A.2	Vapor Density vs. Temperature plot for Acetone and Diethyl Ether.	116
A.3	Liquid Density vs. Temperature plot for Acetone and Diethyl Ether.	117
A.4	Surface Tension vs. Temperature plot for Acetone and Diethyl Ether.	118
A.5	Heat of Vaporization vs. Temperature plot for Acetone and Diethyl Ether.	119

A.6	Vapor Pressure vs. Temperature for Propylene Glycol and Nitromethane	122
A.7	Liquid Density vs. Temperature for Propylene Glycol and Nitromethane	123
A.8	Vapor Density vs. Temperature for Propylene Glycol and Nitromethane	124
A.9	Surface Tension vs. Temperature for Propylene Glycol and Nitromethane	125
A.10	Heat of Vaporization vs. Temperature for Propylene Glycol and Nitromethane	126
A.11	Vapor Pressure vs. Temperature for Methyl and Ethyl alcohol	131
A.12	Liquid Density vs. Temperature for Methyl and Ethyl alcohol	132
A.13	Vapor Density vs. Temperature for Methyl and Ethyl alcohol	133
A.14	Surface Tension vs. Temperature for Methyl and Ethyl alcohol	134
A.15	Heat of Vaporization vs. Temperature for Methyl and Ethyl alcohol	135

List of Tables

<u>Table</u>		<u>Page</u>
2.1	Affect of additional surface tension term	27
4.1	Miscibility chart for benzene and acetone	65
4.2	Liquids immiscible with benzene	66
4.3	Liquids immiscible with acetone	66
4.4	Partial list of three-liquid tests	69
5.1	Results from Tso and Oberle for fission fragments in water	87
5.2	Results from Tso and Oberle for fast neutrons in water	89

Chapter 1

Introduction

1.1 Radiation Induced Nucleation

The term radiation-induced nucleation refers to the phenomena of nucleation (the initial formation of bubbles) of vapor or gas bubbles in liquids due to localized energy deposition or localized ionization along the track of an energized particle.

Homogeneous nucleation is normally not considered an important part of the boiling process in engineering components, since nucleation due to the presence of surface cavities, suspended particles, or non-condensable gas bubbles is the dominant mechanism at small liquid superheats. Pure homogeneous nucleation only becomes important at high superheats.

This phenomena of radiation-induced nucleation of bubbles in a superheated liquid was first reported by D.A. Glaser (1), who was searching for an instrument similar to a cloud-chamber-like detector, which would aid in the study of high energy nuclear events. The cloud chamber utilizes the instability of supercooled vapors against droplet formation, so it seemed promising to attempt to devise an instrument which could take advantage of superheated liquids against bubble formation. Glaser

made an experimental test with superheated diethyl ether. In the absence of any radioactive source a superheated state was able to be maintained for a few seconds. But when a radioactive source was brought near the superheated liquid, it immediately erupted into vapor.

This series of experiments showed that bubble chambers could be a practical device for the study of high energy nuclear events, and led to the highly sophisticated bubble chamber technology which exists today.

Since the existence of the radiation-induced nucleation phenomena was thus demonstrated, the question soon arose of whether or not this would have any affect on nuclear reactor coolants or moderators. Recently, it was desired to know whether this phenomena would have any affect on the sodium void problem in sodium cooled fast reactors. Liquid sodium can attain very high superheats on engineering surfaces. Nucleation of this highly superheated sodium will lead to violent flashing, resulting in the sudden ejection of sodium from one or more coolant channels. The rate of sodium ejection is related to the amount of superheat attained. Since a reactor is an intense source of radiation, the possibility that this radiation, through radiation-induced nucleation, might place an upper limit on the superheat attainable in reactor coolants was a factor worth studying.

1.2 Experimental Methods

There are presently two experimental methods employed to study the radiation-induced nucleation phenomena. The major difference between these two methods is in the manner in which the superheated state of the liquid is attained.

The first, and up to now the most widely used method, is the so-called expansion method. The second is a constant pressure type method. Both of these methods will be reviewed, emphasizing both their advantages and disadvantages.

1.2a Expansion Method

The expansion method is similar to the bubble chamber method of operation. The test liquid is heated to a temperature considerably above its normal boiling point, but is kept at a pressure which still maintains it as a stable liquid. (In other words, the test liquid is kept under a pressure higher than the saturated vapor pressure corresponding to the temperature to which the liquid is raised.) The expansion process then occurs. (Expansion is the sudden lowering of the pressure to a predetermined pressure at which the test liquid is superheated.) The pressure is thus reduced from an initial value, at which the liquid is subcooled, to a lower value, where the test liquid is superheated. This method has been used by Becker(2), Deitrich (3), and El-Nagdy (4).

1.2b Constant Pressure Method

This method, devised by Bell (5), attains the superheated state of the test fluid by maintaining a constant pressure and gradually heating the test liquid. Nucleation from the surface of the test liquid does not occur since the test liquid is not in contact with a solid surface. This is accomplished by suspending the test liquid in the form of a bubble (approximately one-half inch in diameter) between two other liquids, a supporting fluid and a cover fluid. A detailed description of this experimental technique will be given in a later section of this work.

1.2c Advantages and Disadvantages

A major disadvantages of the expansion method is the short duration (a few seconds) of the superheated state of the test liquid. Any effect of radiation on the liquid must therefore be observable during this short period of superheat..

If a reactor (as in Deitrich (3)) or an accelerator (as in El-Nagdy (4)) is used as the source of radiation, then a further complication, that of synchronizing the radiation burst with the expansion in the test chamber, is encountered.

Another disadvantage of the expansion method is that of surface cavities. These will cause boiling on surfaces of the chamber well before the radiation - induced nucleation phenomena can appear. (This problem

has been solved to some degree by El-Nagdy (4), by cooling the test chamber walls just prior to and during the expansion process.)

The constant pressure heating method can maintain a high degree of superheat for an indefinite period of time in the absence of radiation since the technique of suspending the test bubble eliminates surface effects.

The one main disadvantage of this method is that the requirements of this three-liquid configuration are such that it is very difficult to find compatible supporting and cover fluids for many test fluids of interest. The expansion method on the other hand has no such liquid compatibility requirement, and can be used for any liquid desired. A detailed discussion of these compatibility requirements will be given later.

1.3 Objectives of Present Work

The constant pressure heating method was begun at M.I.T. by C.R. Bell (5) who formulated a theory and constructed the experimental apparatus. Some preliminary experimental work with water as the test fluid was also done by Bell (5). This work was continued by Tso (6), who extended the experimental work with water, and performed preliminary analytical work with benzene.

The present work included experimental work with water and propylene glycol, and analytical work (utilizing

Bell's method) with water, propylene glycol, benzene, acetone, and nitromethane. Modifications were also made to the experimental apparatus.

Chapter 2

Theory

2.1 General Introduction

Two theories have been proposed to explain the formation of bubbles by radiation. The first theory, the "Electrostatic theory", was proposed by Glaser (7), and the second theory, the "thermal spike" theory, was proposed by Seitz (8).

Actually there are only two ways in which energy can be extracted from ions to produce bubbles: either the energy of the electric field due to the charges of the ions is converted into the work of formation of bubbles, or the recombination energy of the ions is given off as heat, which produces a so called "thermal spike", and finally bubbles.

The thermal spike theory has generally been accepted as the correct theory, but a short discussion on the electrostatic theory will be presented, since it also did a reasonable job of predicting operating conditions for a number of bubble chambers.

This thesis will use the theoretical approach of Bell (5), which is based on the thermal spike theory.

2.2 The Electrostatic Theory

In order to predict the operating conditions for

a bubble chamber, a theory was needed to quantitatively describe the conditions under which ionizing events could nucleate bubbles in a superheated liquid. Glaser(?) then developed his electrostatic theory.

The electrostatic theory was a microscopic model of an ionization-triggered bubble nucleation mechanism. It was assumed that an ionizing particle produces clusters of electric charges of like sign within a liquid, and that the mutual electrostatic repulsion of these charges could then fracture a superheated liquid to produce bubble nuclei large enough to grow to visible size, using the thermal energy from the liquid. An approximate treatment of the effect of electrostatic forces on bubble nucleation was made, which assumed a number "N" (it was known that a number of charges were required for this mechanism to work) of electronic charges to be distributed uniformly over the surface of a potential bubble nucleus. This treatment formulated an "electrostatic pressure effect", which predicted that a bubble carrying "N" like charges would grow if the pressure on the liquid were less than the saturated vapor pressure at the ambient temperature by a certain amount. This difference,

$\Delta P = P_{\infty}(T) - P$, where: P is the pressure on the liquid and $P_{\infty}(T)$ is the saturated vapor pressure over a flat liquid -vapor interface, is given by:

$$\Delta P > \frac{3}{2} \left(\frac{4\pi}{N^2 e^2} \right)^{\frac{1}{3}} [\sigma(T)]^{\frac{4}{3}} [\epsilon(T)]^{\frac{1}{3}} \quad (2.1)$$

where:

e = electronic charge

$\sigma(T)$ = surface tension of the liquid at temperature T

$\epsilon(T)$ = dielectric constant of the liquid at temperature T

With N taken as 6, this formula had fairly good success in predicting the operating conditions of a number of liquids, such as hydrogen, deuterium, and helium.

Even though the theory met with some initial success, serious objections arose. One of these considered the fact that in order to rupture the superheated liquid, the N charges must be deposited within a sphere of radius "r", where r is given by:

$$r = \frac{2\sigma(T)}{P_{\infty}(T) - P} = \frac{2}{3} \left(\frac{2N^2e^2}{\pi} \right)^{\frac{1}{3}} [\sigma(T)]^{-\frac{1}{3}} [\epsilon(T)]^{-\frac{1}{3}} \quad (2.2)$$

For typical operating conditions for certain liquids, such as some organic liquids, this gives a radius of the order of 10^{-6} cm.. This requires that an ionizing particle must leave a cluster of six charges, of the same sign, in this small volume. It was obvious that this does not happen often enough in primary ionizations to account for the observed number of bubbles.

A contradiction with the theory was also found when alpha particles were used as the ionizing agent. To agree

with this theory, the alpha particle was required to deposit 900 charges, of the same sign, in a region 2×10^{-6} cm. in diameter. This is greater than the maximum ionization attained by an alpha particle during the slowing down process, even granting the possibility of the required charge separation. The total energy loss of the alpha particle, however, was sufficient to explain the observed effects, so another model for the microscopic mechanism was sought. (For a more detailed description of the electrostatic theory and its disadvantages, references (4), (9), and (10) are recommended.)

2.3 Thermal Theory

The thermal theory suggests that local heating by ions and δ -rays (knocked-on electrons) could produce bubbles along the track of ionized particles.

It was assumed that the primary mechanism for the deposition of this local thermal energy occurred through the δ -rays formed by the primary ionizing particle. These knock-on electrons would lose energy by collisions with molecules. The energy of the δ -ray is thus rapidly converted to kinetic energy of the molecules of the medium. The primary ionizing particle thus produces along its path a series of "thermal spikes", which then act as nuclei for bubble formation.

Seitz (8) suggested that this thermal energy could also be obtained from the heat energy released

in ion recombination at the end of δ -rays, rather than just coming from molecular excitation.

The basic assumption of this thermal spike model is that the minimum energy required to form a bubble of critical size is provided from the thermal spike created in a small initial volume by the incident particle. This minimum energy (E_m) required for bubble formation will be given in the next section.

2.4 Minimum Energy for Bubble Formation

The minimum energy (E_m) required for the formation of a critical nucleus is composed of a number of terms.

Norman and Spiegler (11) give E_m as:

$$E_m = \frac{4}{3} \pi R_c^3 \rho_v \Delta H + 4\pi R_c^2 \left(\sigma_l - T_l \frac{d\sigma}{dT} \right) + 2\pi \rho_l R_c^3 \dot{R}^2 + F \quad (2.3)$$

where:

- R_c = critical bubble radius
- ρ = density
- ΔH = enthalpy change per unit mass
- σ = surface tension
- T = temperature
- \dot{R} = velocity of the bubble wall
- F = viscous losses

and the subscripts v and l refer to the vapor and liquid states.

The first term on the RHS is the energy required to heat and vaporize the mass of liquid involved and expand it against the external pressure. The second term is the energy required to form a surface in the liquid. The third term is the kinetic energy given off to the liquid by the motion of the vapor wall. An expression for \dot{R} is given (11) below

$$\dot{R} = \frac{4D}{R_c \left(\frac{\rho_v}{\rho_e}\right)^{1/3}} \quad (2.4)$$

where D is the thermal diffusivity.

The viscous loss term, F , has been shown ((11), (2), (12)) to be negligible compared to the other terms.

Deitrich (12) also uses equation (2.3) as the E_m required for bubble formation.

Becker (2) uses the following equation for E_m :

$$E_m = \frac{4}{3} \pi R_c^3 \rho_v \Delta H - \frac{8}{3} \pi R_c^2 \sigma + 4 \pi R_c^2 \sigma - 4 \pi R_c^2 \left(T \frac{d\sigma}{dT} \right) \quad (2.5)$$

Seitz (8), El-Nagdy (4), and Bell (5) use the E_m equation given below;

$$E_m = \frac{4}{3} \pi \left(R_c^2 \sigma + \rho_v \Delta H R_c^3 \right) \quad (2.6)$$

Bell ((5) pg. 257) has also derived equation (2.6) from a purely thermodynamic viewpoint, which will be considered below.

Two systems are shown below. System I is liquid only, while system II contains a vapor bubble in the liquid. (See FIG.2.1 below) The energy required to go from system I to system II will be found.

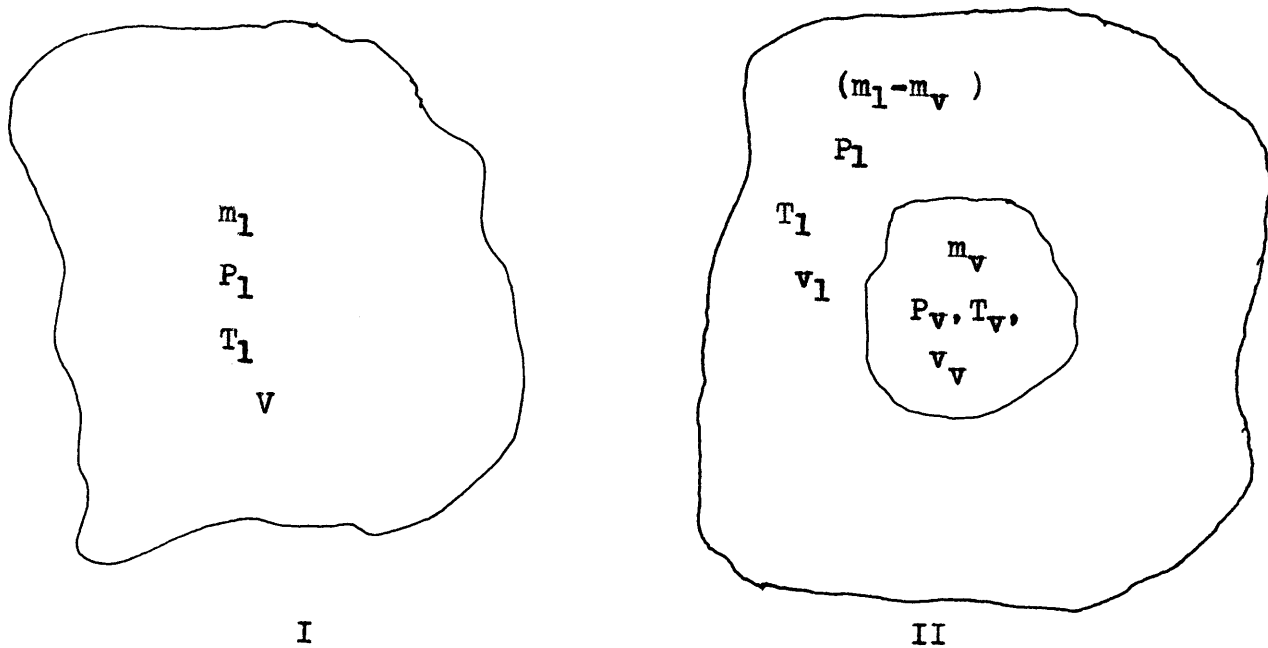


FIG. 2.1

The system parameters are defined as follows:

m = mass of the fluid

P = pressure

T = temperature

V = volume , v = Specific volume

The subscripts v and l again refer to the vapor and liquid states.

From the first law of thermodynamics

$$U_{II} - U_I = Q_{II} - W_{II} \quad (2.7)$$

where U_x = internal energy of system x
 Q_x = energy added to system x
 W_x = work done by system x

The total energy terms are now converted to specific terms,

$$(m_l - m_v)u_l + m_v u_v - m_l u_l = Q_{II} - W_{II} \quad (2.8)$$

The work done by the system (W_{II}) is composed of two parts: the work done to create the void, and the work done to form the surface. W_{II} is given by

$$W_{II} = P_l m_l (v_v - v_l) + A\sigma \quad (2.9)$$

where σ = surface tension of embryo
 A = surface area of the vapor embryo

Substituting equation (2.9) into (2.8) and rearranging terms,

$$u_v - (u_l + P_l v_l) = \frac{Q_{II}}{m_v} - P_l v_v - \frac{A\sigma}{m_v} \quad (2.10)$$

Now $P_v v_v$ is added to both sides of equation (2.10):

$$(u_v + P_v v_v) - (u_l + P_l v_l) = \frac{Q_{II}}{m_v} - P_l v_v - \frac{A\sigma}{m_v} + P_v v_v \quad (2.11)$$

From the definition of enthalpy:

$$h = u + Pv \quad (2.12)$$

Substituting this into equation (2.11) ,

$$m_v (h_v - h_l) = Q_{II} + m_v v_v (P_v - P_l) - A\sigma \quad (2.13)$$

Now, assuming (5) that the change in enthalpy ($h_v - h_l$) is approximately equal to the heat of vaporization:

$$h_{fg} \cong h_v - h_l \quad (2.14)$$

Also, a number of substitutions can be made:

$$m_v = \frac{4}{3} \pi r^3 \rho_v \quad (2.15)$$

$$A = 4\pi r^2 \quad (2.16)$$

$$v_v = \frac{1}{\rho_v} \quad (2.17)$$

where ρ = density

r = bubble radius.

For a critical embryo the equilibrium condition gives;

$$P_v - P_l = \frac{2\sigma}{R_c} \quad (2.18)$$

Utilizing the above substitutions, equation (2.11) is reduced to:

$$Q_{II} = \frac{4}{3} \pi R_c^3 \left[\rho_v h_{fg} + \frac{\sigma}{R_c} \right] \quad (2.19)$$

where Q_{II} is the energy which must be added to the system in order to create the critical embryo. (In other words, $Q_{II} = E_m$)

Equation (2.19) is exactly the same equation as the E_m equation employed by Seitz, El-Nagdy, and later by Bell. (Equation (2.6)) This is the equation which was used in the present work.

It was noticed that some investigators had included an additional surface tension term in their E_m equation (11), (3), (2). This term was of the form $T \frac{d\sigma}{dT}$

Seitz(8), El-Nagdy(4), and Bell(5) did not include this term. It was thus decided to see whether or not this additional term was significant. If this term were significant, then the original E_m equation

$$E_m = \frac{4}{3} \pi R_c^3 \left(\frac{\sigma}{R_c} + \rho_v h_{fg} \right) \quad (2.20)$$

would be changed to

$$E_m = \frac{4}{3} \pi R_c^3 \left(\frac{\sigma - T \frac{d\sigma}{dT}}{R_c} + \rho_v h_{fg} \right) \quad (2.21)$$

Calculations were made for each of the liquids studied to see whether or not this additional term would greatly affect the E_m equation.

The results of these calculations (TABLE 2.1) show that the $T \frac{d\sigma}{dT}$ term is negligible for the liquids studied (water, propylene glycol, nitromethane, benzene, acetone). The σ term in itself is only a small fraction of the E_m equation. The addition of the $T \frac{d\sigma}{dT}$ term does not significantly change this fraction.

This is true for the liquids studied in this work. But it does not necessarily hold for all liquids. In the case of liquid hydrogen and deuterium (used to a great extent in bubble chambers), this additional term is seen to significantly increase the contribution of the surface tension terms.

Therefore, before this additional term can be neglected, it must first be determined to what degree this term affects the E_m equation.

For the liquids studied in this work, this term was neglected, since it was proven to be negligible.

AFFECT OF ADDITIONAL SURFACE TENSION TERM

	A) $\rho_v h_{fg} \frac{\text{lb}}{\text{ft}^2}$	B) $\frac{\sigma}{r} \frac{\text{lb}}{\text{ft}^2}$	C) % of Total B, % of A	D) $\frac{\sigma - T \frac{d\sigma}{dT}}{r} \frac{\text{lb}}{\text{ft}^2}$	E) % of Total D, % of A
WATER	180.1×10^3	2.56×10^3	1.4%	5.12×10^3	2.0%
PROPYLENE GLYCOL	98.05×10^3	0.365×10^3	0.3%	1.92×10^3	1.9%
NITRO- METHANE	193×10^3	0.88×10^3	0.4%	3.35×10^3	1.7%
ACETONE	93.2×10^3	0.34×10^3	0.36%	0.88×10^3	0.95%
BENZENE	122.6×10^3	0.73×10^3	0.59%	1.89×10^3	1.5%
HYDROGEN	41.97×10^3	2.83×10^3	6.74%	13.05×10^3	31.09%
DEUTERIUM	66.29×10^3	4.04×10^3	6.09%	19.90×10^3	30.02%

TABLE 2.1

2.5 Energy Balance Method of Bell

In his work Bell(5) postulated that the energetic particles involved in the nucleation process can be thought of as producing long cylindrical regions of energetic molecules along their path. Macroscopically, this cylindrical region can be thought of as a vapor cylinder. This vapor cylinder will have a diameter of approximately 100 \AA ((5) pg63). A vapor cylinder in a liquid will tend to form into the more stable configuration, that of a sphere (or vapor bubble in this case). Since the total vapor track length is several orders of magnitude greater than the critical embryo diameter, it is highly unlikely that the total length of the vapor cylinder will reconfigure itself into a single vapor sphere. It is more likely that this long vapor cylinder will break up into smaller fragments, and that these fragments will reconfigure into individual embryos.

This process, as described by Bell(5), is shown schematically in FIG.2.2. Also shown is a typical energy deposition curve for a heavy charged particle interacting with matter. In the first part of the track the energy deposition to the electronic system of the stopping medium is the dominant energy transfer mechanism, while in the later part of the track the energy deposition to the medium through nuclear elastic

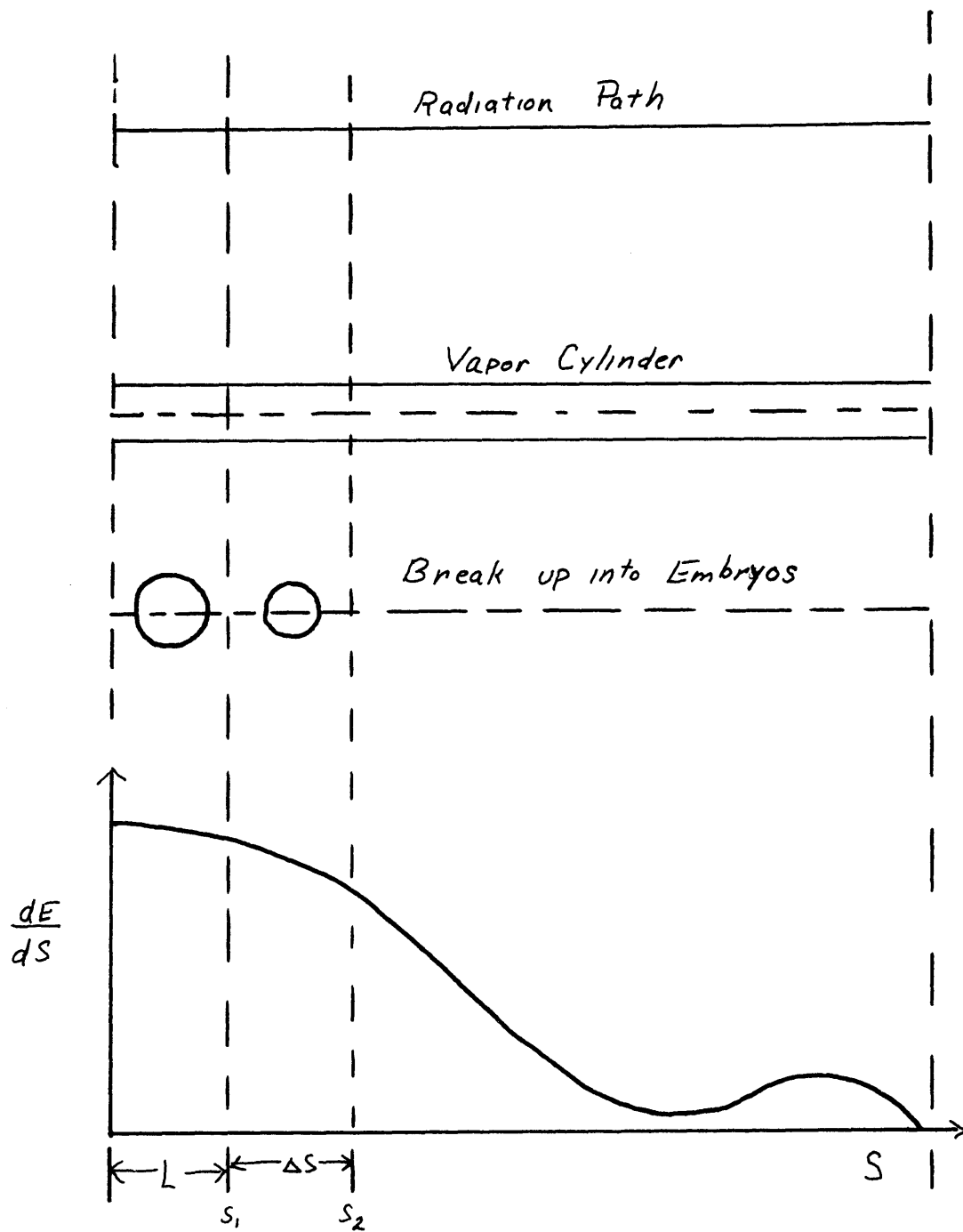


FIG 2.2

collisions will be dominant.

If a section of the radiation particle track length is taken (say s_1 to s_2 , or Δs) and assigned to one particular embryo, then the energy available to this embryo from the energetic radiation particle is the integral of the energy deposition rate, dE/ds , over the distance, Δs . This energy available to the embryo (or the energy lost by the particle) is given by

$$\Delta E = E(s_1) - E(s_2) = \int_{s_1}^{s_2} \left[\frac{dE}{ds}(E) \right] ds \quad (2.22)$$

where $\left[\frac{dE}{ds}(E) \right] ds$ is a function of the particle energy at position s . But the energy deposition rate, dE/ds , is a function of energy, and not position(13). Therefore the integral in equation (2.22) cannot be solved directly. An approximation has been made ((5),74) for the average energy deposition rate:

$$\left(\frac{dE}{ds} \right)_{AVG} = \frac{1}{E(s_2) - E(s_1)} \int_{E(s_1)}^{E(s_2)} \left[\frac{dE}{ds}(E) \right] dE = \frac{E(s_1) - E(s_2)}{\Delta s}$$

OR

$$\frac{- \left[E(s_1) - E(s_2) \right]^2}{\Delta s} = \int_{E(s_1)}^{E(s_2)} \frac{dE}{ds}(E) dE \quad (2.23)$$

The minimum superheat, or the threshold condition, for radiation-induced nucleation will be determined by the largest value of ΔE along the particle track. Assuming that the energy lost by the particle is equal to the energy made available to the embryo, and that the track breaks up in a uniform manner ($\Delta s = L = \text{constant}$, (5) pg.74), then the maximum value for ΔE will occur where dE/ds is maximum, which is at the beginning of the radiation track in the stopping medium. (From $s = 0$, to $s = L$, as shown in FIG.2.2). $E(0)$ would simply be the initial energy of the energetic particle. If a value for $\Delta s = L$ is assumed, then equation (2.23) would contain only one unknown, $E(L)$.

Bell (5) assumed that this break up length is given by

$$L = ar^* \quad (2.24)$$

where r^* is the critical radius of the embryo

"a" is a dimensionless parameter

At this point it will only be mentioned that Bell ((5) 203) postulated: $a = 6.07$. More will be said about this dimensionless parameter in chapter 6.

The basic concept behind the energy balance method is that the energy available from the radiation particle is equal to the energy required for bubble nucleation. The energy available, E_a , is given by

equation (2.23). The energy required for bubble formation was given by equation (2.6):

$$E_m = \frac{4}{3} \pi (r^{*2} \sigma + \rho_v \Delta H r^{*3}) \quad (2.6)$$

There is another factor which must be added to the above equations. This factor is commonly referred to as an "energy sink", and arises from the formation of gas due to molecular dissociation in the stopping medium. In the liquids studied in this work, hydrogen is the gas produced by the dissociation process. The total energy loss for all the hydrogen formed in a track length L (or ar^*) is given by

$$\Delta E = \frac{Q \Delta E G(H_2) 10^6}{N_{AV}} \quad (2.25)$$

where Q and $G(H_2)$ are constants, and ΔE is the same ΔE as in equation (2.23). This additional term is usually subtracted from the available energy, E_a , term.

The final form of the energy balance equation is thus:

$$\frac{4}{3} \pi r^{*3} \left[\frac{\sigma}{r^*} + \rho_v h_{fg} \right] = \Delta E \left[1 - \frac{Q G(H_2) 10^6}{N_{AV}} \right] \quad (2.26)$$

where the LHS is the minimum energy required for bubble formation (E_m) and the RHS is the total energy available, E_a .

When equation (2.26) is satisfied, then the conditions for radiation-induced nucleation have been met.

Besides being an energy sink, the production of the hydrogen gas also affects the dynamic equilibrium of a critical embryo. The original mechanical equilibrium condition for a critical embryo is given by:

$$P_v - P_l = \frac{2\sigma}{r^*} \quad (2.27)$$

Taking the hydrogen gas into account, equation (2.27) becomes:

$$P_v + P_g - P_l = \frac{2\sigma}{r^*} \quad (2.28)$$

The effect of this hydrogen gas is to reduce the vapor pressure requirement inside the critical nucleus for a nucleus of a particular size, and thus reduce the superheat required for that critical nucleus.

An equation for P_g (the gas pressure term) is ((5), pg122)

$$P_g = \frac{3R T_v \Delta E G(H_2) 10^4}{4\pi r^{*3}} \quad (2.29)$$

P_g cannot be calculated directly from equation (2.29), since r^* is a function of P_g (in addition to being a function of P_l), and ΔE is also a function of P_g , since $E(s_2)$ depends on r^* .

Before equation (2.29) can be solved, an expression must be found for dE/ds in equation (2.23). A number of energy deposition formulas have been suggested. The one which is most widely used is that given by Segre(13). This has also been modified for fission fragments. The equation is given below:

$$\frac{1}{N} \frac{dE}{ds} = \frac{4\pi e^4}{m_0 v^2} (Z_1)_{eff}^2 \sum_i \nu_i Z_i \ln \left(\frac{1.123 m_0 v^3}{(\bar{I}_i/\hbar) e^2 (Z_1)_{eff}} \right) + \frac{4\pi e^4 (Z_1)^2}{v^2} \sum_i \nu_i \frac{Z_i}{M_i} \left[\ln \left(\frac{M_1 M_i v^2 (a_{i,2}^{SCR})_i}{(M_1 + M_2) Z_1 Z_i e^2} \right) \right] \quad (2.30)$$

The symbols used in equation (2.30) are defined below:

- e = charge on an electron
- N = number of molecules of stopping medium per unit volume (molecular density)
- m_0 = electron mass
- v = velocity of the particle going through the stopping medium
- Z_1 = atomic number of the particle
- Z_i = atomic number of the i^{th} atom in the stopping medium
- ν_i = number of i^{th} atoms per molecule
- \bar{I}_i = mean ionization potential of the i^{th} component
- M_1 = mass of the particle (amu)
- M_i = mass of the i^{th} atom (amu)
- \hbar = Planck's constant divided by 2π

$(Z_1)_{\text{eff}}$ = effective charge on the particle.

An approximate relationship for the above term is given by Segre (13):

$$(Z_1)_{\text{EFF}} = (Z_1)^{1/2} \frac{\hbar v}{e^2} \quad (2.31)$$

a_{1i}^{SCR} = impact parameter beyond which energy loss by the particle is effectively zero due to screening of nuclei by atomic electrons for the i^{th} atom.

An expression for the impact parameter is given by Claxton (16) :

$$a_{1i}^{\text{SCR}} = \frac{a_H}{[(Z_2)^{2/3} + (Z_i)^{2/3}]^{1/2}} \quad (2.32)$$

where a_H is the radius of the first Bohr orbit for the hydrogen atom.

Equation (2.30) must be evaluated for each particular charged particle-stopping medium case. The solution to equation (2.30) will have the general form of

$$\frac{dE}{ds} = \rho_l \left[A \ln B E + \frac{C}{E} \ln D E \right] \quad (2.33)$$

where A,B,C,D are constants

ρ_l = is the density of the stopping medium

E is the energy of the radiation particle.

The first term in equation (2.33) represents the energy deposition to the electronic system of the stopping medium through ionization and excitation of the atoms, and the second term represents the energy deposition to the stopping medium through nuclear elastic collisions between the energetic particles and the nuclei of the stopping medium. In the cases considered in this work, the second term is negligible, and may be neglected. (This approximation is shown to be valid by Bell (5) pg. 117, and by Segre (13) pg 166.)

Equation (2.33) can thus be reduced to

$$\frac{dE}{ds} = \rho_e A \ln(BE) \quad (2.34)$$

Equation (2.34) shows that the energy deposition rate, dE/ds , is a function of the particle energy, E . This fact was mentioned earlier in connection with equation (2.22).

Equation (2.34) is now substituted into equation (2.23), and the result takes the general form:

$$\frac{[E(s_1) - E(s_2)]^2}{E(s_1) \ln E(s_1) - E(s_2) \ln E(s_2) - B[E(s_1) - E(s_2)]} = Ca \rho_e r^* \quad (2.35)$$

where B and C are constants

a = Bell's parameter

ρ_e = density of the stopping medium

r^* = critical radius of embryo

A substitution is now made for r^* , using equation (2.28):

$$r^* = \frac{2\sqrt{\quad}}{P_v + P_g - P_1} \quad (2.36)$$

It is now possible to calculate, using an iterative procedure, P_g .

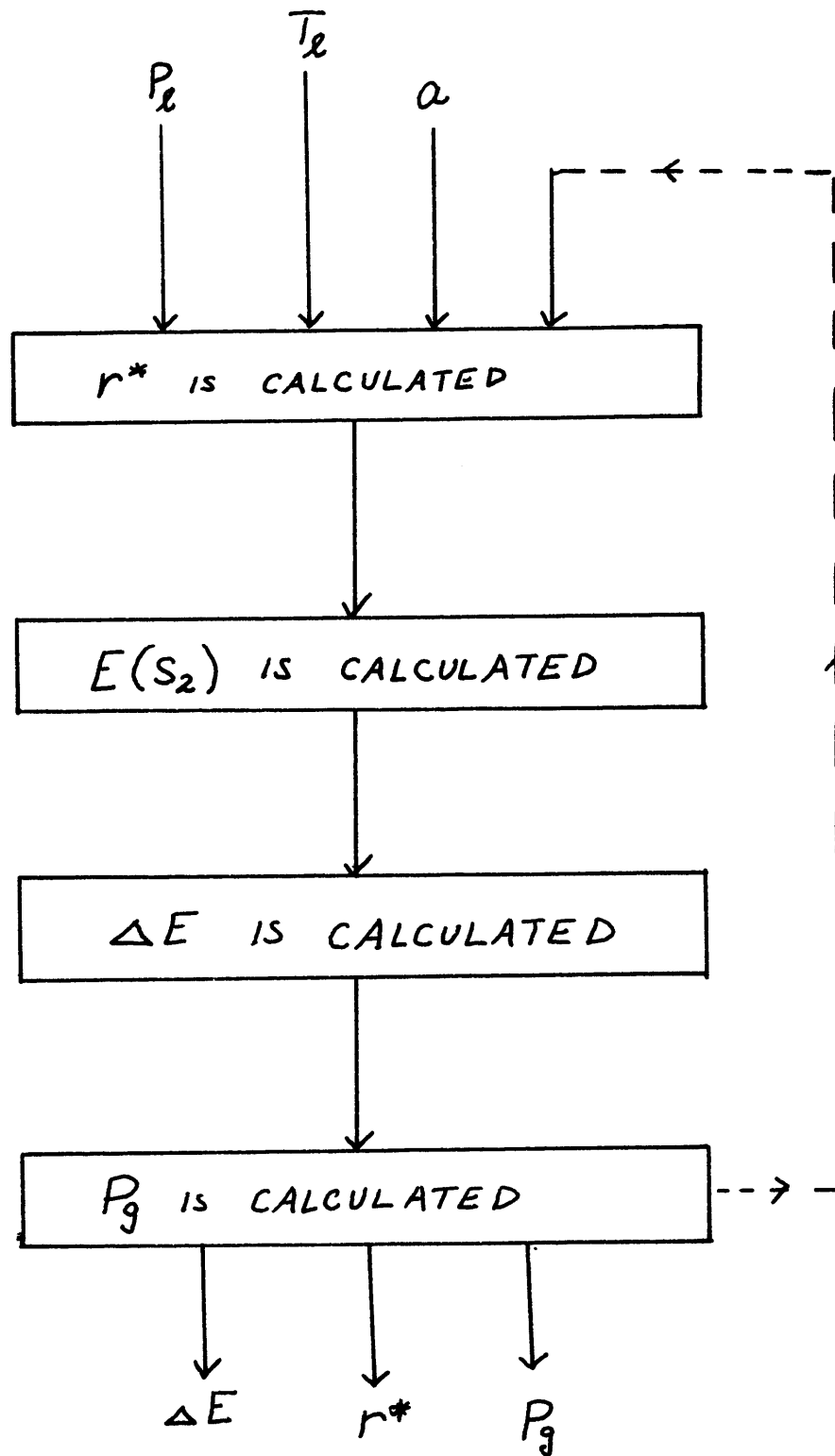
The first step in this procedure is to guess a value of P_g . r^* is then calculated from equation (2.28) (P_v , P_1 , and $\sqrt{\quad}$ are known). The next step is to calculate $E(s_2)$ from equation (2.35). ΔE can now be found by recalling that

$$\Delta E = E(s_1) - E(s_2)$$

$E(s_1)$, the initial particle energy, is always known. P_g is now calculated using equation (2.29). If this calculated value of P_g is not equal to the original P_g guess, then another value of P_g is assumed, and the procedure is continued until the two values converge. FIG. 2.3 gives a simplified flow chart of this calculational procedure.

The convergence of this series will give correct values of P_g , r^* , and ΔE , for a given set of values of P_1 , a , and T_1 .

Once P_g has been obtained, the superheat temperature can be obtained. A complete program has been developed by Bell((5), pg 122), which calculates the superheat

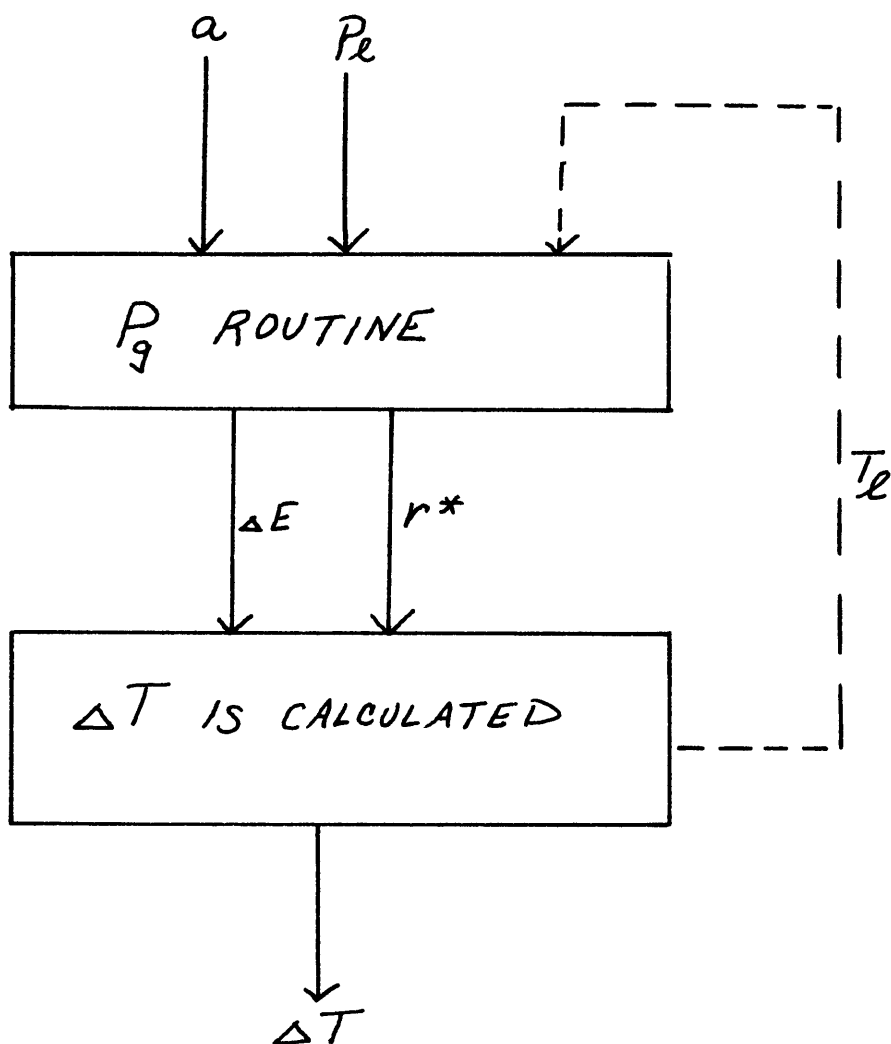


P_g ROUTINE

FIG. 2.3

threshold for various pressures and "a" values. It is an iterative procedure involving the system temperature, T_1 . A brief description of the program operation will be given.

There are three independent variables: the system pressure, P_1 , the system temperature, T_1 , and the parameter "a". P_1 and "a" are considered independent parameters. The first step of this procedure is to select an initial value of T_1 , for a particular set of P_1 and "a" values. This temperature value is then fed into the P_g procedure mentioned earlier, (the P_g procedure can be considered a subprogram of the entire calculational method for obtaining the threshold superheat.) The convergence of the P_g routine gives the corresponding values of P_g , r^* , and ΔE , for the set of chosen variables P_1 , "a", and T_1 . Using these values of ΔE and r^* , the LHS and RHS of equation (2.26), are calculated. If equation (2.26) is not satisfied, a new value of T_1 is chosen and the process is repeated until the energy balance criteria is met. When this criteria is met, the T_1 obtained is the superheat temperature corresponding to the threshold condition. FIG. 2.4 gives a flowchart of the entire computational process for obtaining the correct T_1 value.



THRESHOLD SUPERHEAT
CALCULATION

FIG. 2.4

2.6 Fission Fragments and Fast Neutrons

In the case of a fission fragment, the fragment itself can directly produce the highly energetic region in the medium which is necessary for radiation-induced nucleation. This is not true of a neutron. The neutron interacts with the nucleus of an atom, through elastic scattering, and transfers some of its kinetic energy to the nucleus, thus producing a charged primary knock-on atom (PKOA). This PKOA then deposits its energy in a manner similar to the fission fragment.

The only change which this introduces into the computer program, is in the initial energy determination. In the case of fission fragments it is known (14) that the most probable fission fragment pair which results from this fission process has the following characteristics:

Light fragment

$$A = 97$$

$$E(s_1) = 95 \text{ Mev}$$

$$Z = 38$$

Heavy fragment

$$A = 138$$

$$E(s_1) = 67 \text{ Mev}$$

$$Z = 54$$

If the energy deposition rates of these two fragments are compared over the track length from $s=0$ to $s=ar^*$ (this is the portion where the largest dE/ds will be obtained) then it is seen that the lighter fragment has the higher dE/ds , and will give a higher ΔE .

Therefore, for the threshold condition, only the light fragment need be considered. Thus, for fission fragments the initial energy is known.

The initial energy of the PKOA must be calculated. Since the energy of the neutron is known, the energy of the PKOA can be calculated from elastic scattering theory (15):

$$E(0)_{\text{PKOA}} = \frac{1}{2} E_n \left[1 - \left(\frac{A-1}{A+1} \right)^2 \right] (1 - \cos \theta) \quad (2.37)$$

where E_n is the neutron energy

A = atomic weight of the PKOA

θ = the angle the neutron is scattered in the center of mass frame of reference.

For a maximum $E(0)$, $\cos \theta$ is taken as zero.

This is the only important difference in the computational procedure for the threshold values.

Chapter 3

Experimental Apparatus and Procedures

3.1 Apparatus Modifications

The experimental apparatus was the same as that used by Bell (5) and Tso (6), with a few modifications.

The original test chamber is shown in Fig. 3.1. The test bubble, X, is suspended in the suspension fluid, H, (Dow Corning 550 fluid for the case of water and propylene glycol) and covered with the cover fluid I (Nujol, a heavy mineral oil, for the case of water and propylene glycol). The test chamber, A, is a cylindrical (10"x 3" diameter) steel chamber. The test bubble is visually observed through the window B. The bubble temperature is recorded by two Chromel-Alumel thermocouples (K and L). The chamber is heated by two electrical heaters (M and N). The cover fluid is introduced into the test chamber from reservoir E through the cover fluid outlet tube J. The suspension fluid is introduced from the bottom of the test chamber from the reservoir Q. There are two cooling devices in the test chamber. One is the condenser, F, which condenses any water vapor in the air space left by previous boiling. The condensate is collected in a container and discharged through a tube into reservoir R. The other cooling device is the convection generator G. This serves not only as a cooling device

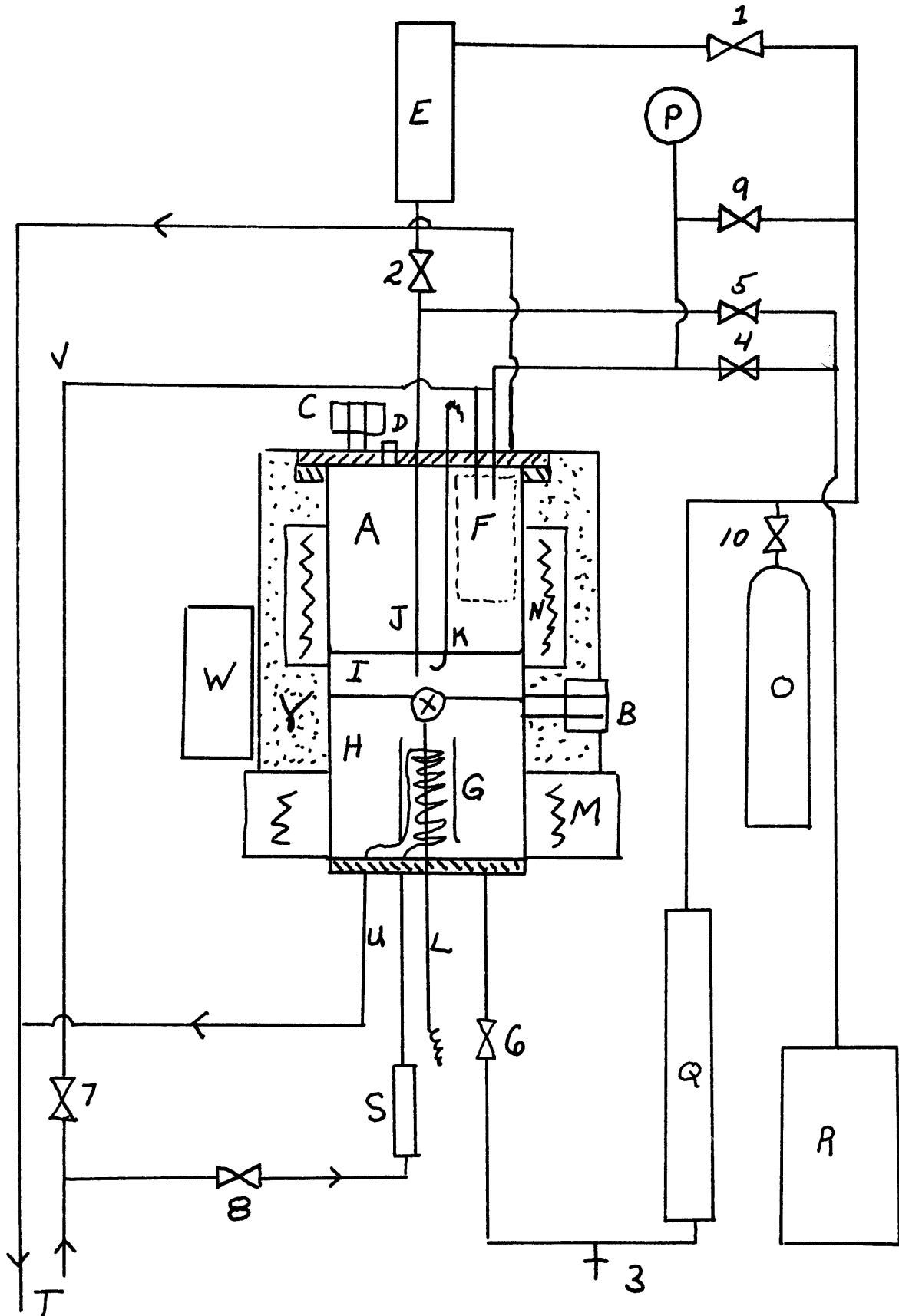


FIG. 3.1

Number 1 to 10	valves
A	boiling chamber
B	observation window
C	light window
D	bubble entrance
E	cover oil reservoir
F	condenser
G	convection generator
H	supporting oil
I	cover oil
J	cover oil outlet
K	top thermocouple
L	bottom thermocouple
M	bottom heater
N	top heater
O	air pressurizer
P	pressure gauge
Q	supporting oil reservoir
R	waste tank
S	flow indicator
T	supply water line
U	convection generator cooling lines
V	condenser cooling lines
W	neutron source
X	water bubble
Y	fibre-glass insulation

when the chamber is being cooled down, but it serves the important function of keeping the test bubble centered during the experimental run. Since this convection generator is such an important part of the apparatus, it is shown separately in FIG. 3.2 . The manner in which the bubble is kept centered is also shown in this figure. The cooling water through the convection generator coils causes a convection current which circulates the supporting fluid such that the flow is radially towards the top of the generator, down through the generator, and radially out at the bottom. In this way the bubble is kept radially in place in the test chamber. The vertical position of the bubble is set by adjusting the supporting oil level.

Two important modifications were made. The first, and most significant, was a change in the method of illuminating the test chamber. In the original design a high intensity lamp was placed above window C, and this was considered adequate. It provided sufficient light to see the test bubble, but it was of considerable strain to the eyes, thus affecting the ease and accuracy of obtaining the data, since all data was visually obtained. The modification which was made placed the light source directly into the chamber, giving a far better illumination of the test bubble. FIG. 3.3a shows the original method, and FIG.3.3b shows the final illumination method. (Only the section of the chamber which supports the lighting system is shown in FIG.3.3)

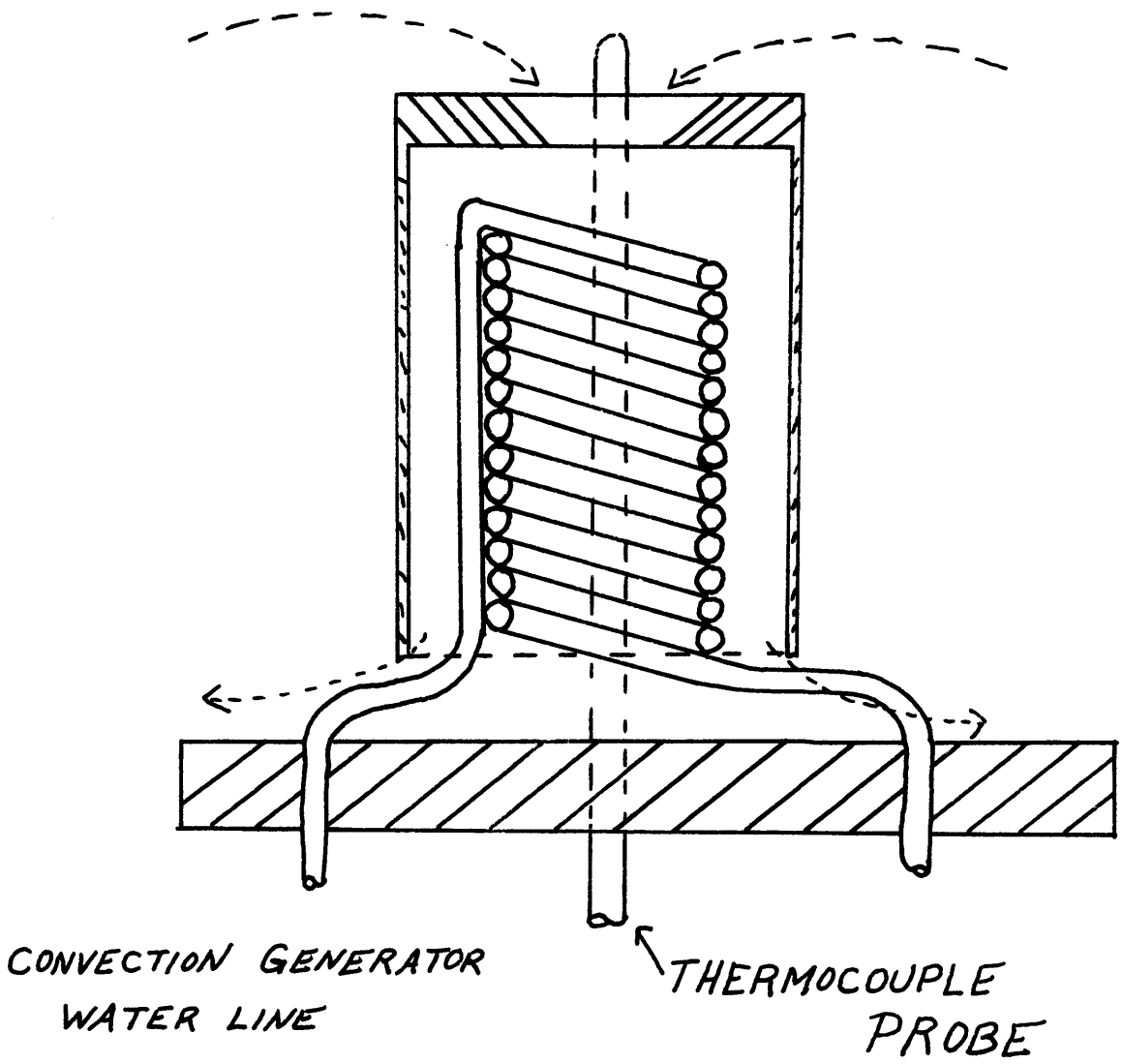


FIG. 3.2

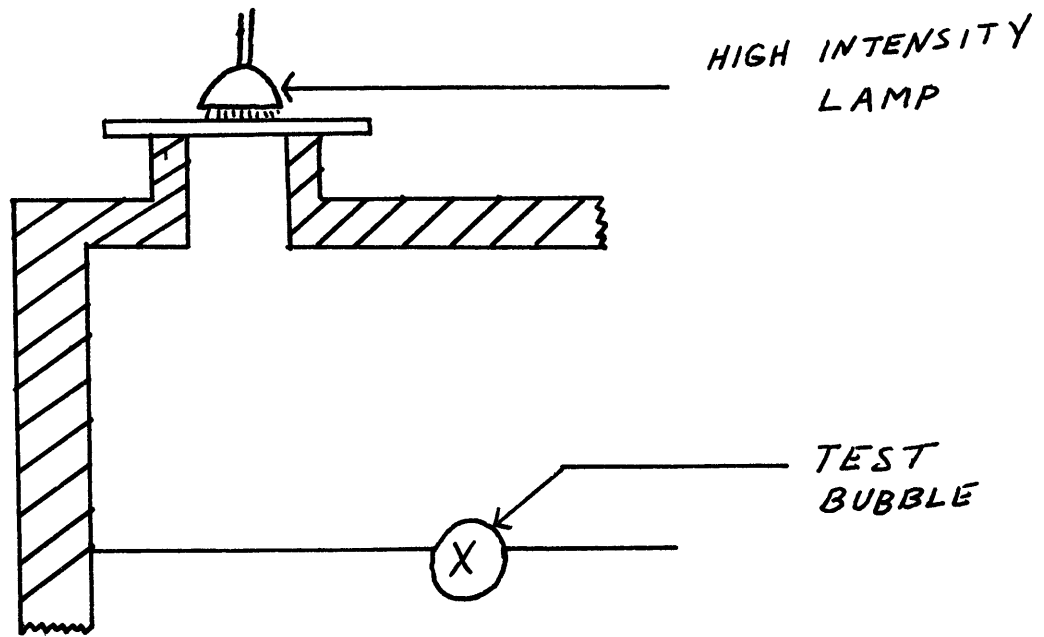


FIG. 3.3a

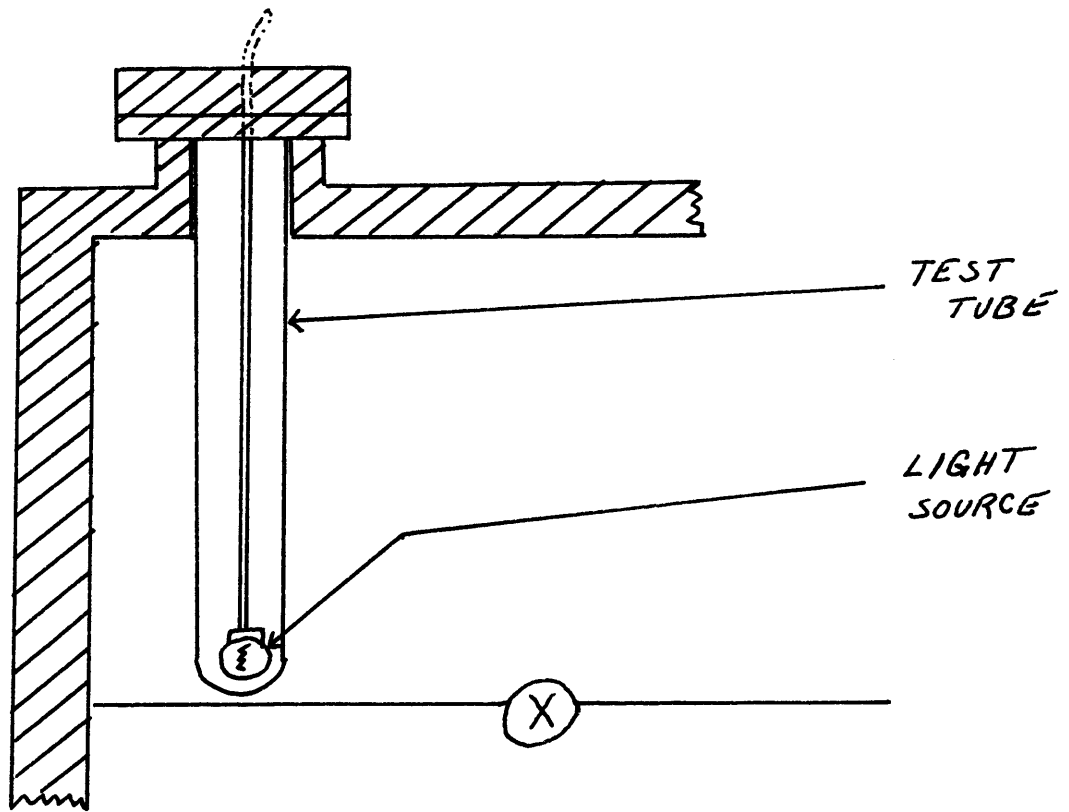


FIG. 3.3 b

This modification required a great amount of work. Since it was not desired to construct a new chamber, it was necessary to work through the existing window C. This created a number of problems, the greatest being that of obtaining a pressure seal at window C. The problem was eventually solved by using the combination of metal rings and hard rubber gaskets to sandwich in the test tube flange. (see FIG.3.3b) Pressures of up to 100 psig were obtainable with this design.

The other modification was to introduce a mirror system for the observation of the bubble. The original design required the experimenter to place his eye directly in front of observation window B. This was an extremely uncomfortable position, and had to be maintained for the length of the experimental run which often exceeded a half-hour.

The mirror system (shown in FIG.3.4) permitted the experimenter to observe the bubble from a distance, and made it easier to monitor all gauges and recorders indicating the temperature and pressure of the test chamber.

The other equipment which should be mentioned is the radiation source, a 5 curie Pu-Be source, and its associated shielding.

The source itself is a small cylindrical element, which is contained in a rectangular aluminum container. This is attached to a masonite block. This entire unit is kept in a shielded storage container until the source

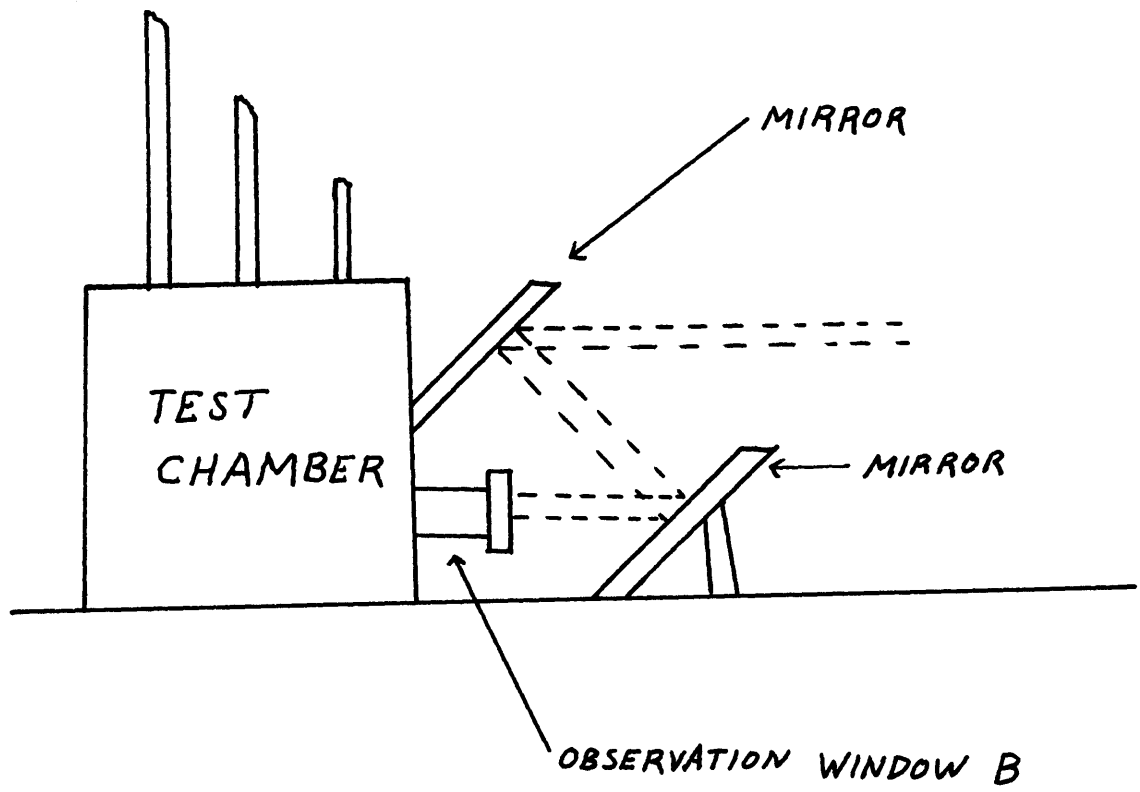


FIG. 3.4

is needed. It is then placed in a shielded housing which has been constructed adjacent to the test chamber.

(The source and housing are shown in FIG. 3.5)

The pressure gauge P was tested for accuracy with a dead weight tester, and it was found that the gauge read approximately 3 psi too low. The calibration curve is shown in FIG.3.6 .

3.2 Experimental Procedure

The procedure for a typical experimental run will be outlined to describe the operational procedure.

Before beginning any experiments with a new test liquid, it is important to thoroughly clean the inside of the test chamber. (Washing with water and then with acetone is recommended.).

The operational procedure is outlined below:

- 1) Introduce the suspension fluid by opening valves 6 and 10, and closing all others. This will force the suspension fluid from the reservoir Q , into the test chamber. The supporting fluid level should be brought to near the top of window B (as shown in FIG.3.1). Once the desired level is reached, valves 6 and 10 are closed.
- 2) The cover fluid is next let into the chamber by opening valves 1,2, and 10. Approximately

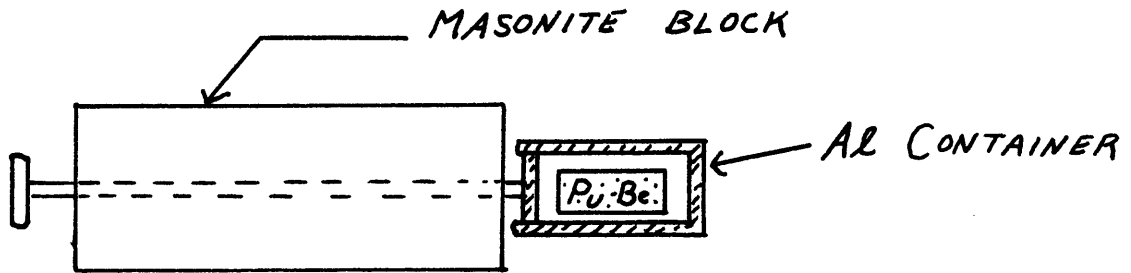


FIG. 3.5. a

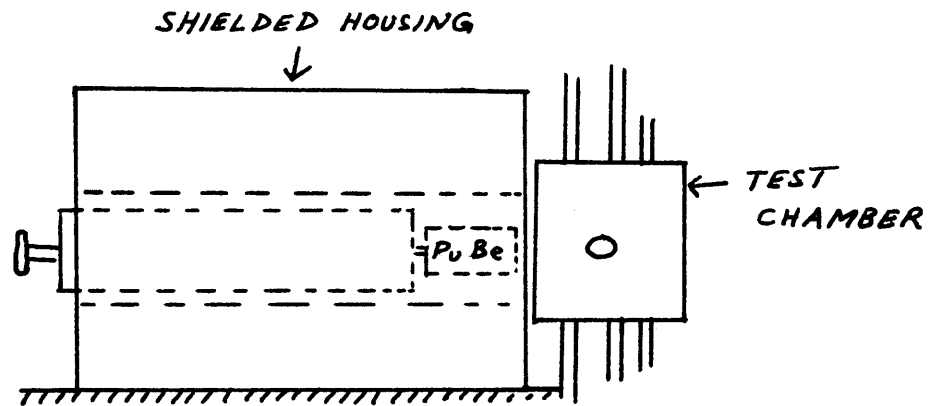


FIG. 3.5 b.

CALIBRATION CURVE FOR PRESSURE GAUGE

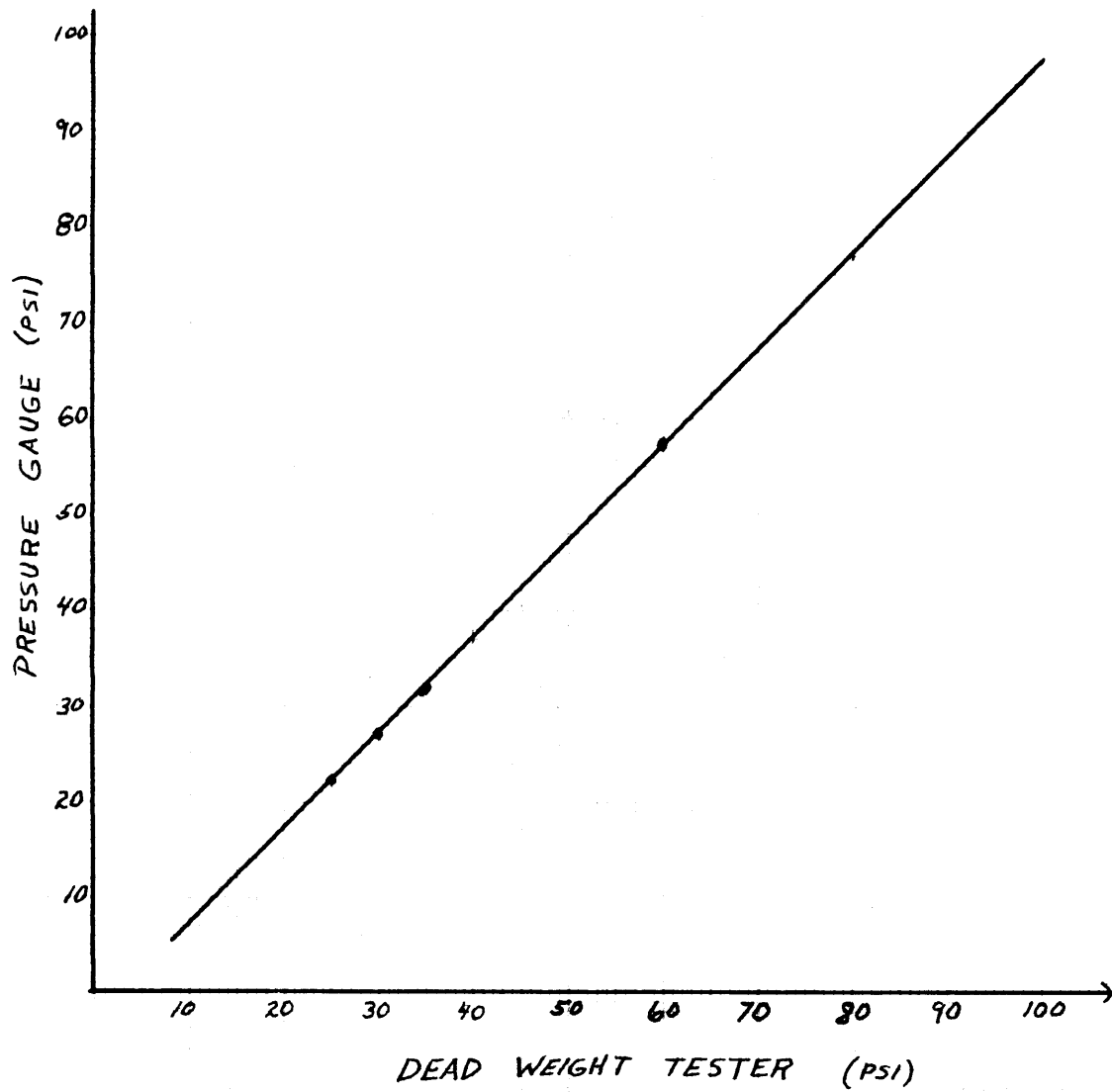


FIG 3.6

an inch of cover fluid is sufficient. When the desired level is reached, valves 1,2, and 10 are closed.

- 3) Valve 8 is opened to allow the convection generator to start flowing.
- 4) The test bubble is then introduced through opening D , by means of an eye dropper. The test bubble is placed above the center of the convection generator.
- 5) After the bubble has been introduced, opening D is closed, and all valves, except 8, are closed.
- 6) Valves 9 and 10 are then opened, with valve 10 being adjusted to the desired pressure.
- 7) Heaters M and N are turned on, and the temperature is constantly monitored through thermocouples K and L .
- 8) Once nucleation is observed, or the run is to be terminated, both heaters, M and N , are turned off, valve 7 is opened, and valve 8 is turned on full (if it were not already fully opened). The chamber is then left to cool down. The time required for it to cool down depends on the final temperature which was reached during the heating process. A final temperature of 500 F will require approximately 45 minutes.

9) When the chamber has cooled down the top layer of liquid must be drawn off, since the test bubble will have broken up and must, in any case, be removed and a new test bubble put into the chamber. This is done by raising the liquid level (by opening valves 6 and 10) until all bubbles are above the opening of the cover oil outlet tube J. All valves are then closed. Valves 9 and 10 are opened, thus pressurizing the chamber. Then valve 5 is opened. This will draw off the top layers of fluids and eject them into reservoir R .

When this has been completed all valves are closed, and the system is ready for another experimental run, beginning with step 1 of this procedure.

3.3 Experimental Difficulties

While running the experiment a number of problems may arise which can create serious difficulties, leading to a premature termination of the experiment.

One problem to be avoided is that of mixing of the cover and suspension fluid. This can occur if valve 6 is opened too quickly or too much, causing the suspension fluid to shoot up into the cover fluid. Also, if reservoir Q is empty and valve 6 is opened, air will shoot through the liquid and cause violent agitation and mixing of the

fluids. The physical properties of the cover and suspension fluids are such that once they are mixed they form a cloudy solution and are very difficult to separate. When mixing occurs the chamber must be emptied and cleaned, and new fluids introduced. It is therefore important that reservoir Q always be filled. The same is true for reservoir E .

Another point to remember is that when cooling down the chamber after a high pressure run, the pressure must not be suddenly reduced. This will cause immediate and violent boiling which will thoroughly mix the fluids. The chamber should thus be cooled down to a temperature below the boiling point of the liquid at atmospheric pressure, and then the pressure can be released.

Another problem might be a flow blockage problem with the convection generator. The tubing used in forming the convection generator is a very small diameter refrigeration tubing. Ordinary tap water is used as the coolant water, and this contains a small amount of chlorine which tends to corrode the inside of the tubing. There are a number of bends in the small diameter tubing which can become blocked due to small particles already existing in the water or produced by corrosion. If the tubing is not periodically cleaned (a weak solution of sodium hydroxide is recommended) the corrosion deposits will soon build up and block the flow. This was the case in the present work. The corrosion deposits were too

thick to be able to be cleaned, so a new convection generator had to be constructed.

During the propylene glycol experimental runs, a change in color of the test liquid was seen to occur at around 300 F. This change is believed to be a chemical characteristic of the liquid. (This characteristic is also seen in other organic liquids.). Also, small dark particles were noticed in the test chamber after a number of experimental runs had been made with propylene glycol. These are believed to be due to residual uranium nitrate particles which remained in the chamber after the propylene glycol test liquid boiled. (The uranium nitrate was introduced to the test liquid for the purpose of providing fission fragments. See section 3.5 for a further discussion on this matter.) These particles required additional cleaning of the chamber.

3.4 Indication of Nucleation

In all previous work on radiation-induced nucleation, the actual production of vapor bubbles in the test liquid proved the nucleation event. In the experimental procedure developed by Bell(5), nucleation is observed through the jumping or break-up of the test bubble. That is, when the bubble is seen to suddenly jump, nucleation has occurred.

For fission fragments at low pressures there is no difficulty at all in observing when nucleation occurs.

The nucleation event at these conditions causes the bubble to actually break up or "explode". At high pressures, nucleation due to fission fragments will cause the bubble to jump suddenly. This is easily seen since it is a fairly large jump. The first jump is the important one, since this gives the minimum superheat value. If the temperature is raised beyond this point, the jumps will be more frequent and become more violent.

For the case of fast neutrons it is more difficult to observe the nucleation event. To begin with, higher temperatures are required, which immediately lengthen the experimental run. At low pressures the nucleation event causes the test bubble to jump in a manner similar to the case of fission fragments in the test fluid. But at high pressures the test bubble jumps only very slightly, and extremely careful observation is required in order to notice this small movement of the bubble. This fact makes it difficult to obtain data for fast neutron-induced nucleation at high pressures.

3.5 Fission Fragments in a Test Liquid

Fission fragments are introduced into the test fluid by dissolving a minute quantity of Uranium Nitrate ($\text{UO}_2(\text{NO}_3)_2 \cdot \text{H}_2\text{O}$), in the test liquid. The amount of Uranium nitrate dissolved can vary. For the case of water, the concentration used was : 0.0087 gm of uranium nitrate to 1.0 gm of water. For the case of propylene

glycol , 0.0029 gm of uranium nitrate to 1.0 gm of test fluid was used.

The fast neutrons from the 5 curie Pu-Be source will cause fission events in the uranium nitrate, thus creating the desired fission fragments.

Chapter 4

Fluid Selection

4.1 Background Information

As mentioned previously, the experimental technique employed by Bell consisted of suspending the test liquid in two other fluids. This gives the important advantage of having the test liquid free from any surface effects.

The test liquid used by Bell(5) and Tso(6) was water. The supporting fluid was a Dow-Corning 550 silicone fluid. The cover fluid was a heavy weight mineral oil, which has the trade name of Nujol. Both experimental and analytical work was done with water.

Tso(6) did some preliminary calculations for benzene as a test fluid, exposed to Pu-Be neutrons. A literature search found benzene(4), acetone(4), and diethyl ether (2) used as test liquids in radiation-induced nucleation studies. It was thus decided to confirm and extend the work of these other investigators, and to obtain analytical results using Bell's(5) constant "a" theory.

4.2 Test Liquid Properties

A number of physical properties are required for the computation of the superheat temperature. These properties are listed below:

- 1.) Vapor Pressure
- 2.) Liquid Density
- 3.) Vapor Density
- 4.) Surface Tension
- 5.) Heat of Vaporization

Data for each of the above physical properties must be known at a number of temperatures, since the calculational procedure requires an empirical relationship between the physical property and the temperature.

This empirical relationship is obtained by feeding the data for various temperatures into a polynomial regression computer program. This program will give an expression of the form:

$$P = A + BxT + CxT^2 + DxT^3 + \dots \quad (4.1)$$

where: P = the value of the physical property
 T = temperature at which the property is to be
 evaluated
 A,B,C,D,.... are constants determined by
 the program.

The polynomial regression program is given in Appendix C.

In addition to benzene, acetone, and diethyl ether, a search was also conducted to find the required properties for methyl alcohol, ethyl alcohol, nitromethane, and propylene glycol.

All required properties were eventually found, and the empirical relationships, along with graphs of the physical property versus the temperature, are given in Appendix A .

4.3 Compatibility Requirements

A simple schematic drawing of the configuration of the liquids is shown in FIG.4.1 below;

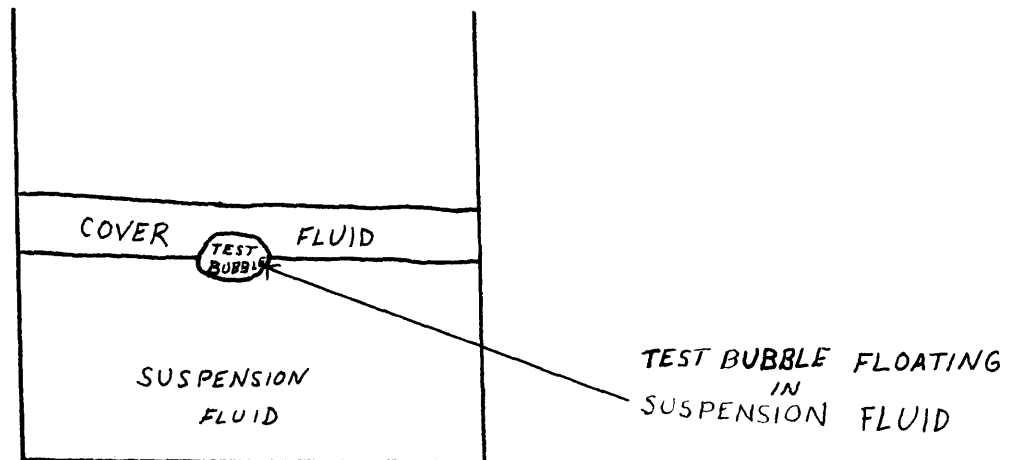


FIG 4.1

The three fluids must exhibit the following characteristics:

- 1.) The three fluids must be immiscible with each other. That is, they cannot be soluble with each other.
- 2.) The relative densities must be such that the supporting fluid has the highest density, the cover fluid the lowest, and

the test fluid density must lie between the two.

- 3.) The boiling points of the cover and supporting fluids must be greater than the boiling point of the test fluid. The lower the test fluid boiling point, the easier the experimental work.
- 4.) The surface tension difference between the test fluid and the other two fluids must be fairly large, with the test fluid having the largest surface tension value.

The fourth factor listed above is not that obvious at first, but it is one of the most important factors affecting the choice of the three liquids.

4.4 Difficulties in Fluid Selection

Benzene and Acetone were originally planned to be used as the test fluids, since some work had already been done on these fluids (4). But benzene and acetone were not able to be used with this three liquid configuration. The problems presented were twofold:

- 1.) The densities of benzene and acetone are very low:

- benzene density	0.87901 gm/cm ³	(20 °C)
-acetone density	0.78998 gm/cm ³	(20 °C)

2.) Benzene and acetone are two of the most universal solvents in use. In other words, they are soluble in almost any liquid.

These two factors seemed to work together. The few liquids which are insoluble with benzene or acetone all have higher densities. This eliminates any possibility for a cover fluid, which must have a lower density.

Evidence of this solubility problem can be seen in any solubility chart. TABLE 4.1 is a small section of a large solubility chart (reference (17) pgs. 58-60), and it is seen that there are indeed few liquids which are insoluble in benzene and in acetone. The liquids which were found to be immiscible with acetone and benzene are listed in Table 4.2 and 4.3 , along with their density. In all cases, those liquids which were immiscible with benzene or acetone had higher densities . An extensive literature search (and consultations with graduate students in the organic chemistry department at M.I.T.) failed to produce a suitable cover fluid for either benzene or acetone.

Therefore, only analytical work was able to be done with benzene and acetone. However the data of El-Nagdy (4) is later compared with these analytical results to determine the "a" value predicted by this data.

	<u>ACETONE</u>	<u>BENZENE</u>
Acetone		M
Isoamyl acetate	M	M
Benzene	M	
Chloroform	M	M
Diethylenetriamine	M	M
Ethyl alcohol	M	M
Ethyl Benzoate	M	M
1,3-Butylene glycol	M	I
Ethyl ether	M	M
Methyl isopropyl ketone	M	M
Triethylenetetramine	M	M
Glycerol	I	I
Propylene glycol	M	I
Trimethylene chlorohydrin	M	M
Carbon tetrachloride	M	M
Nitromethane	M	I
Diethyl ether	M	M
Pyridine	M	M
Diethyl cellosolve	M	M
Triethyl phosphate	M	M

M = miscible I = immiscible

TABLE 4.1

TABLE 4.2

Liquids immiscible with benzene

<u>Liquid</u>	<u>density gm/cm³ (20°C)</u>
1,3-Butylene glycol	1.005
3-chloro-1,2-propanediol	1.326
ethylene glycol	1.1135
glycerol	1.261
1,2-propanediol	1.036
1,3-propanediol	1.053
diethanolamine	1.089
formamide	1.133
hydroxyethyl-ethylenediamine	0.980
nitromethane	1.1138

TABLE 4.3

Liquids immiscible with acetone

<u>Liquid</u>	<u>density gm/cm³ (20°C)</u>
glycerol	1.261

A search was conducted to find a test liquid other than water, and supporting liquids which would be compatible with it. This is a difficult and time consuming procedure, since there are four independent variables which must be taken into account (miscibility, density, boiling point, and surface tension).

The easiest method of search is to begin with the miscibility condition. This is the quickest way to eliminate most of the unsuitable liquids. The first step would be to choose liquids which are immiscible with a large number of other liquids. (The miscibility charts given in references (17)-(21) are recommended for this purpose.)

After obtaining a number of candidates from the miscibility criteria, the boiling points should be checked. The test liquid should have as low a boiling point as possible. (Reference (22) gives the boiling points of most of the commonly used liquid solvents conveniently in order of increasing boiling point.) The possible choices are then checked as to densities. The test liquid must have an intermediate density. (Reference (22) also gives the densities of a large number of liquids in ascending order.)

In addition to the organic liquids there exist some light weight mineral oils which might be able to be used as cover and stopping fluids. These are for the most part clear liquids with high boiling points, and

are immiscible in many organic liquids. But even though they are referred to as light-weight oils, their densities are not much less than that of water. (Nujol has a density of 0.886 gm/cm^3 at 20°C , which makes it heavier than either benzene or acetone.)

Upon completion of the preceeding analysis, a number of possible choices were available. The exact effect of surface tension was not known at this time. Small quantities of the most likely candidates were obtained, and compatibility tests were made. These compatibility tests simply consisted of placing the supporting and cover fluids in a beaker (a similar arrangement as in the test chamber) and then introducing the test fluid. This is an exact simulation of the manner in which it is done in the test chamber.

Table 4.4 gives a partial list of the results observed from the compatibility tests described above. In many cases there resulted what was termed a "spreading effect", where the test liquid did not remain in the shape of a bubble, but spread out over the supporting fluid. This effect is shown in FIG. 4.2.

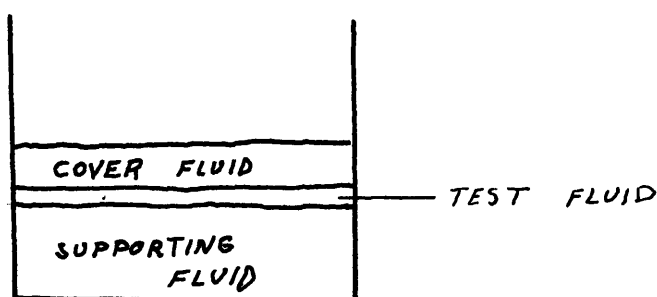


FIG. 4.2

	<u>SUPPORTING FLUID</u> (surface tension in dynes/cm at 20°C)	<u>TEST FLUID</u>	<u>COVER FLUID</u>	<u>RESULT</u>
(1)	Glycerol 63.3	Nitro- methane 37.48	Nujol 23.0	Spreading of the test fluid.
(2)	Ethylene- glycol 46.49	nitro- ethane 32.66	Nujol 23.0	Spreading of the test fluid.
(3)	Glycerol	1,2-dichloro- ethane 32.23	nujol	Test bubble slightly soluble when heated.
(4)	Glycerol	propylene- glycol 36.9	Nujol	Bubble does not remain in bubble shape, spreads.
(5)	Glycerol	salicyl- aldehyde —	ethylene- glycol	test bubble soluble when heated
(6)	DC FS 1265 fluid 26.1	nitro- methane	Nujol	test bubble slightly soluble when heated.
(7)	DC 550 fluid 23.50	propylene- glycol	Nujol	Stable bubble

TABLE 4.4

The surface tension effect is apparent from these results. In the fourth test listed the supporting fluid, glycerol, has a high surface tension (63.3dynes/cm at 20°C), while the test fluid, propylene glycol, has a much lower surface tension (36.9 dynes/cm at 20°C). The result of this test was the spreading of the test fluid over the supporting fluid as shown in FIG.4.2 . In the seventh test listed, the high surface tension glycerol was replaced with a low surface tension (23.5 dynes/cm at 20°C) DC 550 silicone oil. The result of this test was the successful configuration shown in FIG. 4.1 . In both of the cases mentioned the surface tension difference was large, but for a successful configuration it is not only necessary that there be a large difference between surface tensions, but also that the test liquid have the highest surface tension.

In the experimental work with water as the test fluid, the water test bubble showed exceptional stability in the supporting (DC550 fluid) and cover (Nujol) fluids. The surface tension of water is found to be 72.0dynes/cm at 20°C . This tends to support the conclusion arrived at above.

Thus a compatible set of fluids was found:

cover fluid : Nujol

test fluid : propylene glycol

supporting fluid : Dow Corning 550 fluid.

Experimental work was then done using this test fluid.
(Due to time limitations, the search for more compatible fluid sets was not continued to find another possible test fluid.)

4.5 Discussion of Surface Tension

Since the surface tension plays such an important role in the selection of a compatible fluid set, a few words on the nature of surface tension are in order.

Surface tension (σ) is usually defined from a molecular viewpoint. An individual molecule in a body of liquid is subject to forces due to its neighboring molecules. (Theory indicates that these are electrical forces (23)) These forces will fluctuate due to molecular agitation, but when averaged over a finite period, their effect will be zero, so that a molecule can move about in a liquid without doing any work against these forces (24). In other words, the resultant average forces are equal in all directions inside a body of liquid. But when a molecule comes to the surface of this body of liquid, the molecule must ultimately move against unbalanced forces, since it will no longer be surrounded symmetrically by other molecules. At the surface, therefore, there will be an uneven distribution of forces acting essentially normal to the free surface of the liquid. (This will be normally inward, since the electrical force is essentially an attractive force (25)). There is thus a pull toward the interior

of the body exerted on the surface layer.

Since this surface force is uniform due to the averaging effect of the large number of molecules per unit of surface area, it tends to produce a surface with the smallest possible area. (If the liquid is free from gravitational effects, a spherical shape would result.) This inward normal pull is usually defined as the surface free energy. And to extend this surface, work must be done equivalent to this energy. This is usually referred to as the surface tension. (This term is not totally correct, but the idea of a tension in this free surface of a liquid is familiar as an explanation of the tendency of a liquid surface to assume the form having a minimum area.)

The units of surface tension are: dynes/cm , lbf/ft , or ergs/cm² .

Relationships between the surface tension and other physical properties will now be considered.

The first important fact is that as the temperature of the liquid is increased, the surface tension decreases. This is due to the fact that the increase in temperature gives the molecules in the liquid more energy, and thus larger fluctuations, and, since the attractive forces are close-range forces, they will decrease with an increase in the distance between molecules. At the critical temperature the surface tension is zero.

A number of relationships are given between the temperature of a liquid and its surface tension. These are all of the general form

$$\sigma = A - B \times T \quad (4.2)$$

where:

σ = surface tension

T = temperature at which the surface tension is to be calculated

A and B are constants which vary with the liquid. There is also a relationship between the viscosity and the surface tension. An equation relating these two parameters has been formulated by Buehler (27), and is given below:

$$\sigma^{\frac{1}{4}} = \frac{\log(\log \eta) + 2.9}{I/\rho} \quad (4.3)$$

where: σ = surface tension

η = viscosity in millipoise

I/ρ = a constant which varies for different liquids.

A relation between surface tension, density, and temperature has been given by Macleod(34) :

$$\frac{\sigma}{(D-d)^4} = \text{constant} \quad (4.4)$$

where; σ = surface tension
 D = liquid density
 d = vapor density

Very recently there has been developed a correlation between surface tension and the dielectric constant, and surface tension and the index of refraction (28). The relation between the surface tension and the dielectric constant is shown in equation (4.5)

$$\sigma = 165.0 \left[\frac{(\epsilon_s - 1)}{(2\epsilon_s + 1)} \right] - 9.1 \quad (4.5)$$

where: σ = surface tension in ergs/cm²
 ϵ_s = static dielectric constant

Equation (4.5) is good for all liquids with zero dipole moment. These include: hexane, octane, benzene, p-xylene, carbon tetrachloride, p-dichlorobenzene, CS₂, H₂, N₂, O₂, A, Br₂, Cl₂.

For molecules with non-zero dipole moments, the relation is of similar form, but includes the index of refraction, n , instead of the dielectric constant.

This correlation is shown below:

$$\sigma = 286.0 \left[\frac{(n^2 - 1)}{(2n^2 + 1)} \right] - 28.6 \quad (4.6)$$

The previous correlations between surface tension and other physical properties (viscosity, density, dielectric constant, index of refraction) are very useful, since surface tension data is difficult to find at more than one temperature.

The previous few paragraphs have been an introduction to the concept of surface tensions. For a more detailed discussion on this topic, references (23) to (28) are recommended.

Chapter 5

Results

5.1 Analytical Results

Analytical results have been obtained using the energy balance method of Bell (5). The results include fast neutrons in the test fluid and fission fragments in the test fluid.

For the case of fast neutrons in the test fluid, the initial energy of the PKOA was 2.12 Mev. This initial energy value is listed on the graphs as "EPKA" (energy of the primary knock-on atom). (The value of 2.12 Mev for this initial energy was obtained through an analysis by Bell((5) pg. 173) considering the Pu-Be neutron source and its associated energy spectrum.)

The test fluids for which analytical results were obtained are:

- 1.) Water (FIG.5.1 and FIG.5.2)
- 2.) Propylene Glycol (FIG.5.3 and FIG.5.4)
- 3.) Benzene (FIG.5.5 and FIG.5.6)
- 4.) Acetone (FIG.5.7 and FIG.5.8.)
- 5.) Nitromethane (FIG. 5.9 and FIG.5.10)

The results are given in the form of a graph of the threshold superheat (amount of superheat) versus the system pressure, for a number of "a" values.

FAST NEUTRONS IN WATER

$E_{PKA} = 2.12 \text{ MeV}$

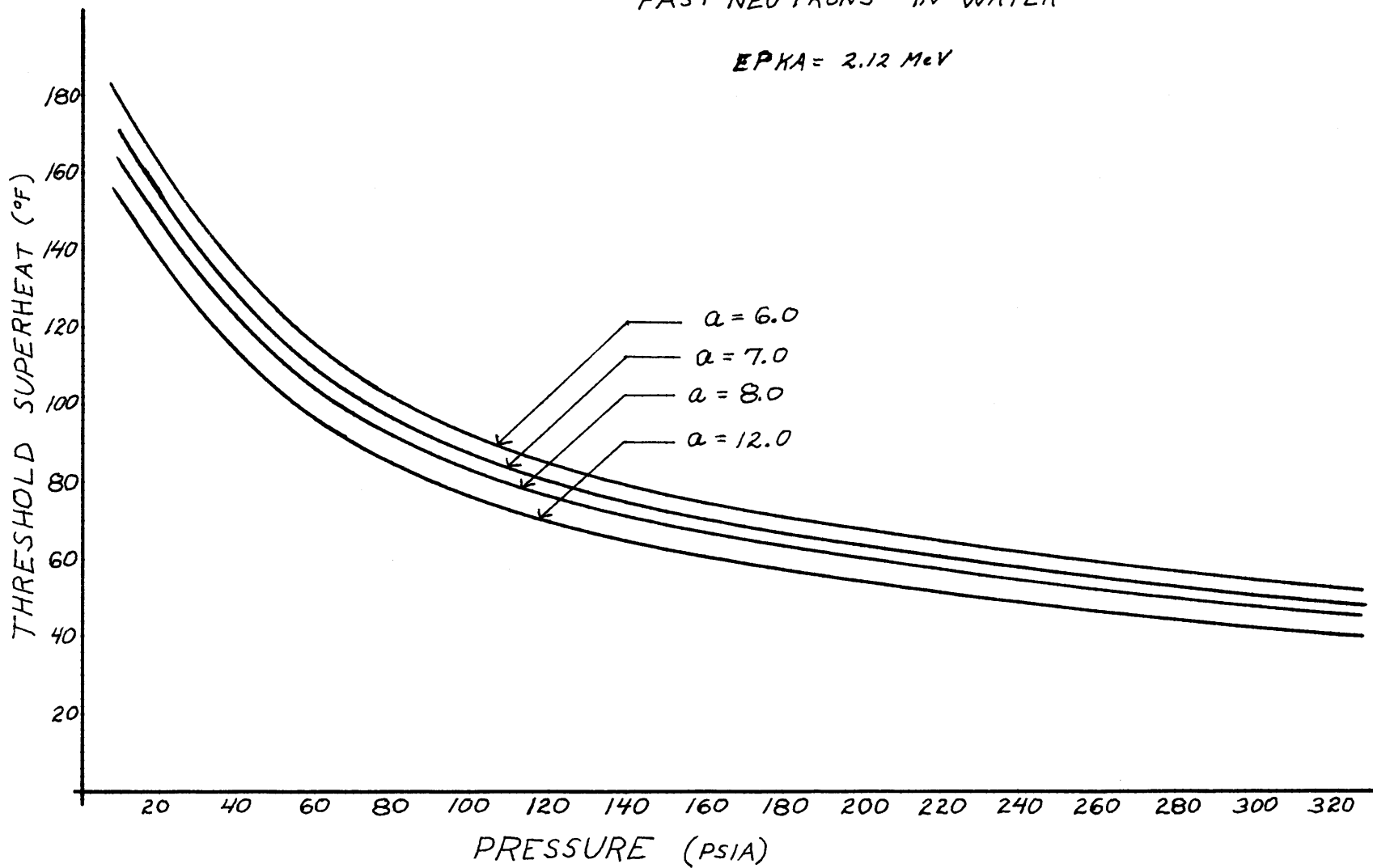


FIG. 5.1.

FISSION FRAGMENTS IN WATER

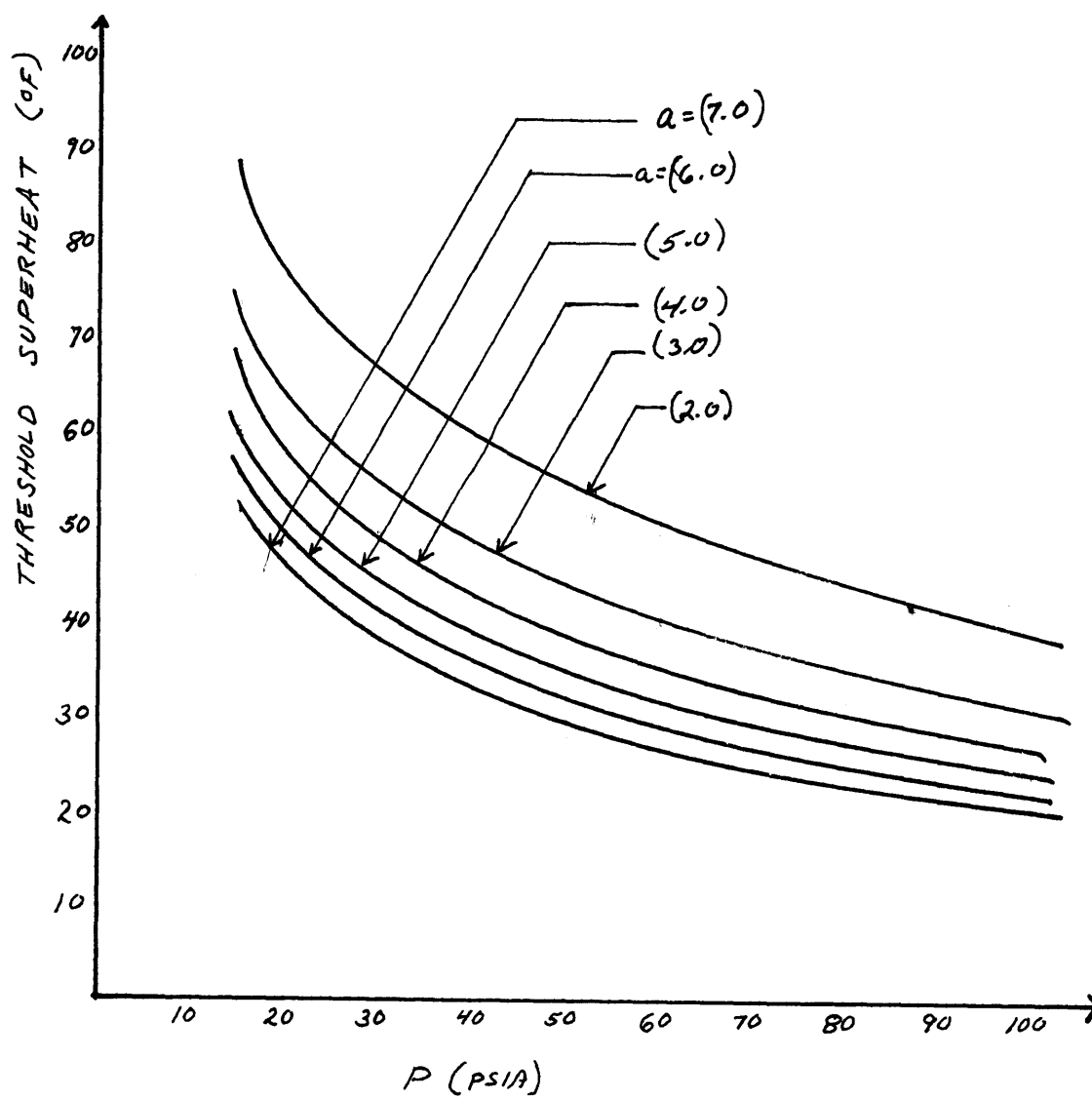


FIG 5.2

FAST NEUTRONS IN PROPYLENE GLYCOL

$$EPKA = 2.12 \text{ MeV}$$

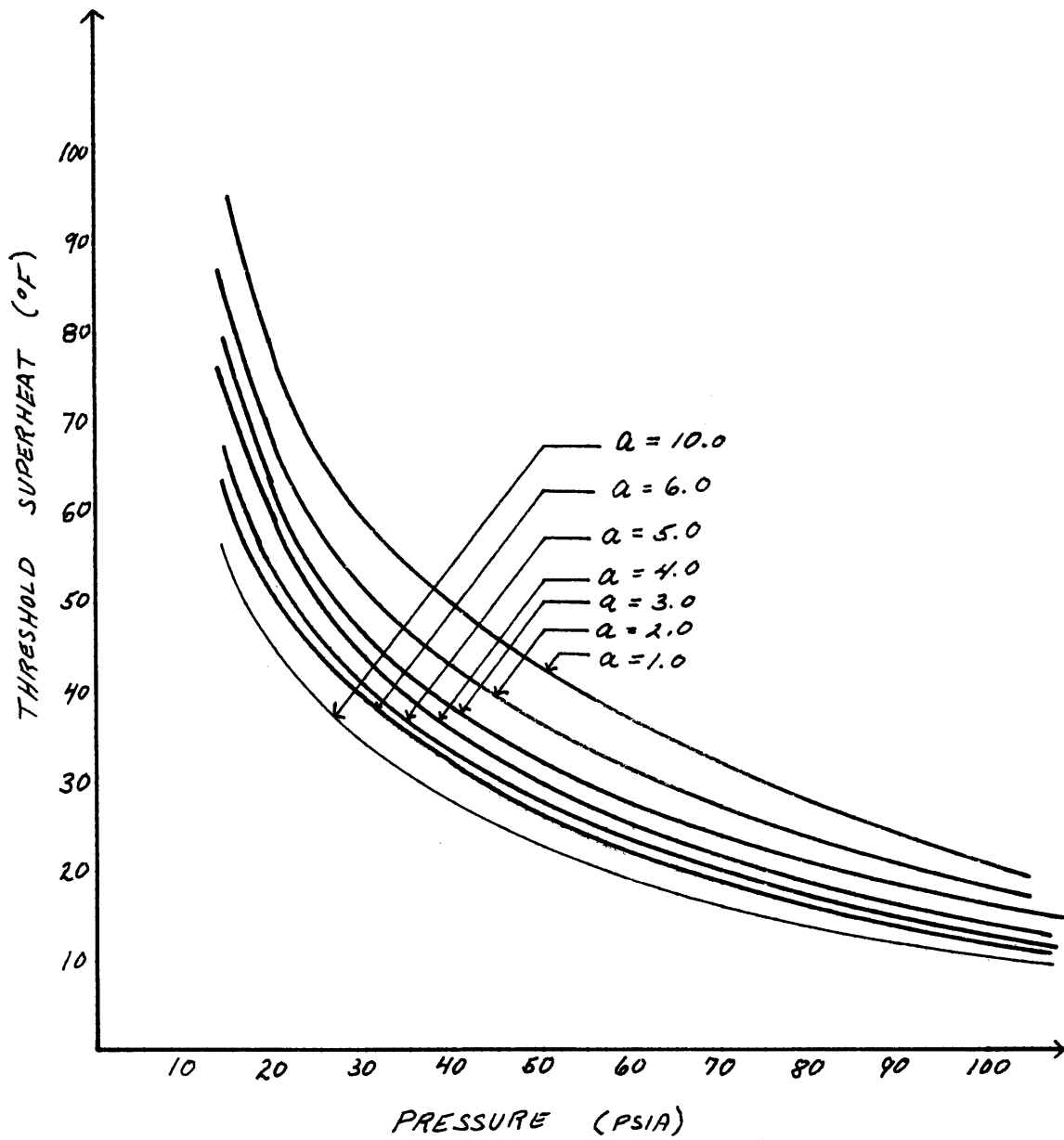


FIG. 5.3

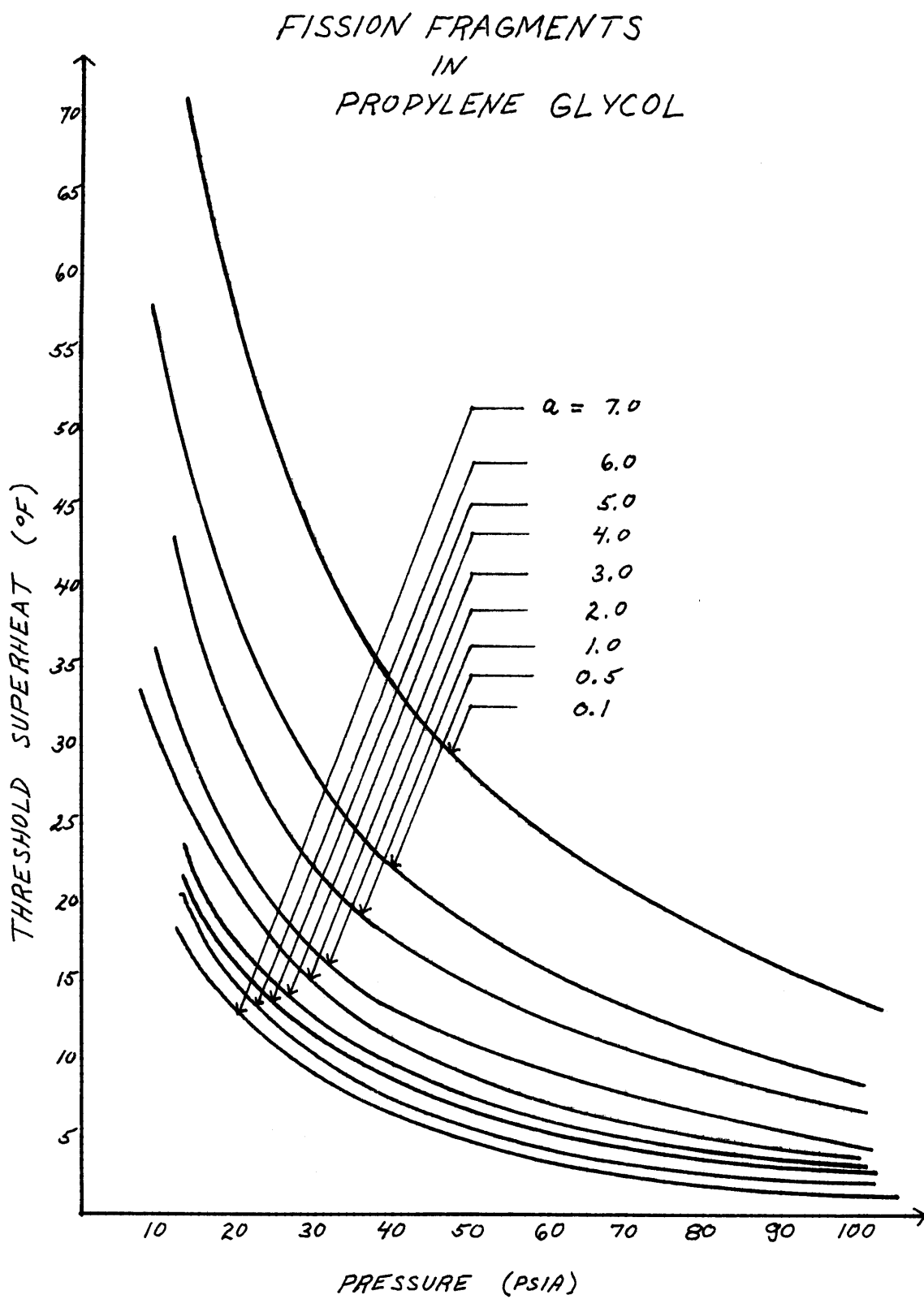


FIG. 5.4

FAST NEUTRONS IN BENZENE

$$EPKA = 2.12 \text{ MeV}$$

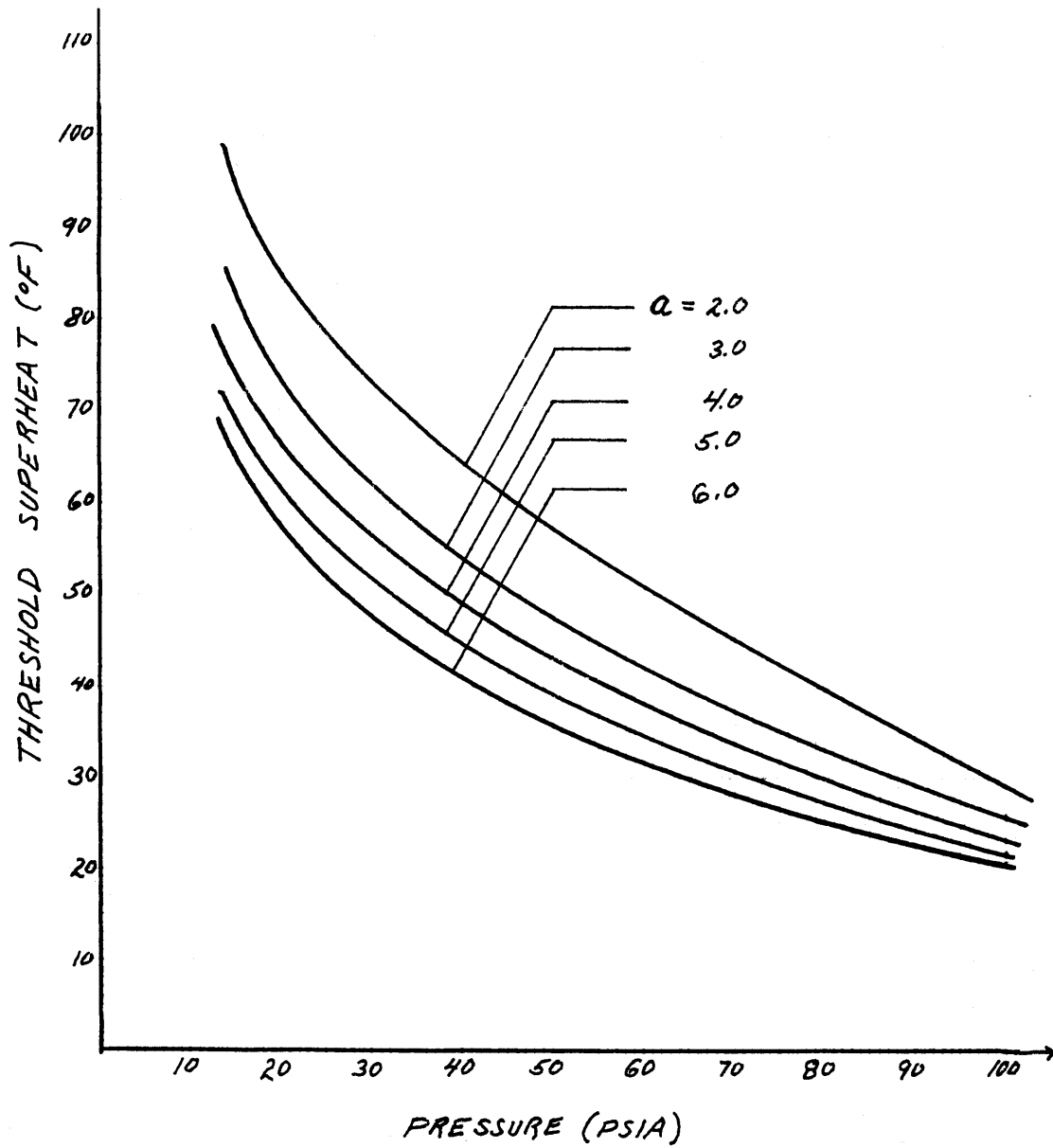


FIG. 5.5

FISSION FRAGMENTS
IN
BENZENE

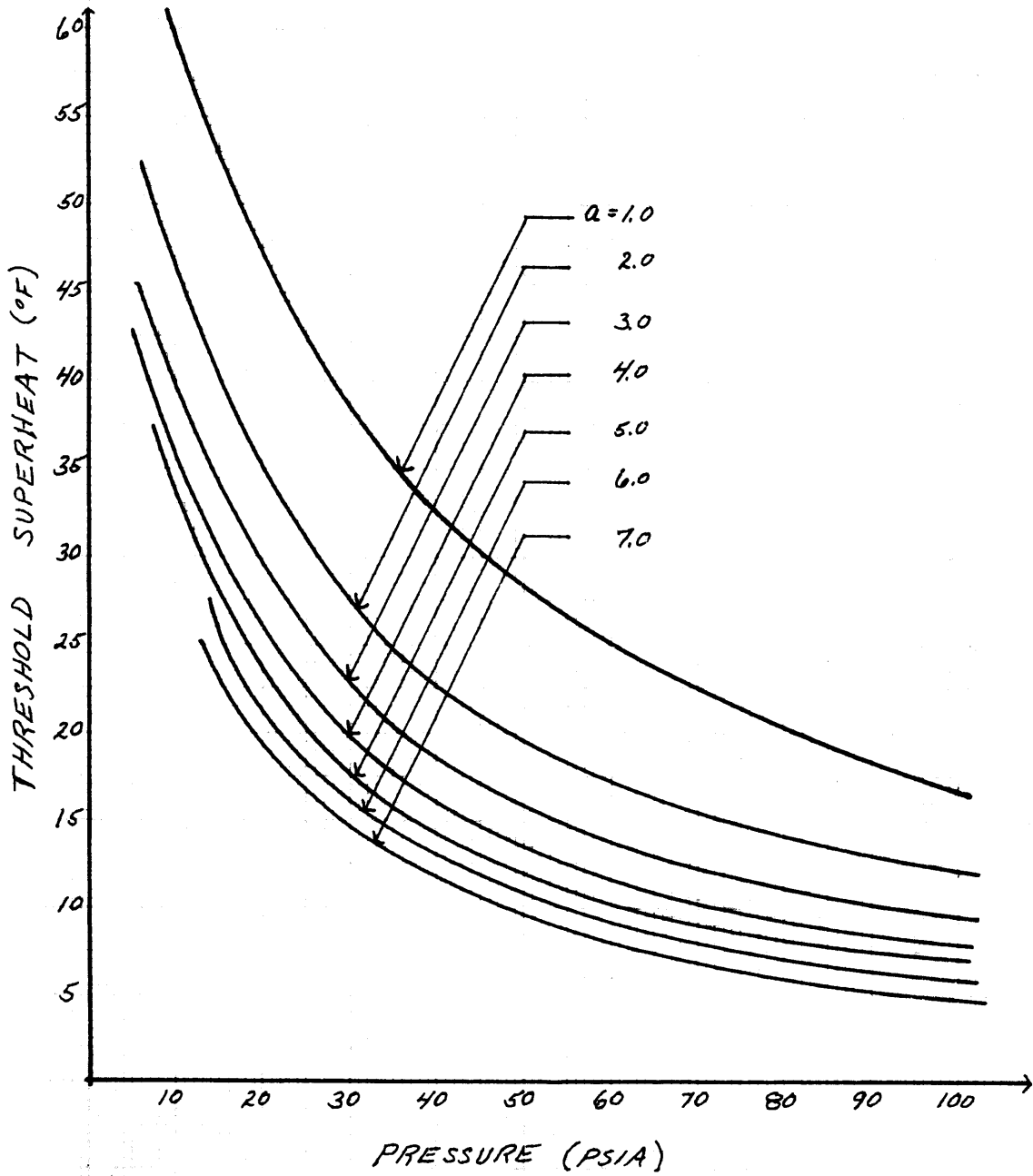


FIG. 5.6

FAST NEUTRONS
IN
ACETONE

$$EPKA = 2.12 \text{ MeV}$$

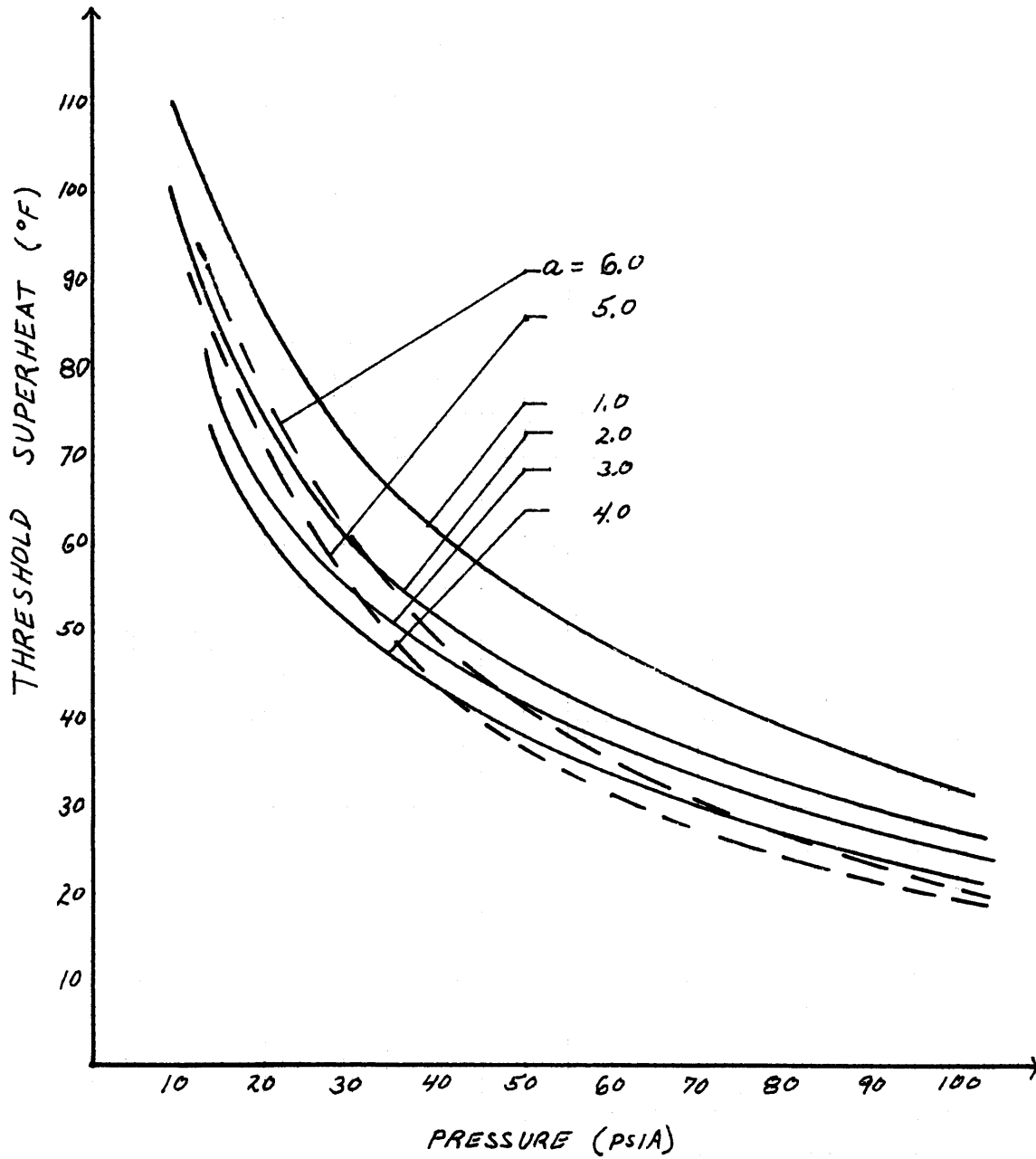


FIG. 5.7.

FISSION FRAGMENTS
IN
ACETONE

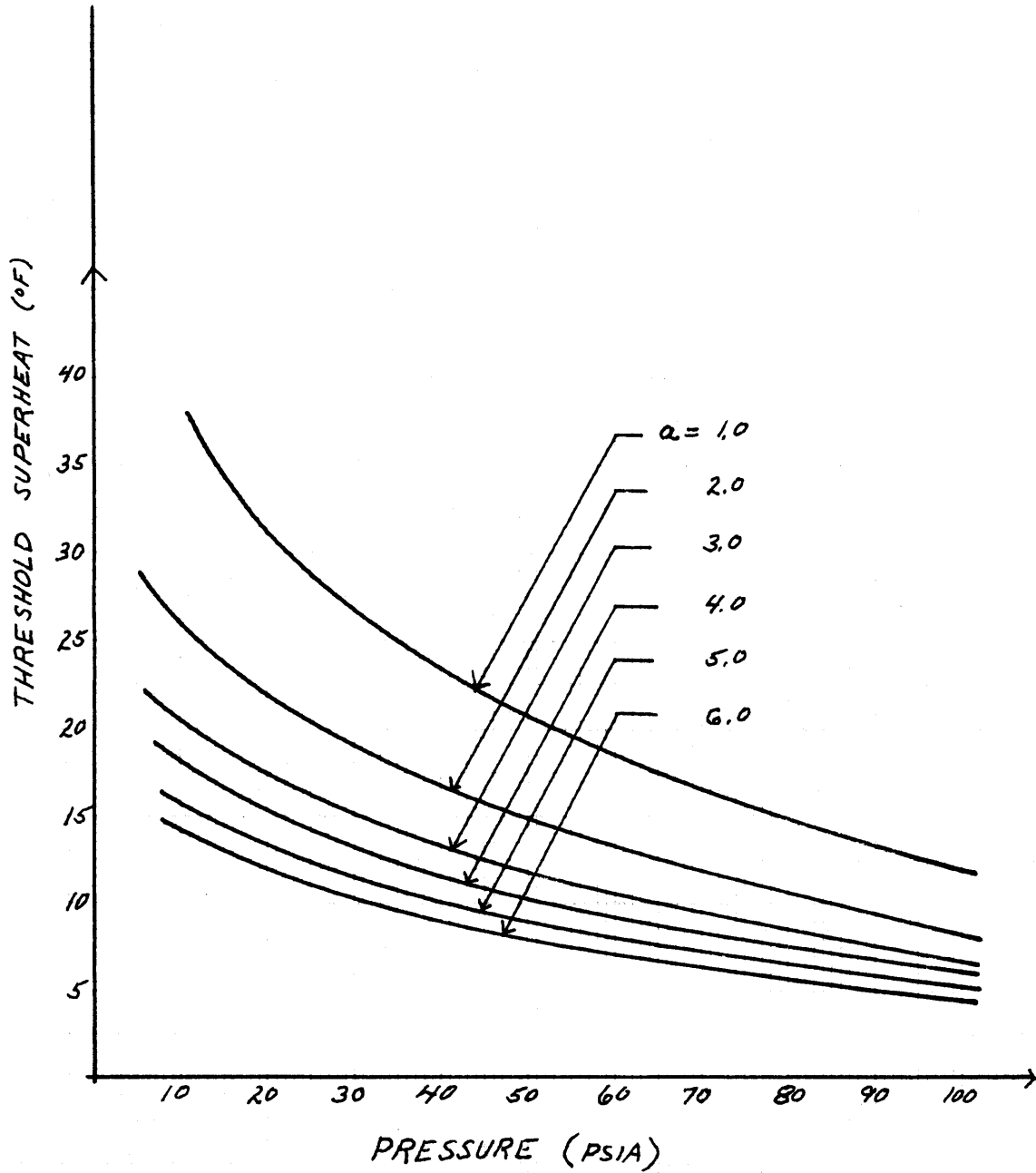


FIG. 5.8

FAST NEUTRONS
IN
NITROMETHANE

EPKA = 2.12 MeV

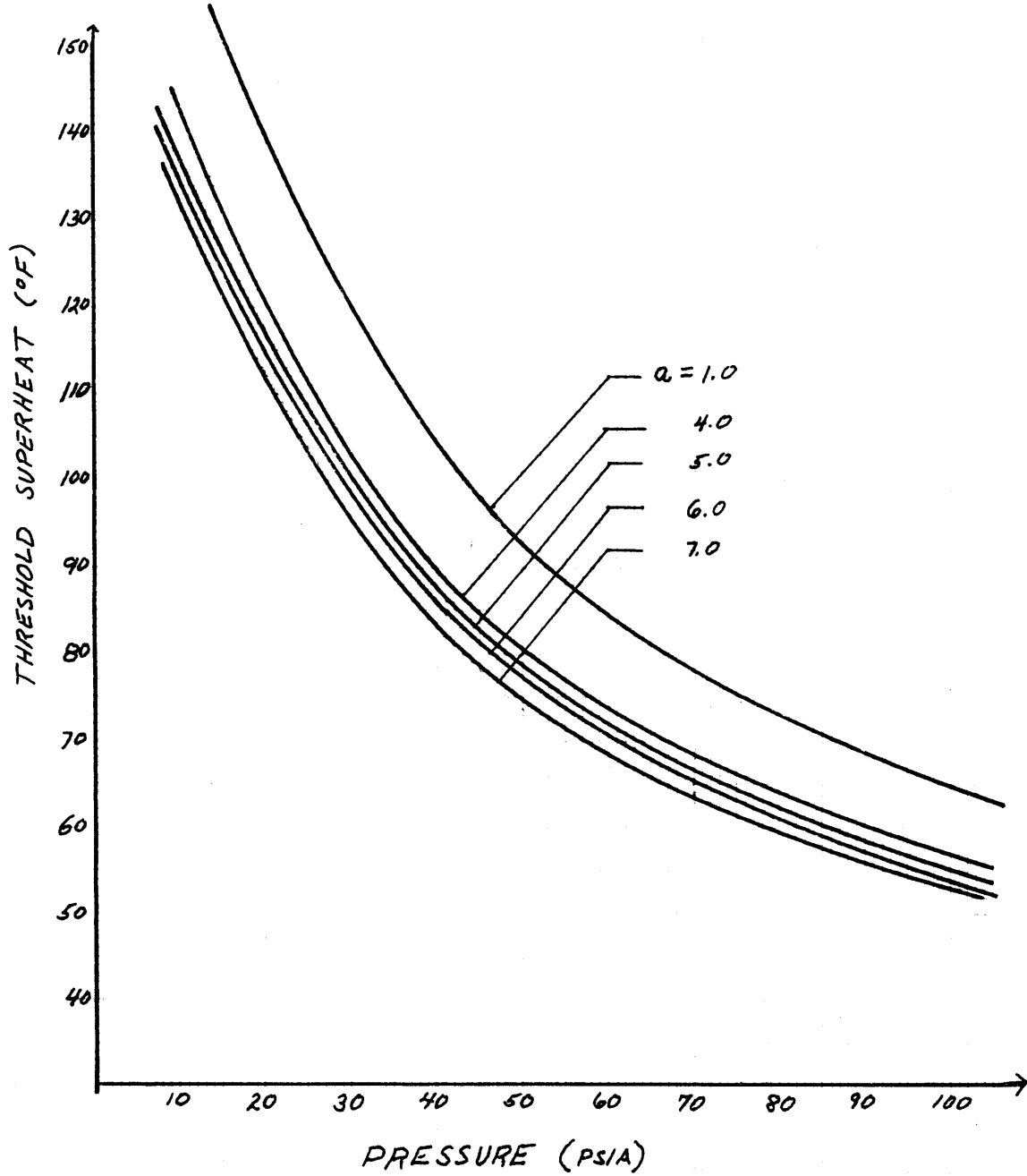


FIG. 5.9

FISSION FRAGMENTS
IN
NITROMETHANE

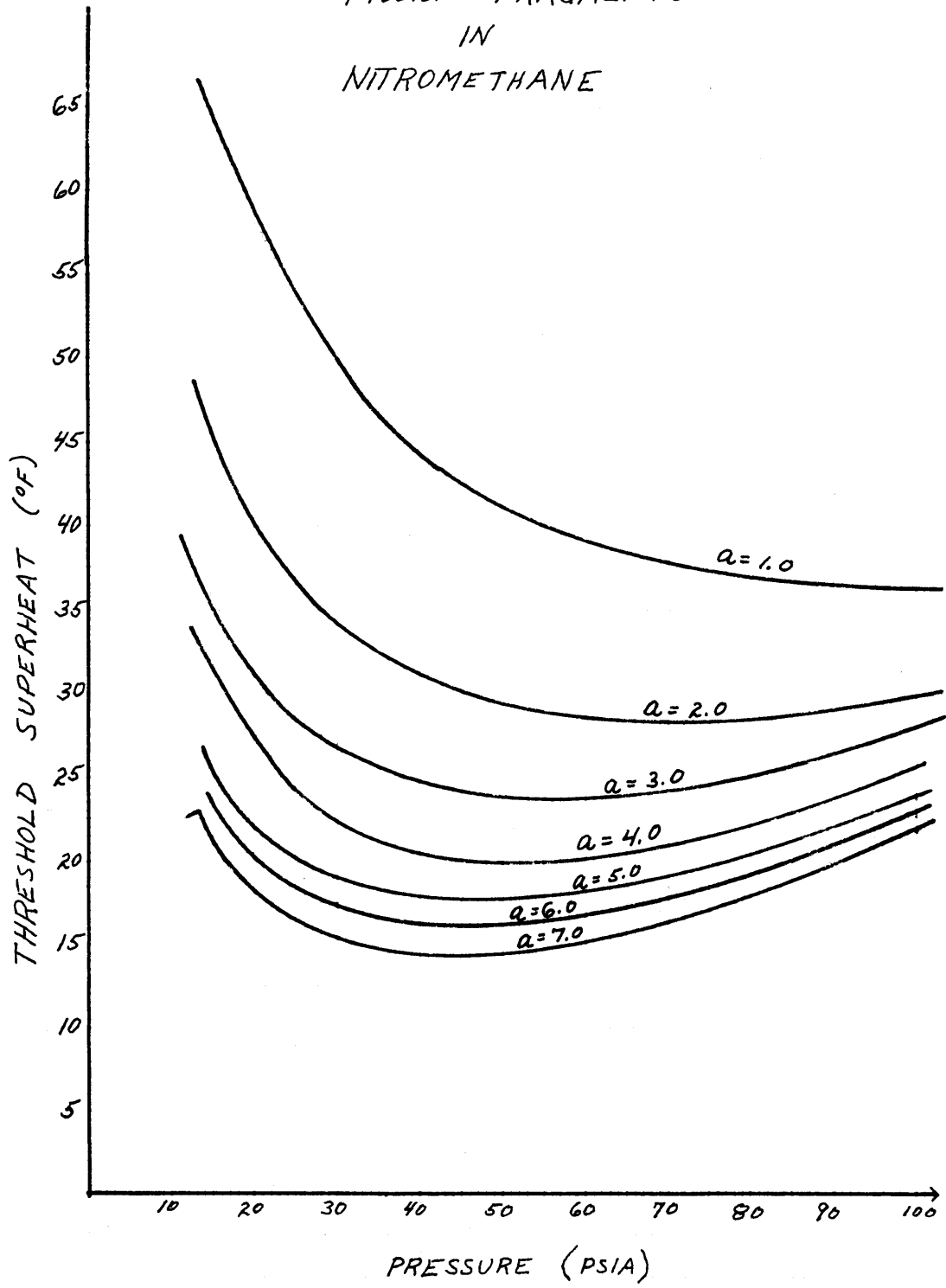


FIG. 5, 10

5.2 Experimental Results

Experimental results were obtained for fission fragments in water and propylene glycol.

For water, fission fragment data was obtained at four pressures: 14.7psia, 32.7psia, 53.7psia, and 74.2psia . These were the same pressures as were tested by Tso(6), since one of the objectives of this work was to attempt to confirm the results obtained by Tso for the fission fragment case.

The results obtained in this work are shown on FIG.5.11. These results and the results obtained by Tso are listed together in TABLE 5.1, shown below.

TABLE 5.1

<u>PRESSURE</u> (psia)	<u>AMOUNT SUPERHEAT (°F)</u>	
	TSO (6)	OBERLE
14.7	63.5 ± 2	62.4 ± 2.5
32.7	49.3 ± 3	48.5 ± 2.0
53.7	38.7 ± 2.5	39.2 ± 4.1
74.2	34.2 ± 2.4	33.3 ± 2.*

As is seen above, the results obtained in this work agree quite well with those obtained by Tso (6).

FISSION FRAGMENTS IN WATER
EXPERIMENTAL RESULTS

OBERLE: 

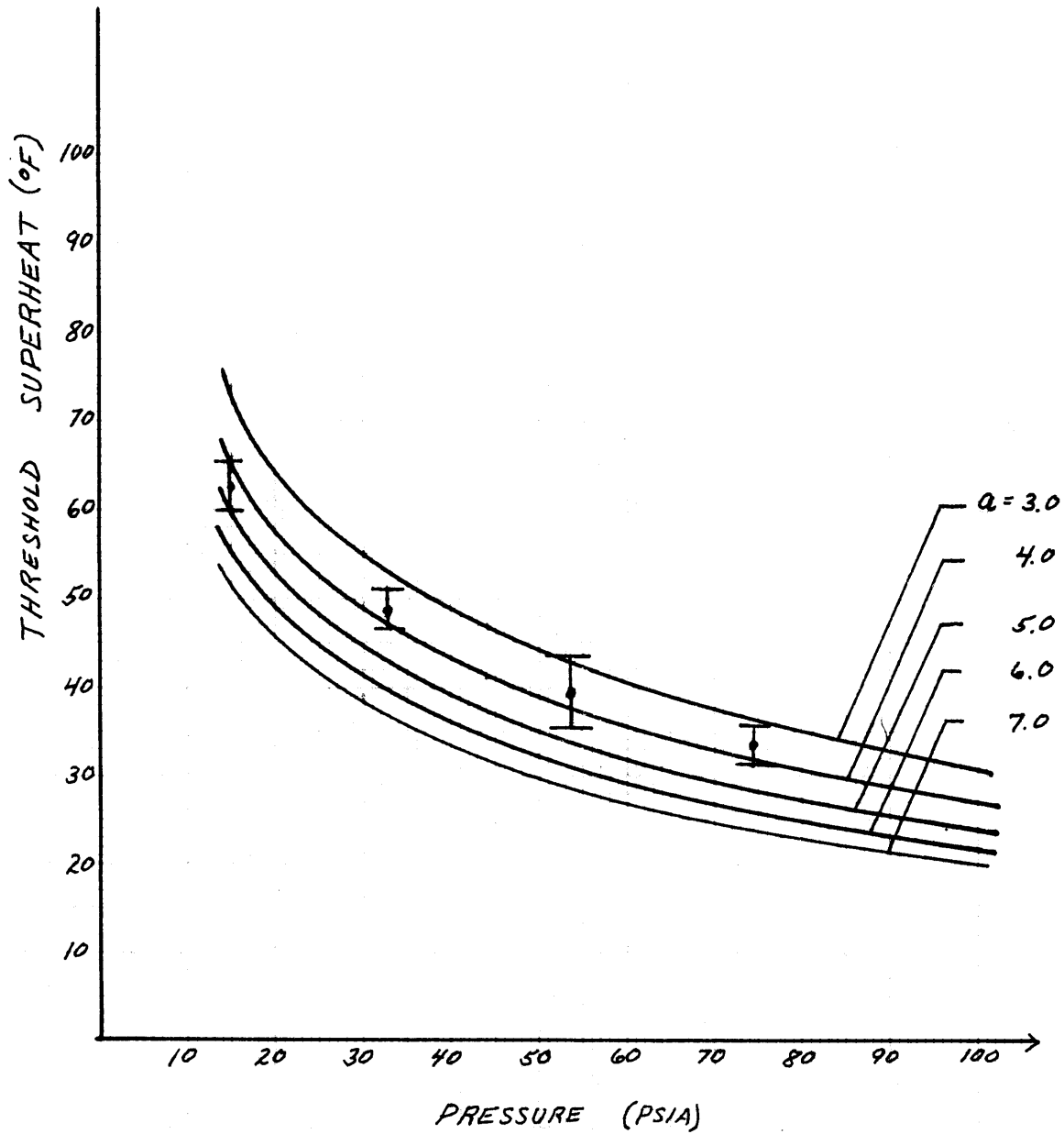


FIG. 5.11

For the case of fast neutrons , only one data point was obtained. This was for the case of fast neutrons in water at 55 psia. A large number of experimental runs were required to obtain one good result for this case. This was due mainly to the fact that this data was at high temperatures , and the convection generator was not very effective in keeping the bubble centered. Therefore, due to the difficult and time consuming experimentation involved, further work was not done with fast neutrons, since work was still to be done with organic liquids.

The result obtained for the single fast neutron result is shown in TABLE 5.2, along with the results of Tso (6) at this same pressure.

TABLE 5.2

	PRESSURE psia	AMOUNT SUPERHEAT (°F)	TEMPERATURE RAMP (°F/min)
OBERLE	55	105.0	2.0
TSO(6)	55	102.4	1.6
"	55	105.9	1.35

Bell (5) and Tso (6) also encountered considerable difficulties with the fast neutrons in water. Tso , ((6) pg. 68) has mentioned the difficulties and reliability of their work.

The experimental data obtained for propylene glycol exposed to fission fragments is shown in FIG.5.12.

The superheat data was obtained at four pressures: 14.7psia, 20psia, 40psia, 60psia.

Considerable difficulty was encountered for the higher pressure (40psia and 60 psia) since high temperatures (around 500°F) were required, and the convection generator was not able to keep the bubble centered. Due to the convection generator problem, more than one bubble was placed into the test chamber for each experimental run, so that if one or more bubbles drifted out of sight, there would, it was hoped, still remain at least one test bubble in sight. This was not always the case, since very often all of the test bubbles drifted out of sight. There were not as many good experimental runs for these pressures as there were for the two lower pressures studied. Due to this fact, and due to the presence and movement of a large number of test bubbles per experimental run, the data obtained at these higher pressures is not considered to be as accurate as that for the lower pressures.

5.3 Sensitivity Study of Superheat Data

The minimum superheat conditions are especially sensitive to the surface tension of the fluid and to the energy deposition of the charged particle. It was

FISSION FRAGMENTS IN
PROPYLENE GLYCOL
EXPERIMENTAL RESULTS

OBERLE: 

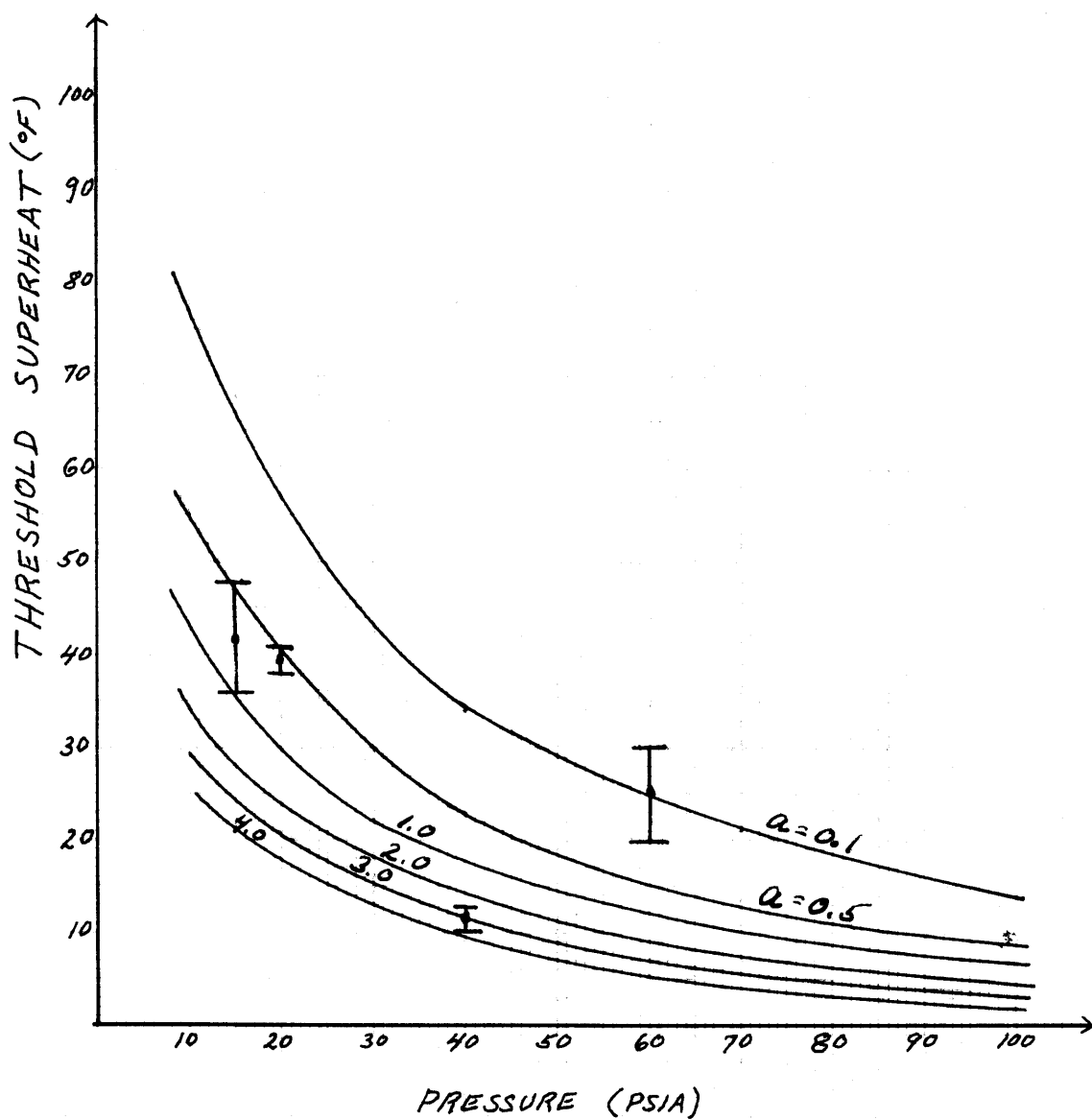


FIG. 5.12

reported by Connolly (33) that variations in these two factors significantly changed the analytical results of his group's work.

Therefore, a sensitivity study was made for water and propylene glycol exposed to fission fragments.

For the case of water, a $\pm 7\%$ variation in the surface tension was studied. The result on the minimum superheat is shown in FIG.5.13 .

A 20% variation in the mean charge of the radiation particle was considered. (The mean charge is the most sensitive factor in the energy deposition calculation. And, as suggested by Bell (5), a 20% variation is conceivable.) The effect of this large uncertainty is shown in FIG.5.14 .

It was seen that a positive uncertainty in the surface tension increased the minimum superheat, while a negative uncertainty decreased the minimum superheat. In the case of the mean charge a positive uncertainty decreased the mean superheat while a negative uncertainty increased it. Therefore, when these two uncertainties were combined to obtain a maximum uncertainty in the minimum superheat, they were combined in the following manner:

maximum positive uncertainty--- +7% in surface tension
-20% in mean charge

maximum negative uncertainty-- -7% in surface tension
+20% in mean charge

The result of the maximum uncertainties are shown in FIG.5.15 .

FISSION FRAGMENTS IN WATER

 $\pm 7\%$ UNCERTAINTY IN SURFACE TENSION

I OBERLE DATA

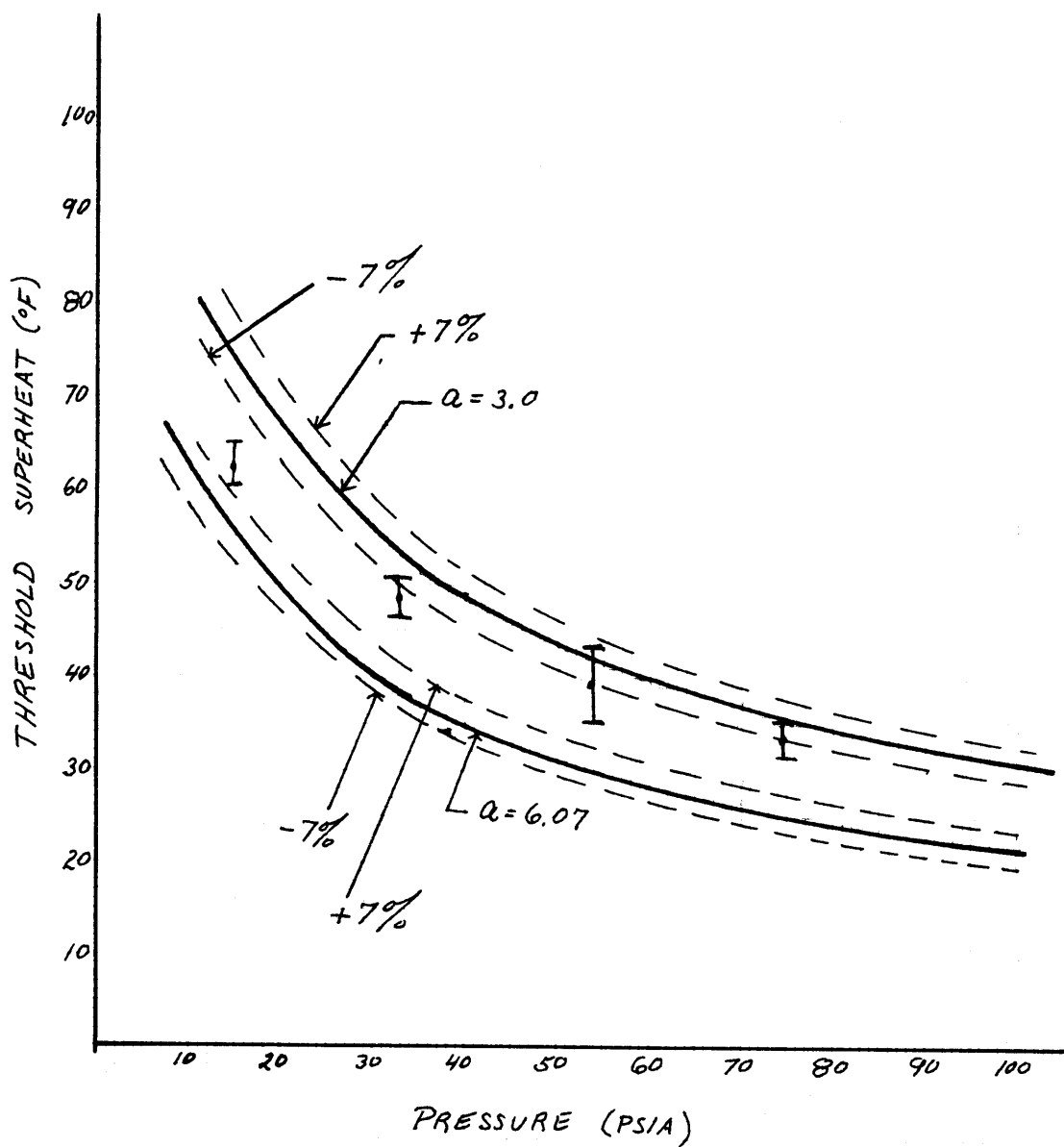


FIG. 5.13

FISSION FRAGMENTS IN WATER

 $\pm 20\%$ UNCERTAINTY IN
MEAN CHARGE

I OBERLE DATA

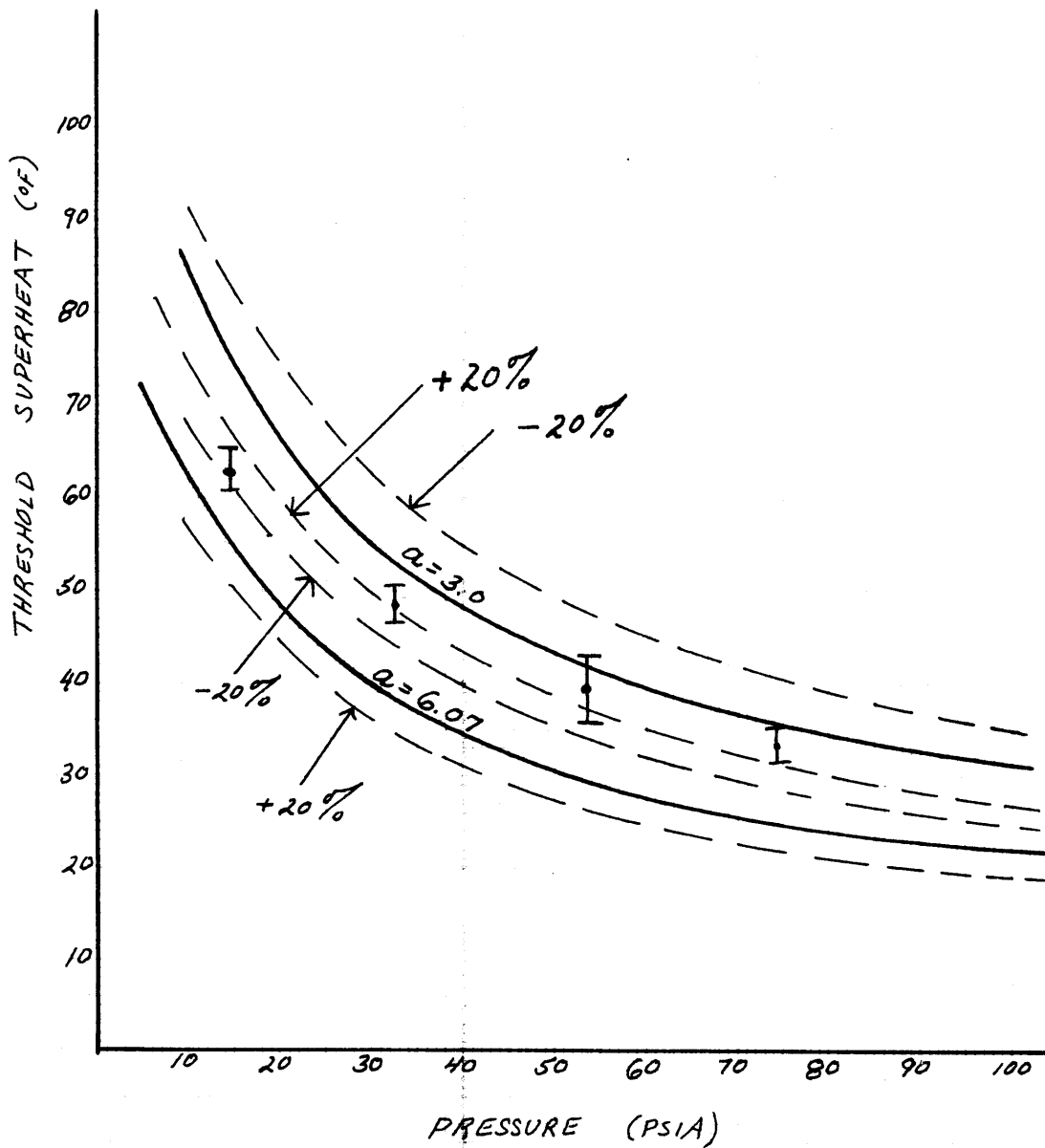


FIG. 5.14

FISSION FRAGMENTS IN WATER

COMBINED UNCERTAINTIES

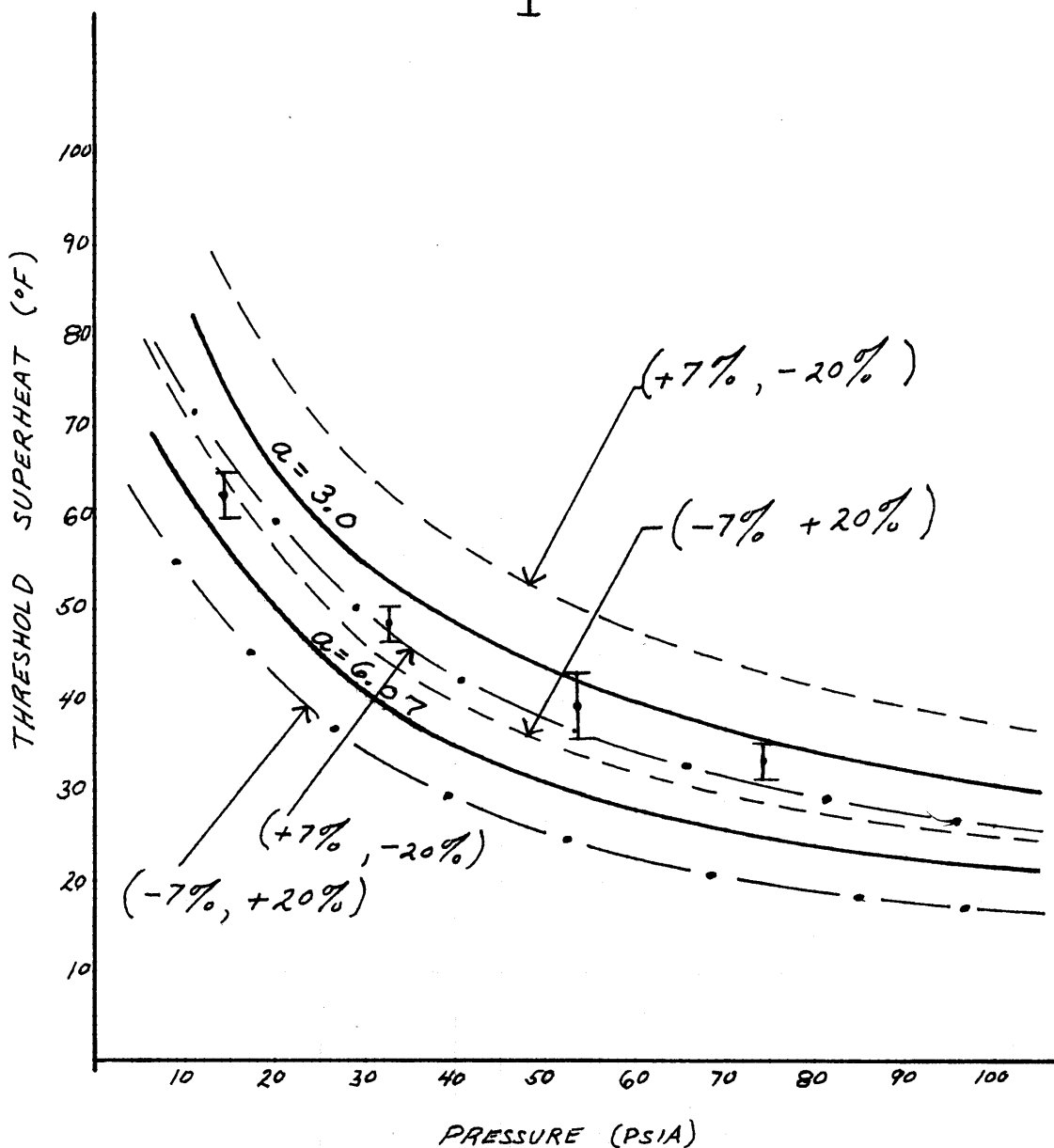
+7% σ +, -20% MEAN CHARGE-7% σ + +20% MEAN CHARGE
 OBERLE DATA


FIG 5.15

This same type of sensitivity study was made for the case of propylene glycol. The percent variations used were:

maximum uncertainties in surface tension-- $\pm 5\%$

maximum uncertainties in mean charge -- $\pm 20\%$

The directional affect of each uncertainty is the same as for water. The results of these studies are shown in FIG.5.16, FIG.5.17, FIG.5.18 .

5.4 Comparison with other results

Experimental results have been obtained by other researchers.

Deitrich (3) has obtained data for the case of fission products in water. His results are shown in FIG.5.19, along with the results from this work.

El-Nagdy (4) has obtained experimental data for Benzene and Acetone exposed to fast neutrons at atmospheric pressure. The fast neutrons were at different energies than those from the Pu-Be source used in this work. His experimental data is shown with the analytical results from the energy balance method of Bell(5). (Adjustments had been made to conform with the neutron energies used by El-Nagdy.) The results are shown in FIG.5.20 and FIG.5.21. (The 14.1 Mev neutrons correspond to an EPKA of 4.0 , and the 2.45 Mev neutrons correspond to an EPKA of 0.695 Mev.

FISSION FRAGMENTS IN
PROPYLENE GLYCOL

$\pm 5\%$ UNCERTAINTY IN
SURFACE TENSION

I EXPERIMENTAL DATA (OBERLE)

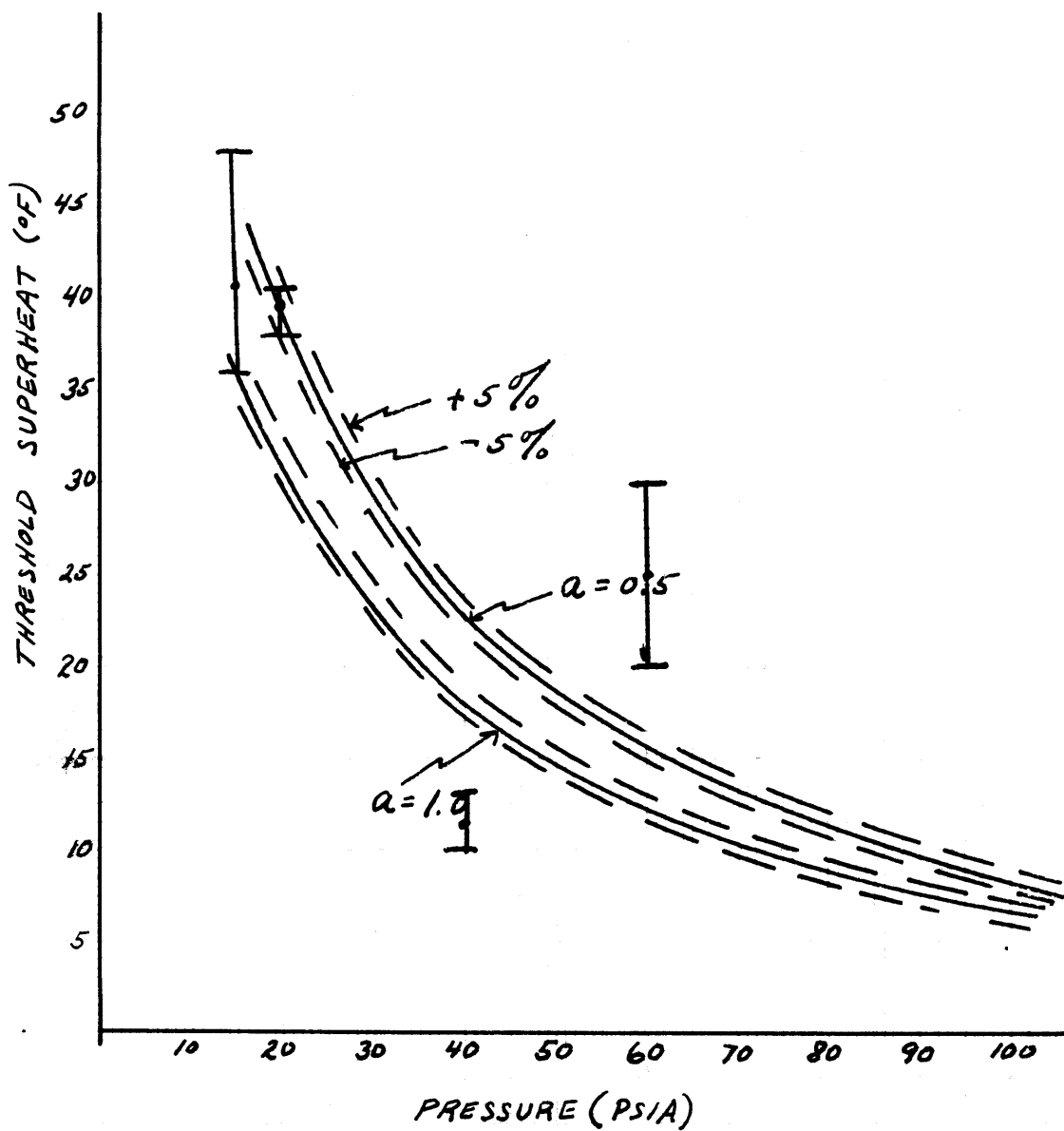


FIG. 5.16

FISSION FRAGMENTS IN
PROPYLENE GLYCOL

$\pm 20\%$ UNCERTAINTY IN
MEAN CHARGE

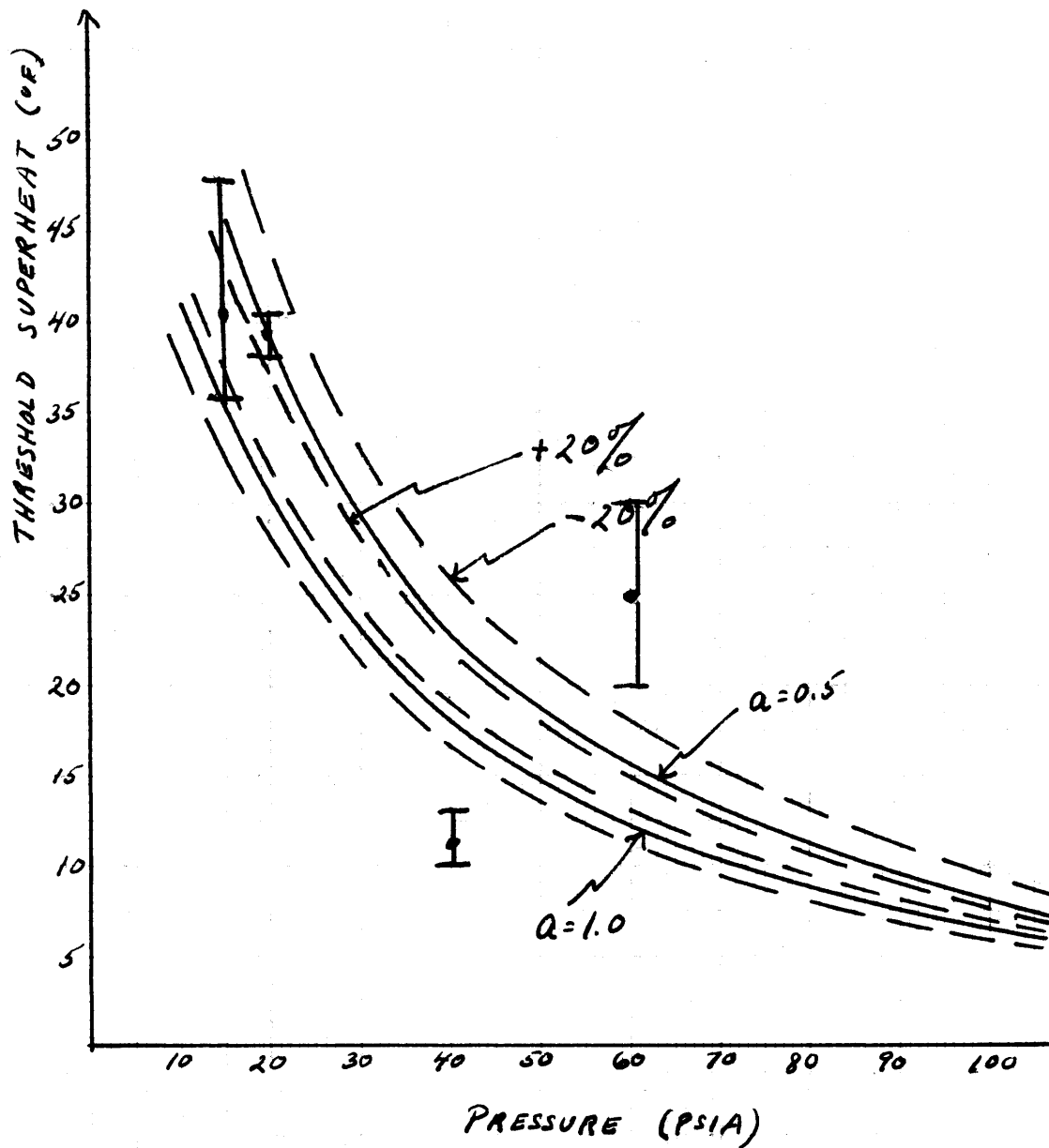


FIG. 5.17

FISSION FRAGMENTS IN PROPYLENE GLYCOL

COMBINED UNCERTAINTIES

+5% , -20%

-5% , +20%

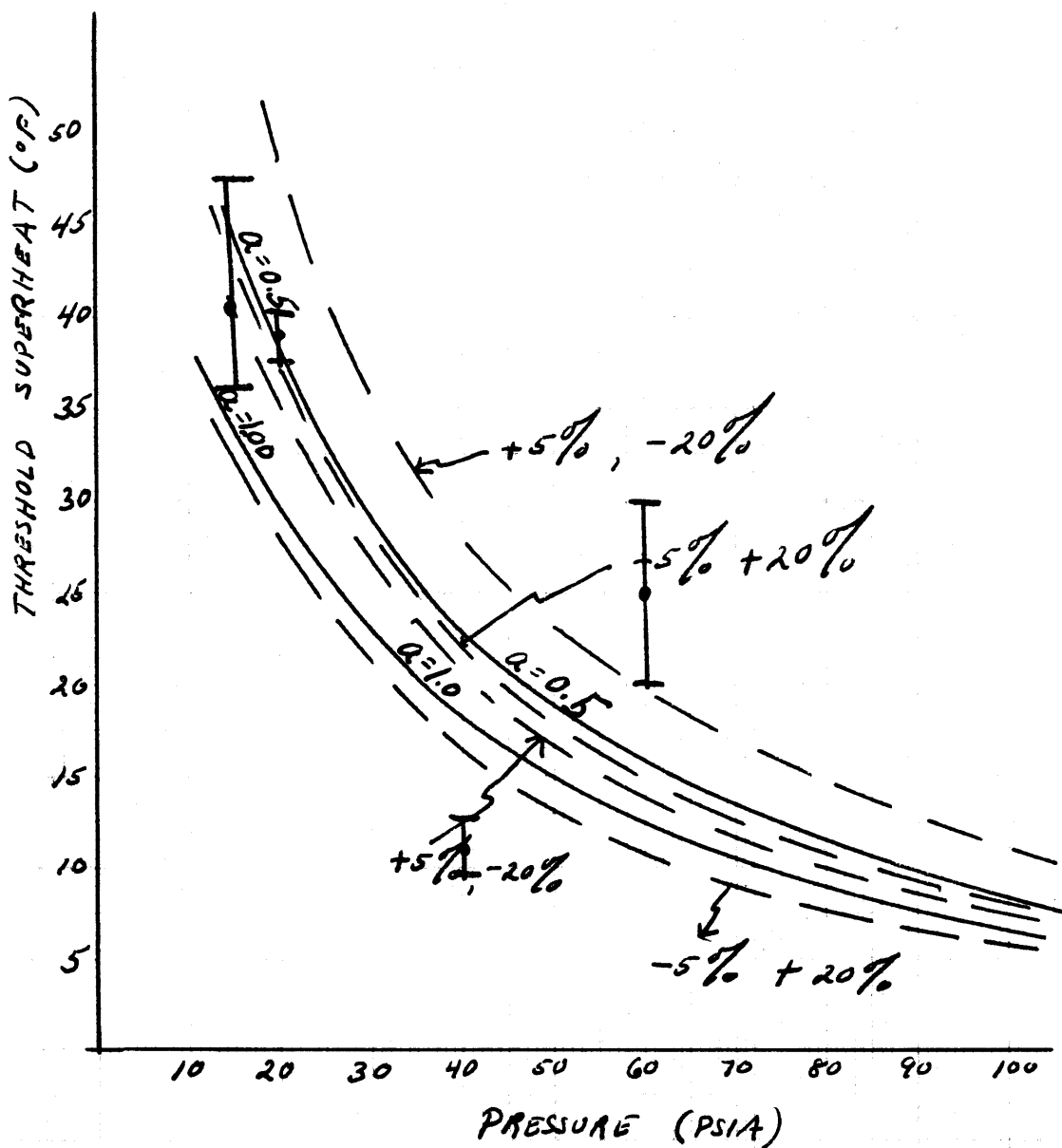


FIG 5.18

FISSION FRAGMENTS IN WATER

■ DEITRICH

I OBERLE

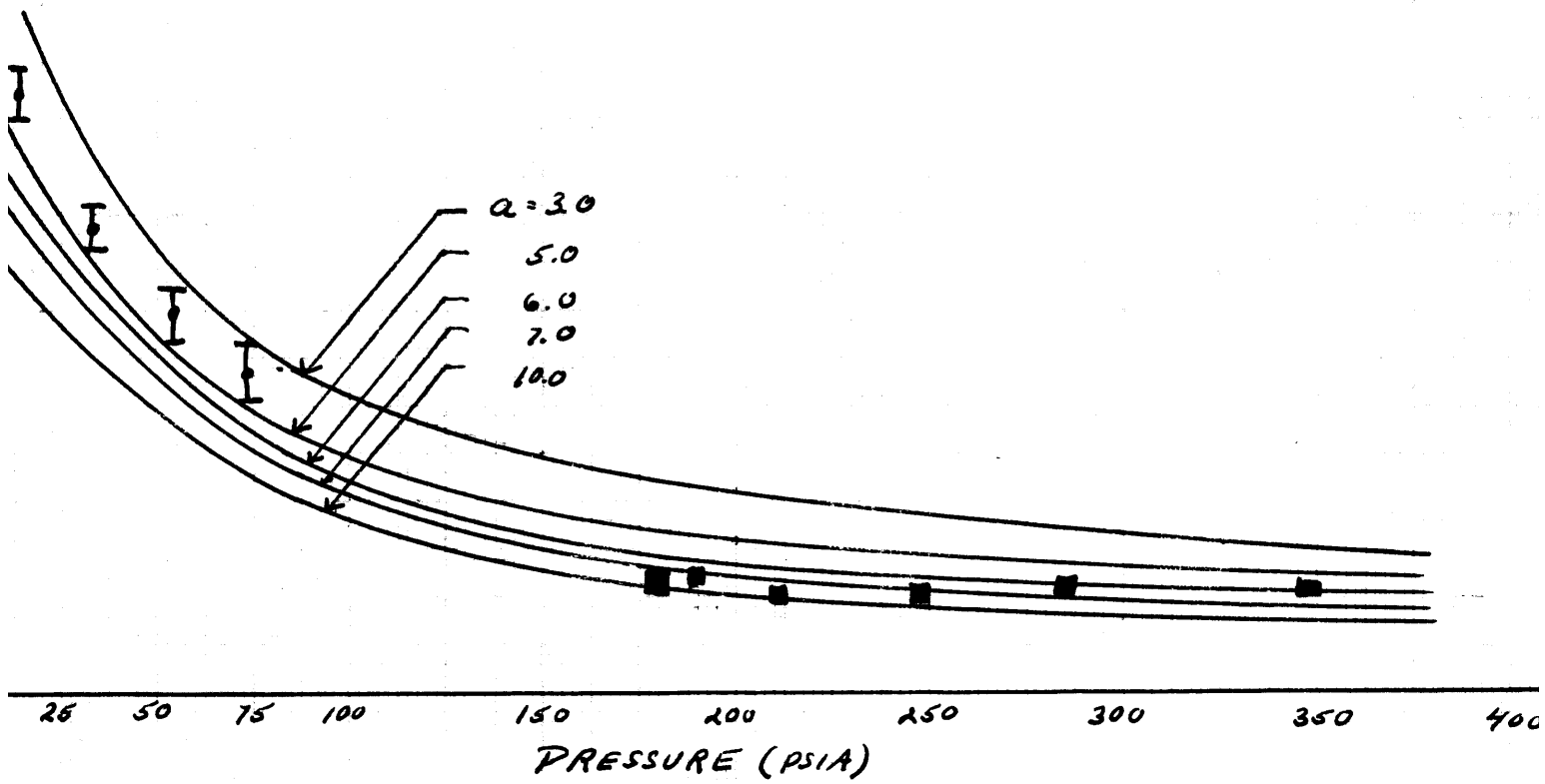


FIG. 5.19

FAST NEUTRONS IN BENZENE

14.1 MeV NEUTRONS ———
 2.45 MeV NEUTRONS - - - -
 EL-NAGDY: 14.1 MeV □
 2.45 MeV △

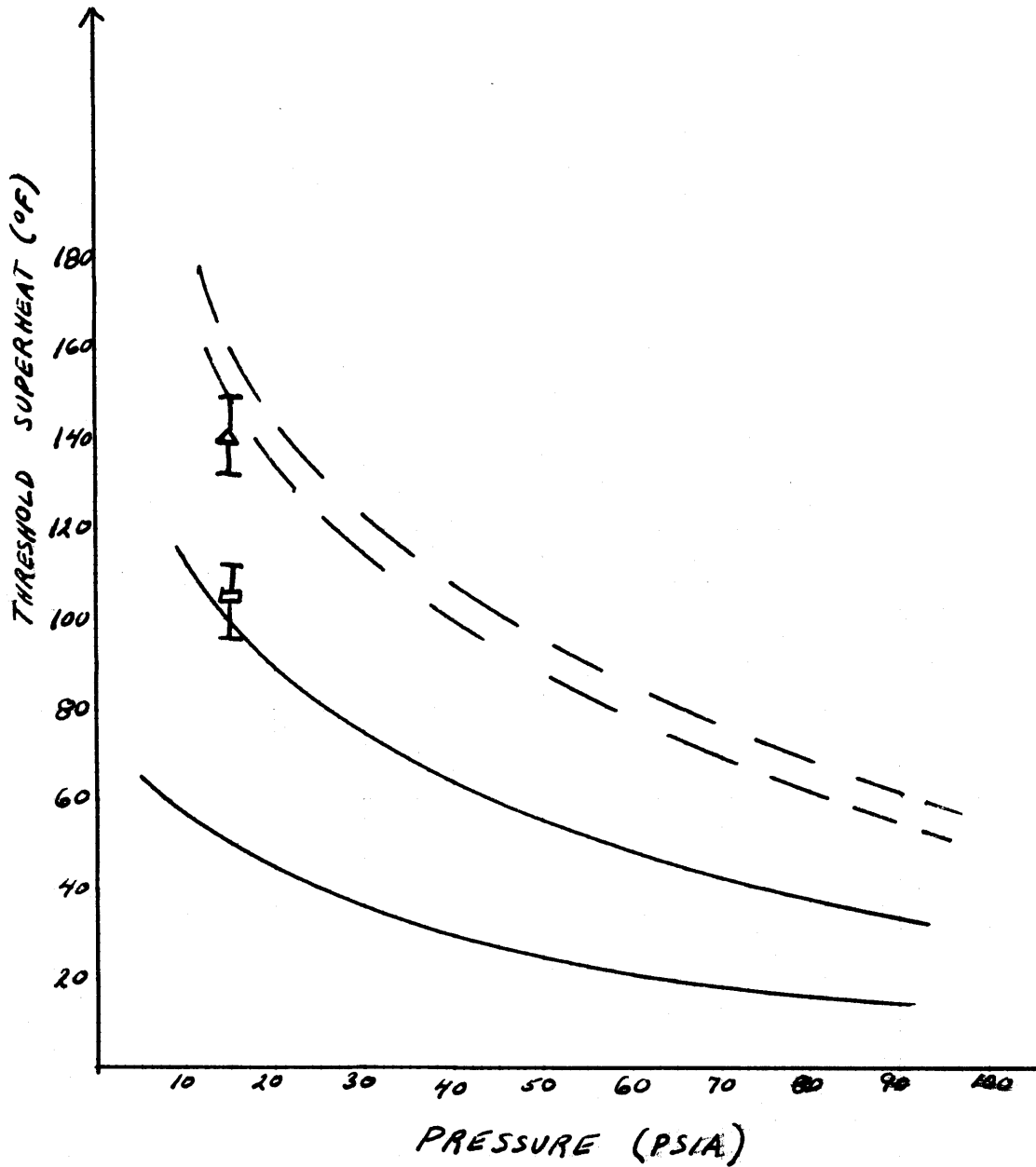


FIG. 5.20

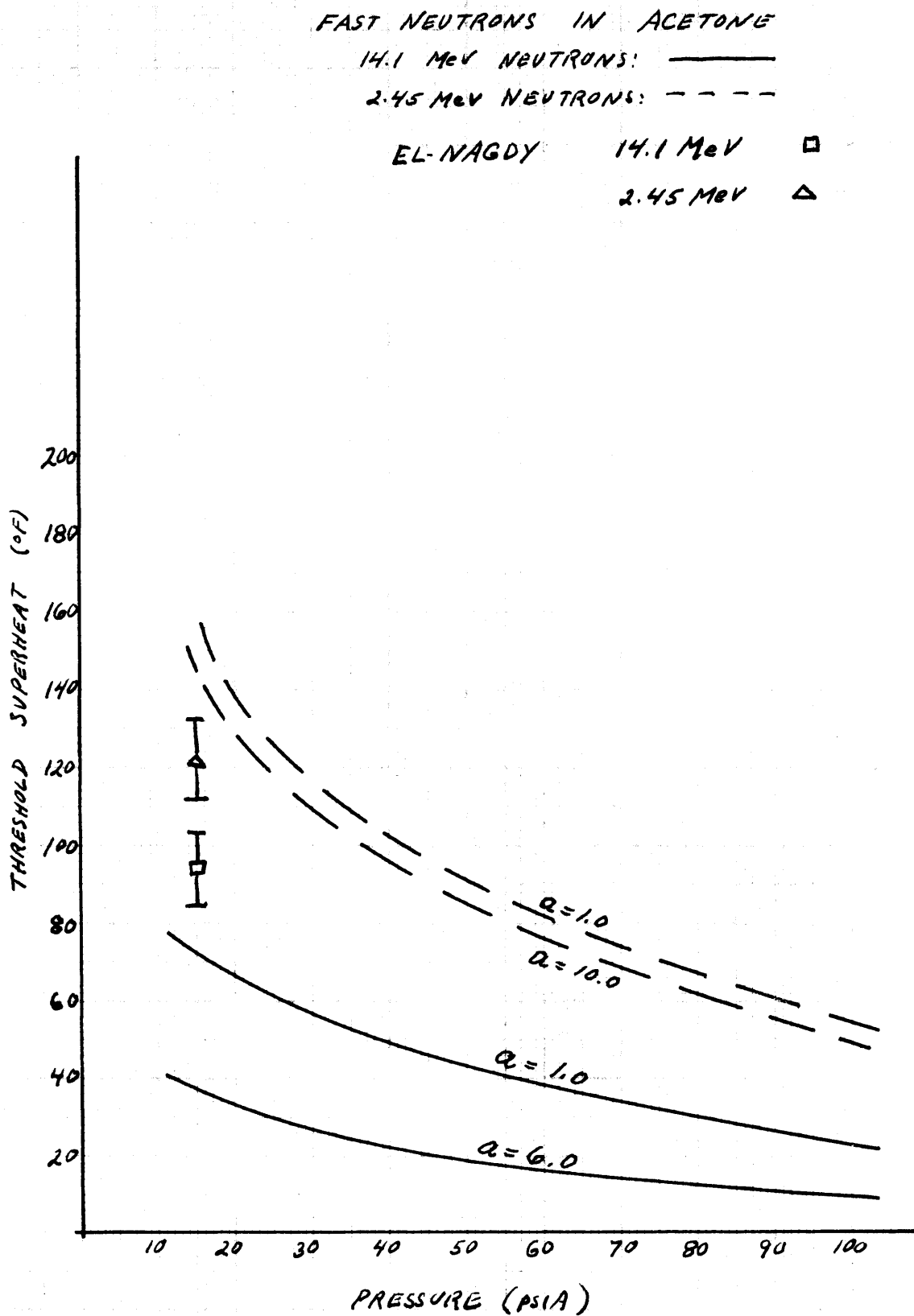


FIG. 5.21

Chapter 6

Conclusions and Recommendations

6.1 Conclusions

The experimental results for fission fragments in water have been shown in FIG.5.11. These results can be considered very reliable, since the nucleation event was very noticeable, and, more significantly, this data was very close to the data of Tso(6), who also did experimental work under these conditions. It is therefore reasonable to conclude that these minimum superheat results for water exposed to fission fragments, can be considered very accurate and reliable.

These experimental results fall between "a" values of approximately 3.5 and 4.5. In any case, the "a" value is less than 6.07, as predicted by Bell (5).

The experimental results of Deitrich(3) have been plotted over calculated "a" curves. (FIG.5.19) These results varied from an "a" value of 10.0, to an "a" value of 5.0. Deitrich's data also seems to be fairly reliable, with the uncertainties in his superheat data of ± 0.5 F .

Therefore, the experimental evidence seems to point to the conclusion that the "constant a " theory of Bell (5) does not hold for the case of fission fragments in water.

There exists, of course, the possibility that there is some error or uncertainty in the analytical calculations for the constant "a" curves.

A sensitivity study was made on the parameters which have the greatest affect on the superheat limits, and thus on the "a" curves. A $\pm 7\%$ variation in the surface tension, and a $\pm 20\%$ variation in the mean charge was considered for water. (FIG.5.13 and FIG.5.14) These two uncertainties were first considered separately, and then jointly (FIG.5.15). In either case, the experimental data did not fall within the $a = 6.07$ band.

The same type of sensitivity study was made for propylene glycol exposed to fission fragments. The conclusions are similar to those for water. For these experiments with propylene glycol, all of the data points were below the $a = 6.07$ line. With all of the uncertainties mentioned above, there is a possibility that the data may all fall within the error band of a single "a" value. More study must be done on this before anything conclusive can be said on this. But in any case, it can be concluded that the "a" value is not 6.07 as stated by Bell (5).

The analytical results for the fast neutrons are similar to those of the fission fragments. The difference being that the fast neutrons require larger superheats.

In benzene and acetone (FIG.5.5 and FIG.5.6), the superheat curves are seen to go downward as "a" increases, and then to reverse direction and go up as "a" continues to increase. The reason for this is not understood at the present time, and further study needs to be done to explain this behavior.

6.2 Rayleigh's criteria

The constant "a" theory of Bell (5) concerned itself with the break up of a cylinder of vapor. It was assumed that the vapor cylinder contains disturbances of all wavelengths. These disturbances are held to be responsible for the break up of the cylinder.

Rayleigh (35) has developed a theory of jet instabilities which, in short, shows that there is a certain wavelength which will lead to the maximum rate of growth of the disturbance, and hence break up.

This certain wavelength has been found by Rayleigh for two extreme cases. In the first case, a vapor jet is surrounded by a liquid; in the second case, a liquid jet is surrounded by a vapor . A schematic of these two cases is shown in FIG.6.1 .

For the first case, that of a vapor surrounded by liquid, Rayleigh found this certain wavelength to be

$$\lambda = (12.96)r_c \quad (6.1)$$

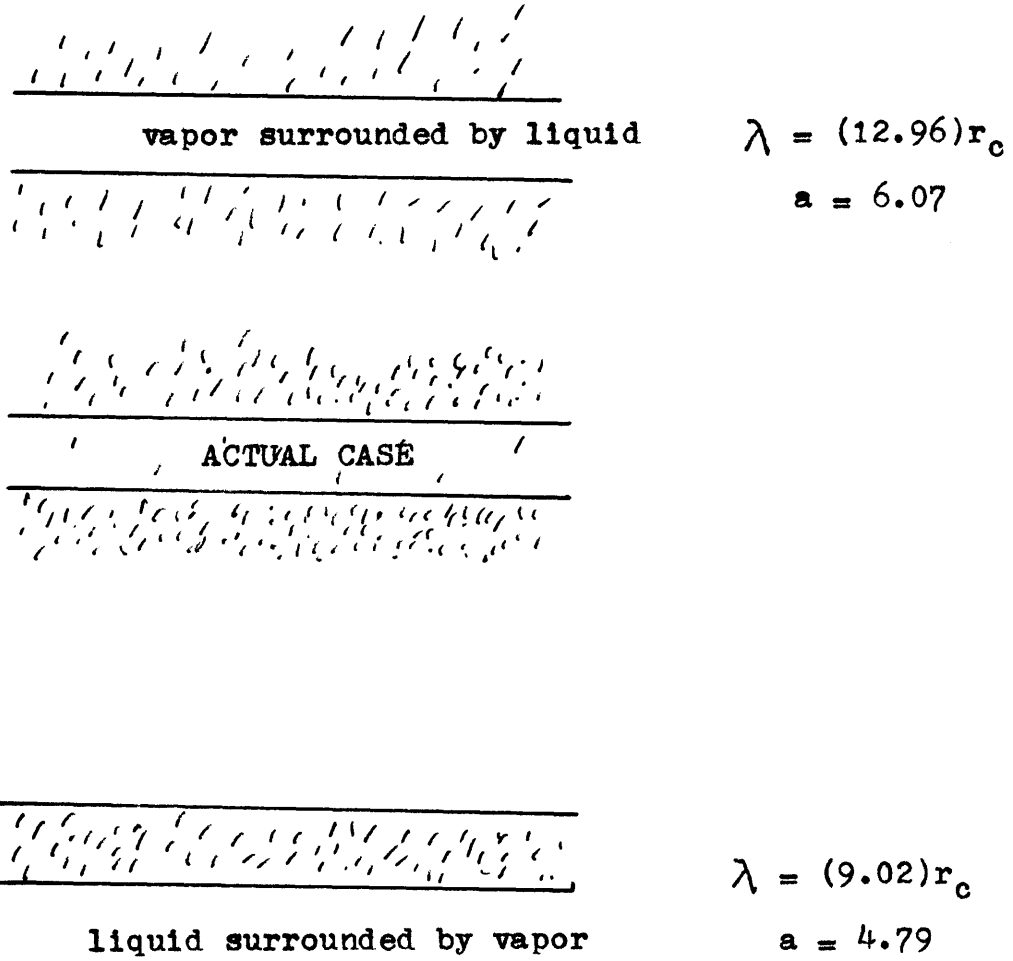


FIG 6.1

where λ is the wavelength

r_c is the radius of the cylinder.

For the case of a liquid jet surrounded by vapor, the wavelength is given by:

$$\lambda = (9.02)r_c$$

This wavelength is related to Bell's(5) work through the relationship

$$\lambda = L = ar^*$$

where r^* is the critical radius of the embryo.

a = Bell's parameter

Beginning with the wavelength for the case of a vapor jet surrounded by a liquid, Bell ((5) pg 200) was able to calculate that the "a" parameter for this case would be equal to 6.07 .

Similar calculations show that for the case of a liquid surrounded by a vapor, with $\lambda = (9.02)r_c$, the resulting "a" value is 4.79 .

The actual case encountered in the radiation-induced nucleation studies, is believed to be somewhere between these two cases. That is, the "a" value should lie between 4.79 and 6.07 . (It is probably closer to 6.07, since the jet is more vapor than liquid.)

6.3 Recommendations

Before undertaking any further experimental work, a number of changes are recommended in the experimental apparatus.

The major problem encountered was that of the bubble drifting out of view. The present method of keeping the bubble centered is by means of the convection generator which was discussed in chapter 3. This convection generator, however, was not able to keep the test bubble centered at all times. It proved exceptionally difficult to keep the bubble centered at high temperatures, and many experimental runs were terminated prematurely due to the test bubble drifting out of view.

A new convection generator is recommended. This should have a larger flow-rate capacity and a coolant inlet temperature as low as possible.

Another recommended modification would be a separate recorder for each thermocouple. This would eliminate the switching back and forth on one chart recorder.

It is seriously recommended that a new chamber be constructed. This new chamber should include a larger observation window, preferably one in which the entire test chamber is visible. It should also include a bright and variable intensity light source, either

inside or outside of the chamber. But it must supply direct illumination of the bubble.

A chamber similar to the one used by T.J. Connolly (31) seems very promising. A sketch of such a type is given in FIG.6.1a . An alternate lighting scheme is shown in FIG.6.1b. Both of these cases must include a convection generator.

The important factors in any new chamber are:

- 1.) The window to observe the bubble should be as large as possible.
- 2.) The light source should be as near as possible to the bubble.
- 3.) A method to keep the bubble in position, such as the convection generator.

Another improvement which can be made, is the degassing of the test liquid. El-Nagdy(4) and Connolly (33) describe a simple method of accomplishing this.

Since it is difficult to find supporting and cover fluids for many test liquids of interest, the concept of a density gradient suspension fluid should be investigated as a possible solution to this problem.

Further experimental work should be done with more organic fluids, preferably with those for which analytical results have already been obtained.

Different radiation sources and types can be tested, such as gamma rays, or alpha particles.

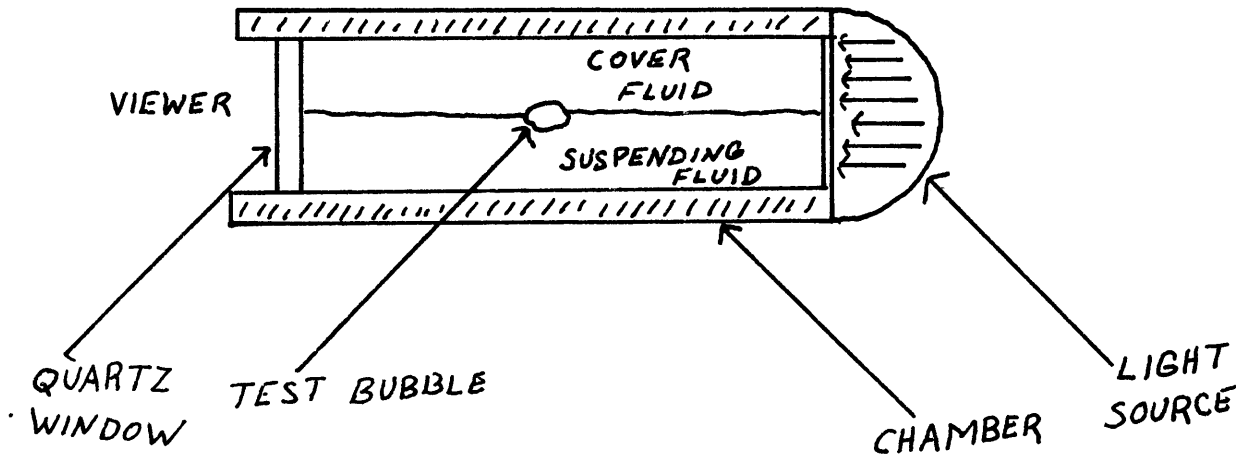


FIG. 6.2a

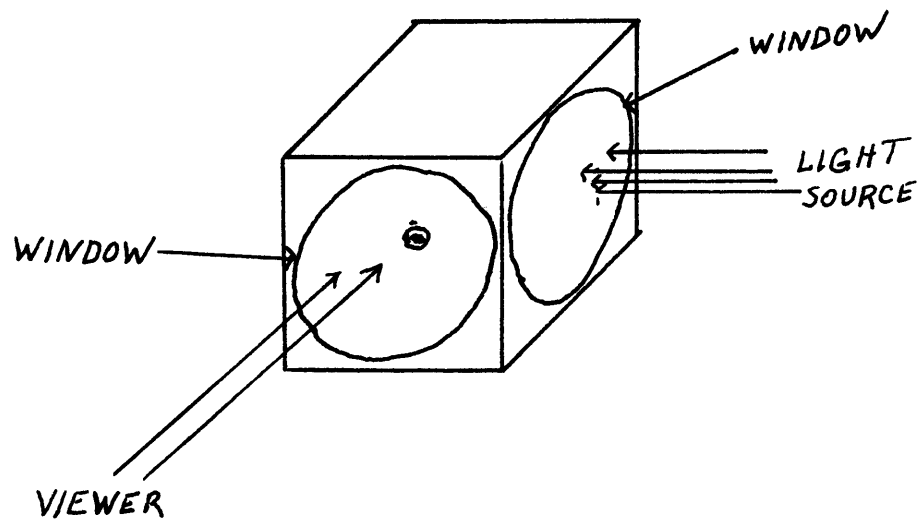


FIG. 6.2b

Theoretical work still remains to be done.

It does not seem that the "constant a " theory holds, at least for the cases in which experimental data was obtained. In any case, it has been shown that even if there is a "constant a " it is not equal to 6.07, but would be somewhat lower.

A possible area of study which might aid in understanding this phenomena, is in the area of the instability and break up of vapor and liquid cylinders, such as the discussion given by Rayleigh.

Appendix A

Physical Properties

A.1 Introduction

Five physical properties of the test liquid are required for the superheat calculations. These are:

- 1.) Vapor Pressure
- 2.) Liquid density
- 3.) Vapor density
- 4.) Surface tension
- 5.) Heat of Vaporization

The variation of these properties with temperature must also be known. A search was made to find tabulated data of these properties at various temperatures. This data was then fed into a polynomial regression computer program, which gave an equation for the physical property as a function of temperature. The equations have the following form:

$$P = a + bT + cT^2 + dT^3 + \dots \quad (\text{A.1})$$

where P = physical property

T = temperature at which the property is evaluated.

a, b, c, d, \dots are constants determined by the program.

The number of terms required depends on the particular case. The output of the computer program gives the amount of improvement for each additional term added to the polynomial. The first three terms are almost always sufficient.

For some properties a relation between the property and the temperature may be given directly. When this was the case, the equation given was used.

The remainder of this appendix will give the final equations which relate the property to the temperature, and it will also present graphs of the physical property versus the temperature over the temperature range of interest.

Each of the five physical properties have been found for each of the following liquids:

- 1.) Acetone
- 2.) Diethyl Ether
- 3.) Propylene glycol
- 4.) Nitromethane
- 5.) Methyl alcohol
- 6.) Ethyl alcohol

The properties for water and benzene have previously been reported by Bell (5) and Tso (pgs. 84-95 (6)).

The properties are listed in the following manner:

- property involved (units) , (reference source)
- temperature dependent equation
- temperature range over which the equation is valid

A.2 Physical Properties of Acetone

1.) Vapor pressure (P_v in mm Hg., T in $^{\circ}\text{C}$) (22)

$$\log (P_v) = 7.23157 - \frac{1277.03}{T + 237.23}$$

$$\text{triple point} < T < 190^{\circ}\text{C}$$

2.) Liquid density (ρ_l lbm/ft³ $T^{\circ}\text{F}$) (4)

$$\rho_l = 66.3909 - 0.36738(T) + 1.9336 \times 10^{-3} (T)^2 - 3.25478 \times 10^{-6} (T)^3$$

$$60^{\circ}\text{C} < T < 230^{\circ}\text{C}$$

3.) Vapor density (ρ_v lbm/ft³ , $T^{\circ}\text{F}$) (4)

$$\rho_v = 0.45065 - 8.2235 \times 10^{-3} (T) + 3.8308 \times 10^{-5} (T)^2$$

$$60^{\circ}\text{C} < T < 230^{\circ}\text{C}$$

4.) Surface tension (σ lbf/ft , $T^{\circ}\text{F}$) (4)

$$\sigma = 1.9457 \times 10^{-3} - 4.8055 \times 10^{-6} (T)$$

$$60^{\circ}\text{C} < T < 230^{\circ}\text{C}$$

5.) Heat of vaporization (HFG Btu/lbm , $T^{\circ}\text{F}$) (4)

$$\text{HFG} = 251.046 + 0.08274(T) - 0.0017143(T)^2$$

$$60^{\circ}\text{C} < T < 230^{\circ}\text{C}$$

The graphs of physical property vs temperature for acetone are shown in FIG. A.1 through FIG.A.5 .

VAPOR PRESSURE vs TEMPERATURE

ACETONE —————
DIETHYL ETHER - - - - -

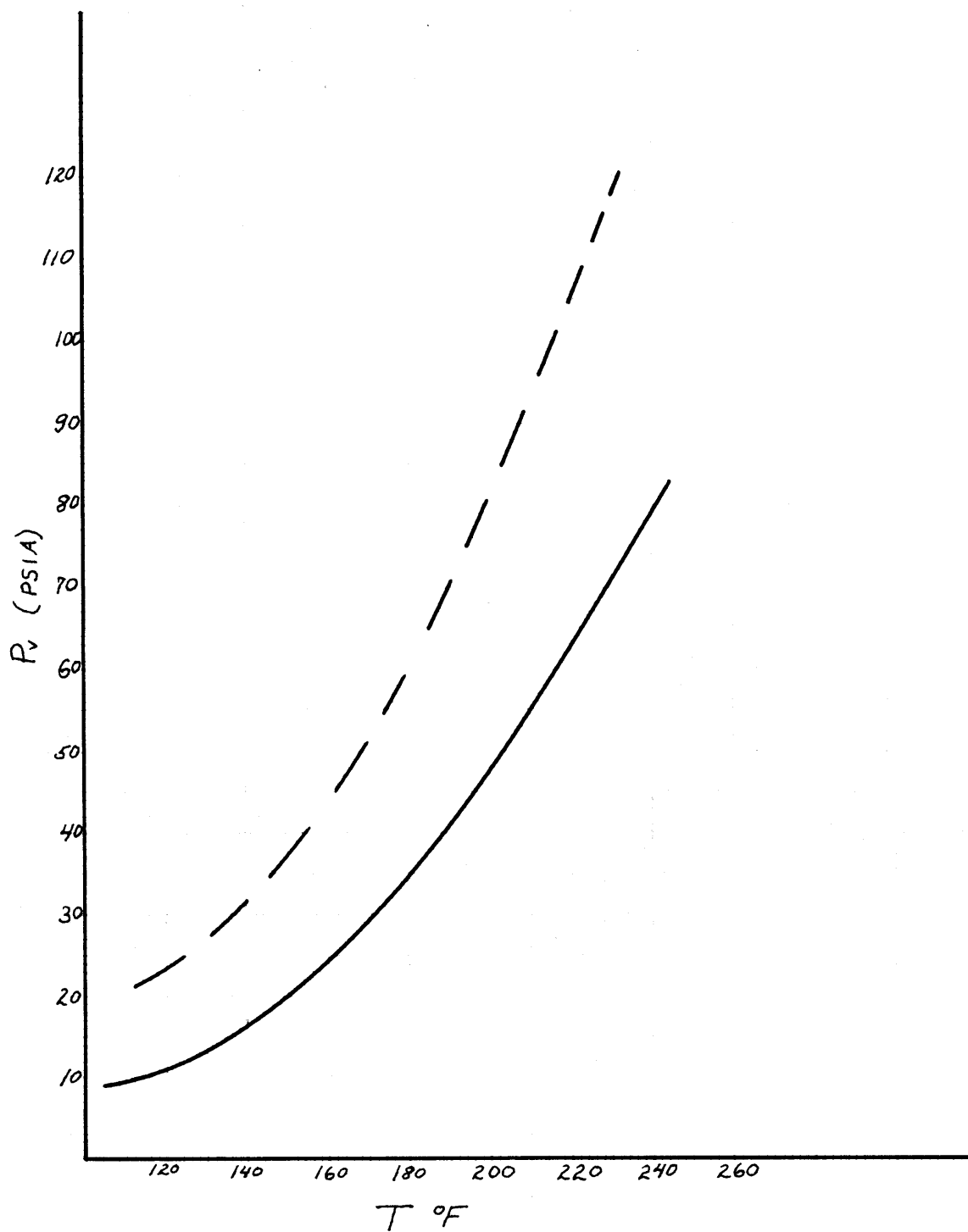


FIG. A.1

VAPOR DENSITY vs TEMPERATURE

ACETONE —————
DIETHYL ETHER - - - - -

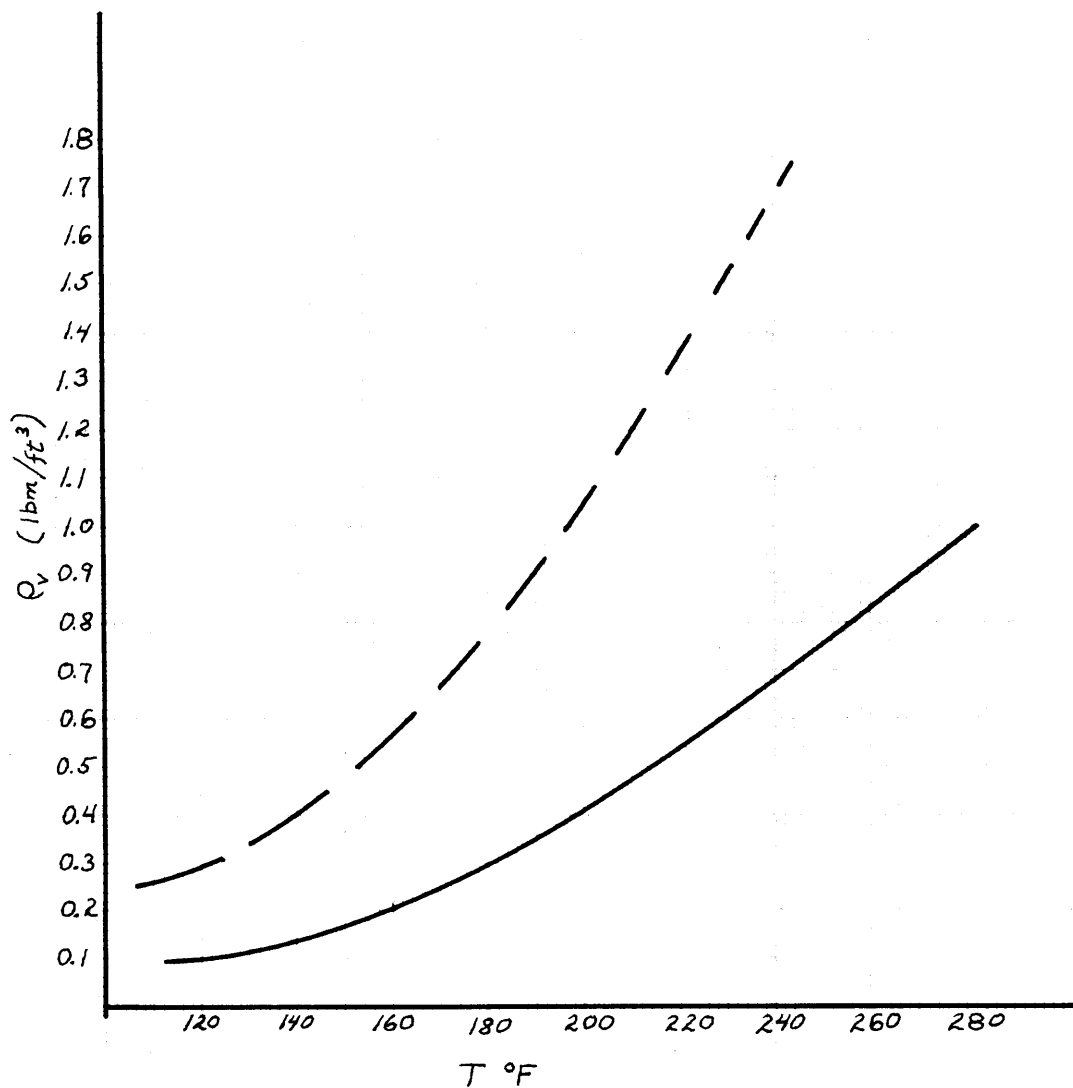


FIG. A.2

LIQUID DENSITY vs TEMPERATURE

ACETONE —————
DIETHYL ETHER - - - - -

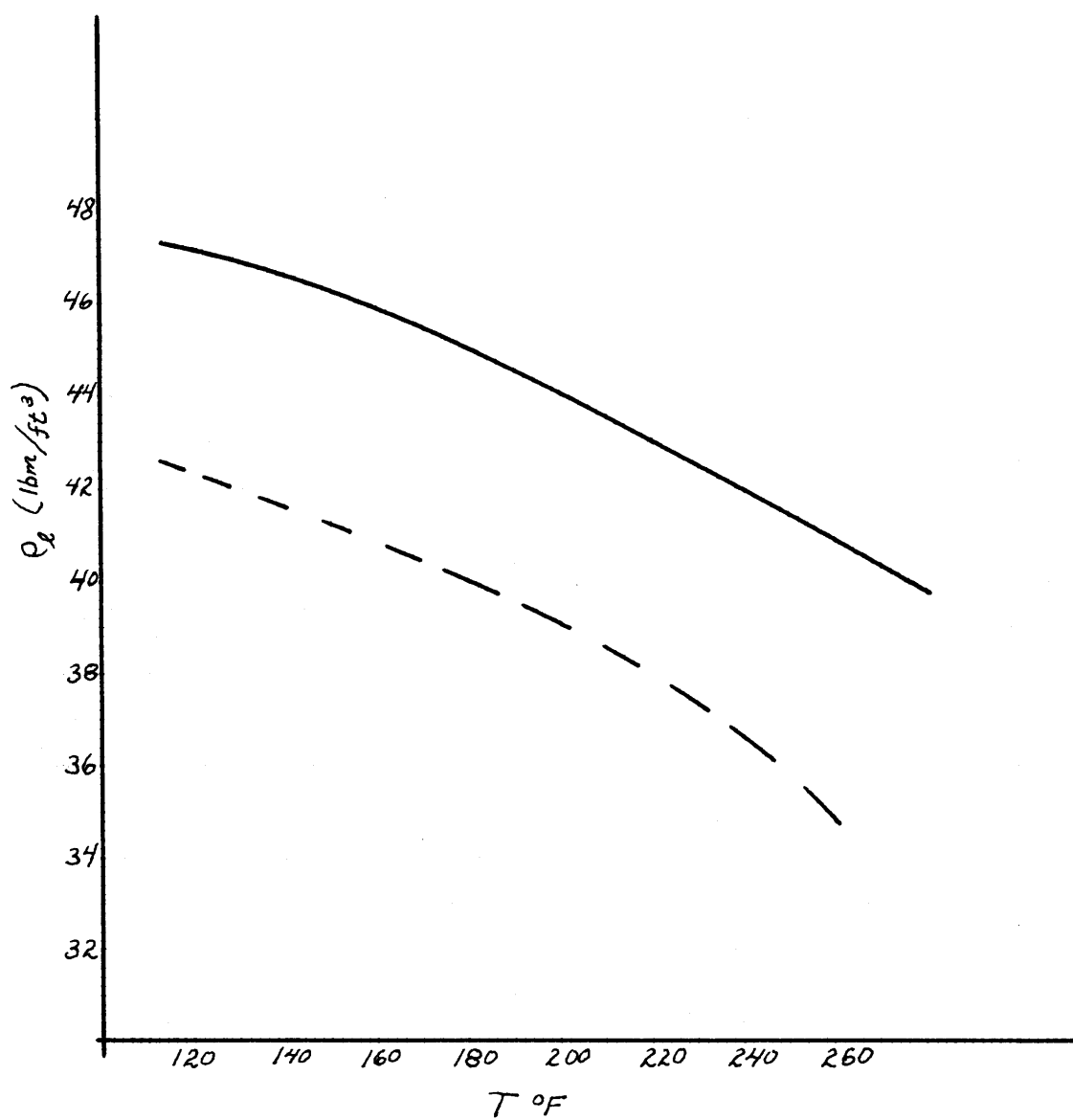


FIG. A.3

SURFACE TENSION vs TEMPERATURE

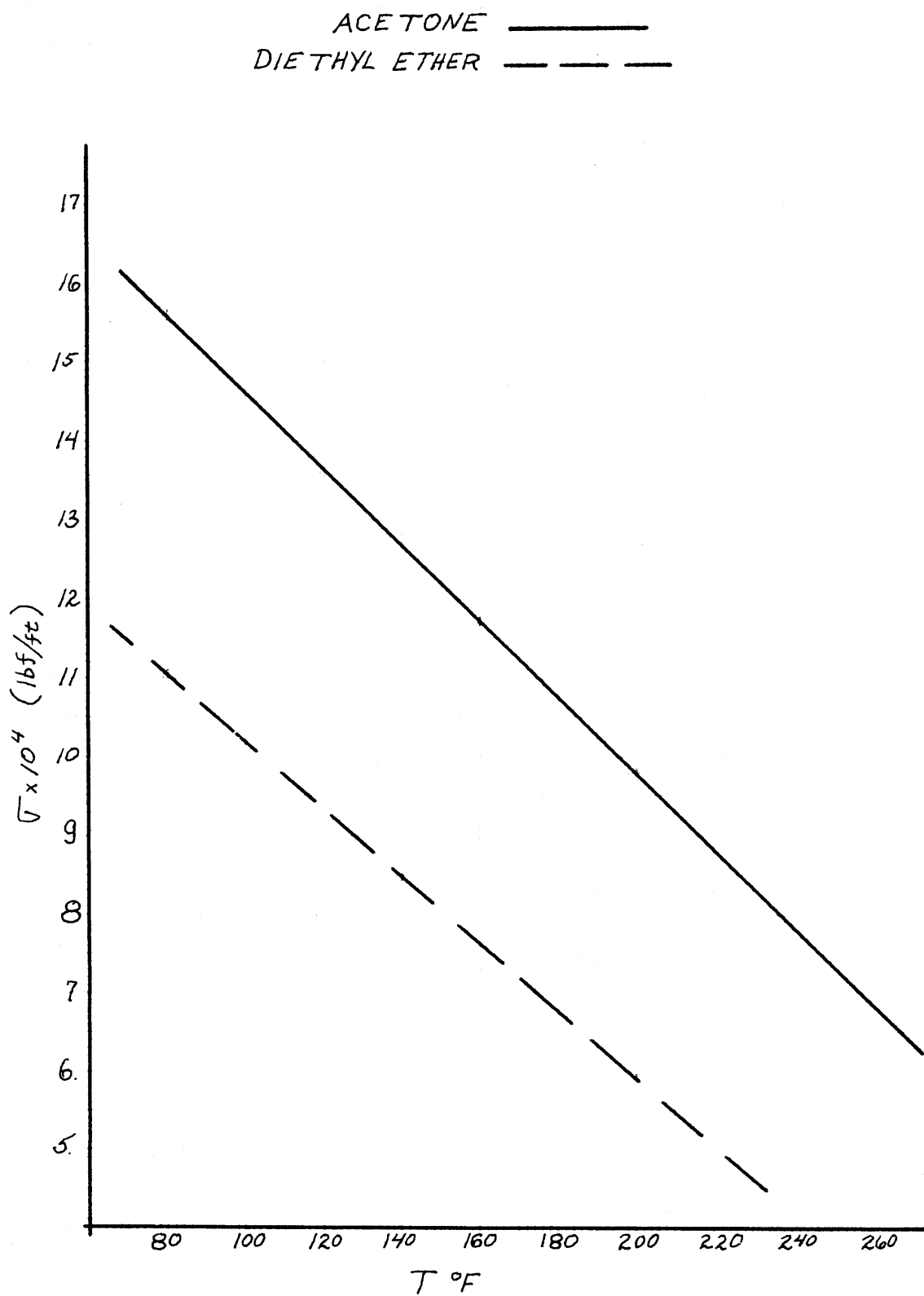


FIG. A.4

HEAT OF VAPORIZATION vs TEMPERATURE

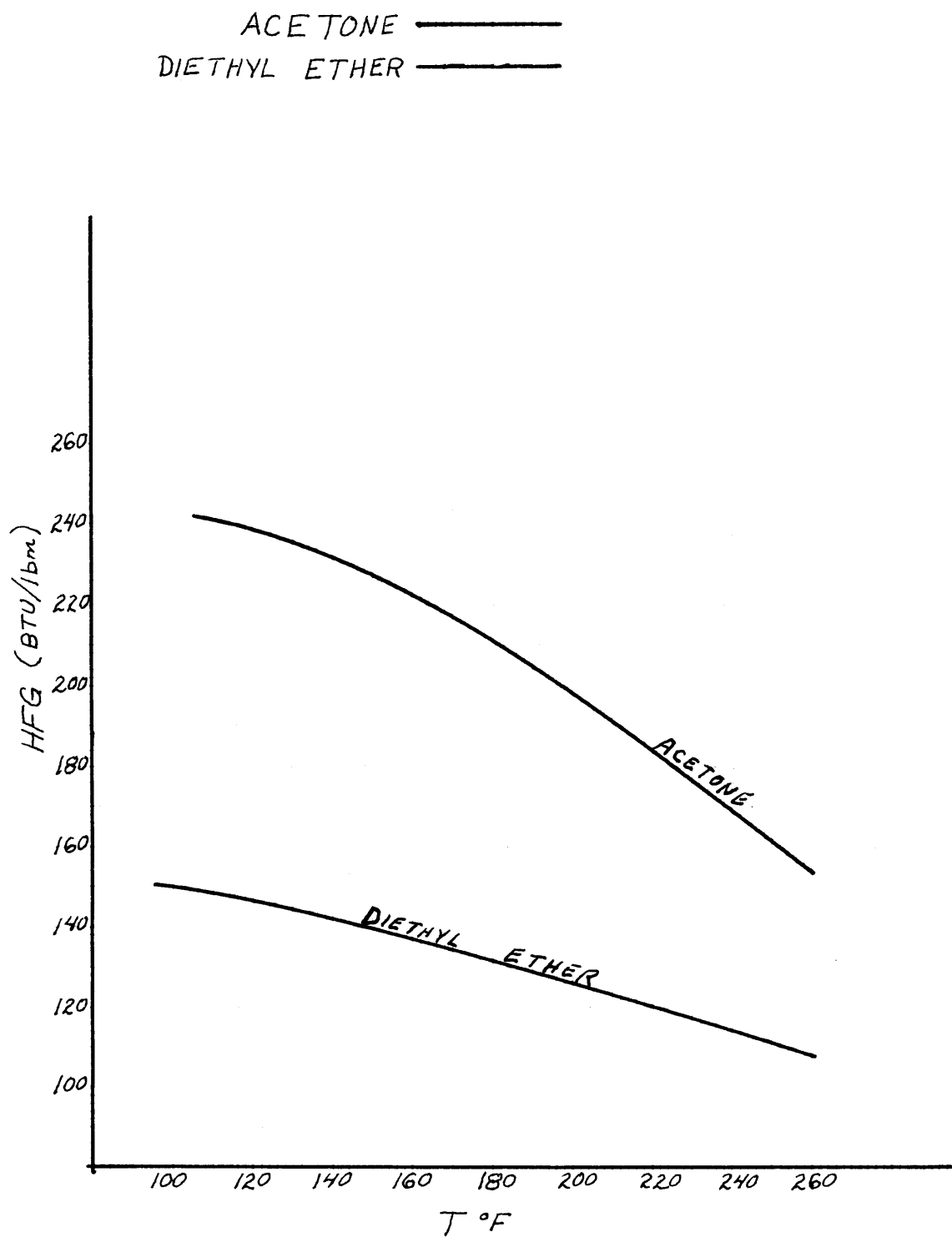


FIG. A.5

A.3 Physical Properties of Diethyl Ether

- 1.) Vapor pressure (P_v psia , $T^{\circ}\text{F}$) (22)

$$P_v = 44.2626 - 0.96031(T) + 0.0056627(T)^2$$

$$80^{\circ}\text{F} < T < 300^{\circ}\text{F}$$

- 2.) Liquid density (ρ_l lbm/ft³ , $T^{\circ}\text{F}$) (29)

$$\rho_l = 45.6089 - 0.005339(T) - 0.00013836(T)^2$$

$$65^{\circ}\text{F} < T < 300^{\circ}\text{F}$$

- 3.) Vapor density (ρ_v lbm/ft³ , $T^{\circ}\text{F}$) (29)

$$\rho_v = 1.53905 - 0.030649(T) + 0.00013358(T)^2$$

$$65^{\circ}\text{F} < T < 300^{\circ}\text{F}$$

- 4.) Surface tension (σ lbf/ft , $T^{\circ}\text{F}$)

$$\sigma = 0.0013942 - 3.81359 \times 10^{-6}(T)$$

$$65^{\circ}\text{F} < T < 330^{\circ}\text{F}$$

- 5.) Heat of vaporization (HFG Btu/lbm , $T^{\circ}\text{F}$) (22)

$$\text{HFG} = 162.277 - 0.00444(T) - 8.31636 \times 10^{-4}(T)^2$$

$$80^{\circ}\text{F} < T < 280^{\circ}\text{F}$$

Graphs are shown on FIG. A.1 through A.5 .

A.4 Physical Properties of Propylene Glycol

1.) Vapor pressure (P_v in mm Hg., $t^\circ\text{C}$) (22)

$$\log(P_v) = 8.9171 - \frac{2645.7}{T + 250.7}$$

$$0^\circ\text{C} < T < 250^\circ\text{C}$$

2.) Liquid density (ρ_l in lbm/ft³, $T^\circ\text{F}$) (29)

$$\rho_l = 66.3836 - 0.0236(T) - 1.1618 \times 10^{-5}(T)^2$$

$$20^\circ\text{C} < T < 280^\circ\text{C}$$

3.) Vapor density (ρ_v in lbm/ft³, $T^\circ\text{F}$) (29)

$$\rho_v = 0.2627 - 0.002735(T) + 6.6505 \times 10^{-6}(T)^2$$

$$20^\circ\text{C} < T < 280^\circ\text{C}$$

4.) Surface tension (σ in lbf/ft, $T^\circ\text{F}$) (22)

$$\sigma = 0.00285136 - 4.71296 \times 10^{-6}(T)$$

$$20^\circ\text{C} < T < 280^\circ\text{C}$$

5.) Heat of vaporization (HFG in Btu/lbm, $T^\circ\text{F}$) (22)

$$\text{HFG} = 396.7268 - 0.11884(T) - 3.7196 \times 10^{-4}(T)^2$$

$$25^\circ\text{C} < T < 300^\circ\text{C}$$

The graphs of property vs temperature are shown on FIG.A.6 to A.10 .

VAPOR PRESSURE vs TEMPERATURE

PROPYLENE GLYCOL —————
NITROMETHANE - - - - -

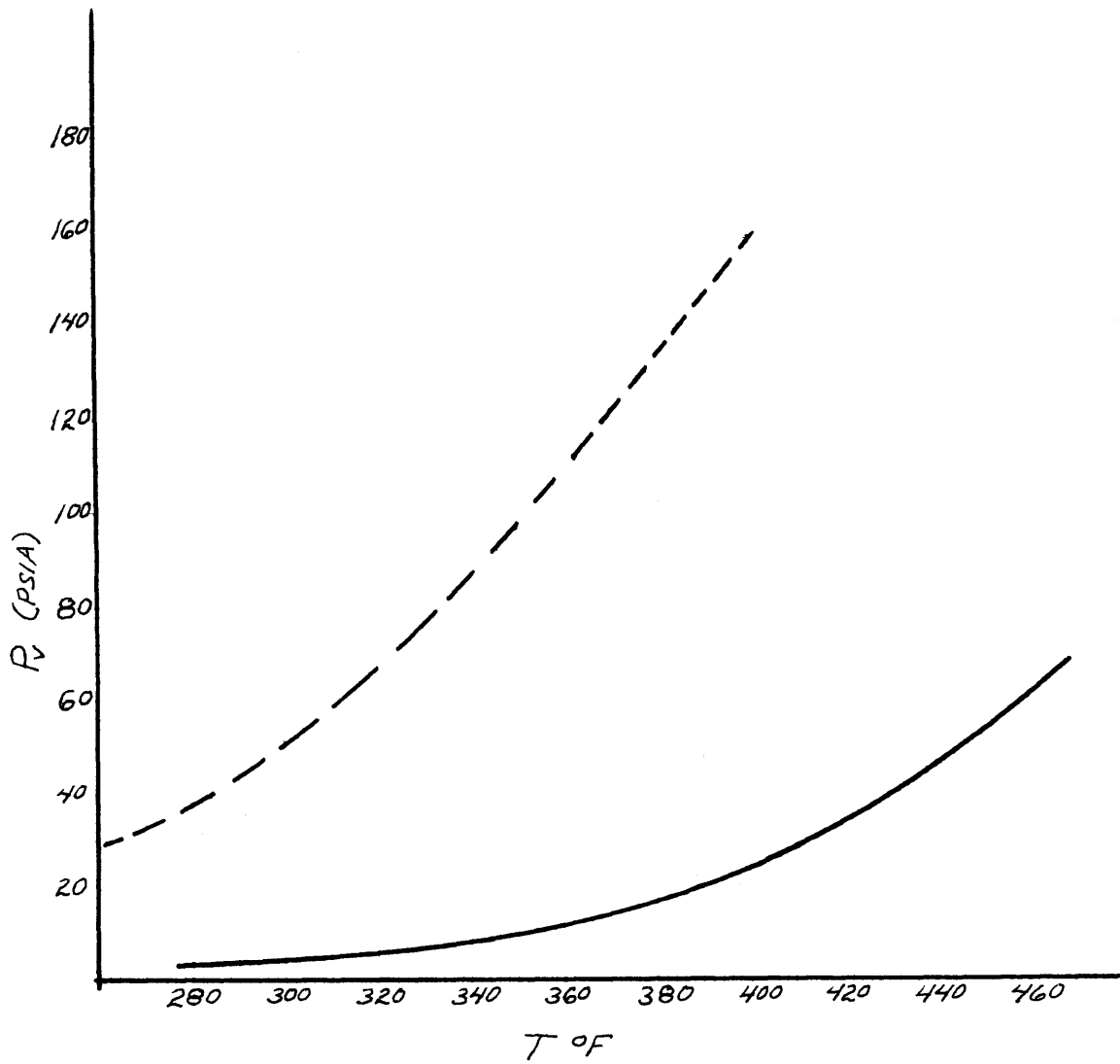


FIG. A.6

LIQUID DENSITY vs TEMPERATURE

PROPYLENE GLYCOL —————

NITROMETHANE - - - - -

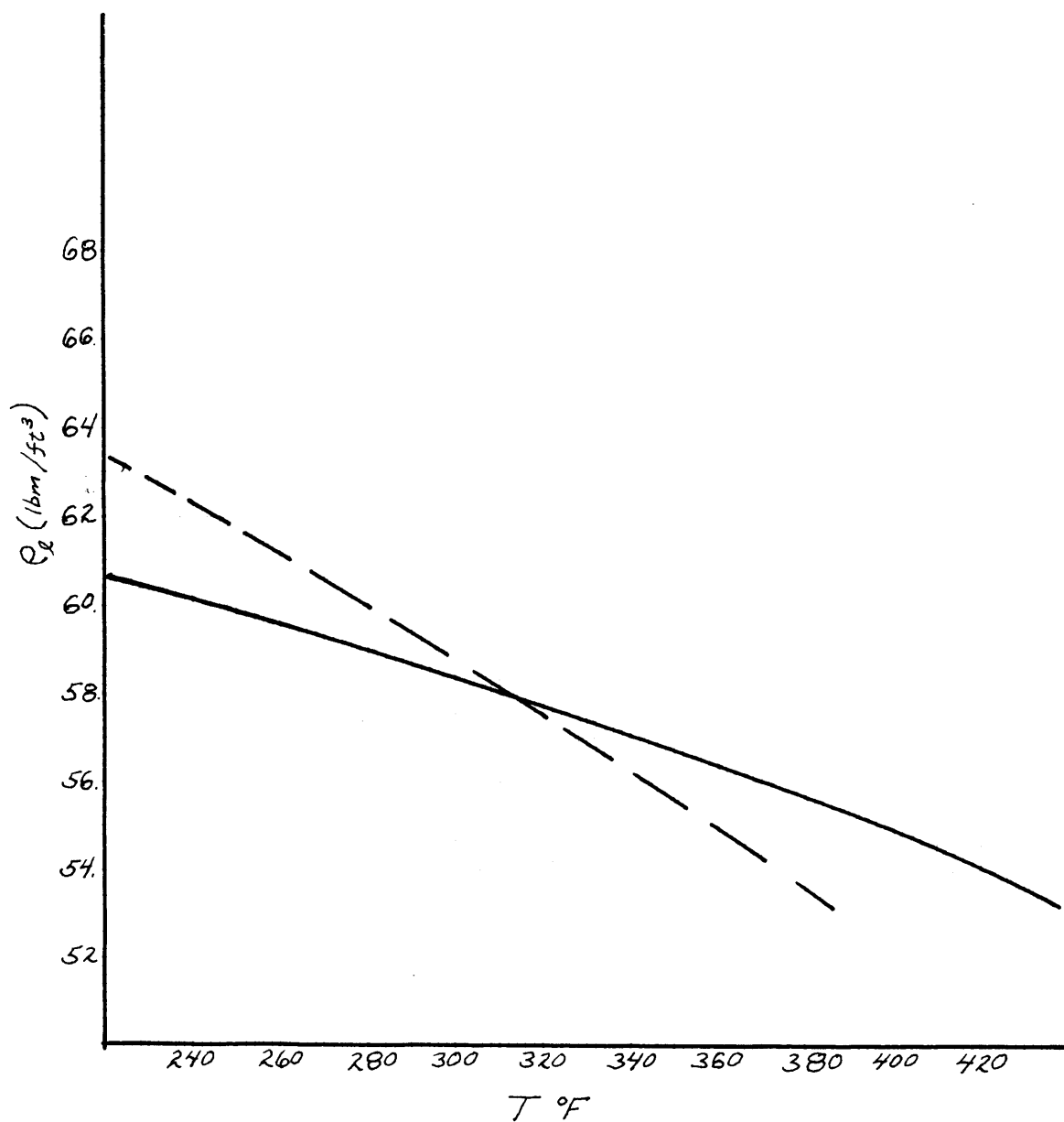


FIG. A.7

VAPOR DENSITY vs TEMPERATURE

PROPYLENE GLYCOL _____

NITROMETHANE - - - - -

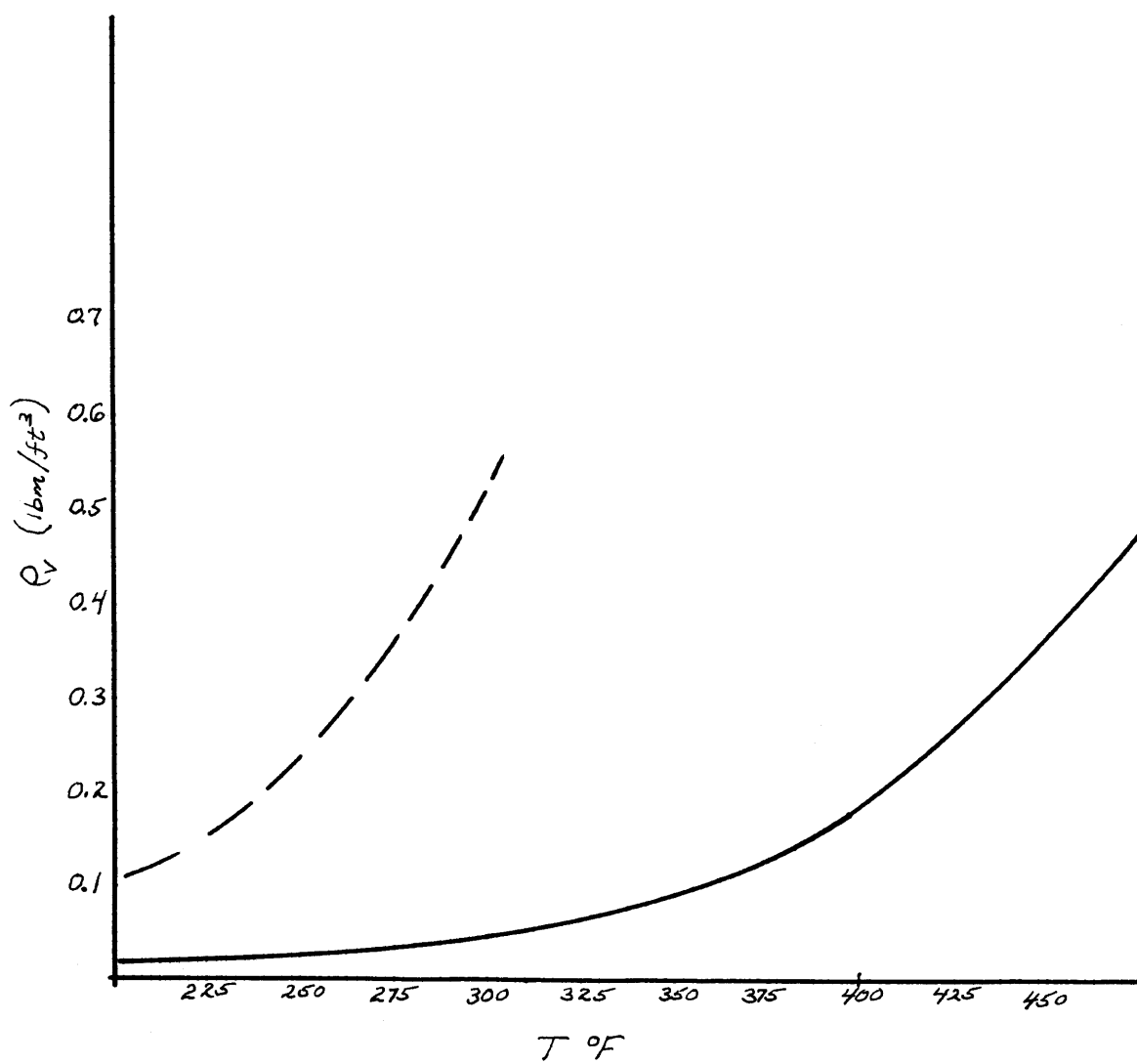


FIG. A.8

SURFACE TENSION vs TEMPERATURE

PROPYLENE GLYCOL _____

NITROMETHANE - - - - -

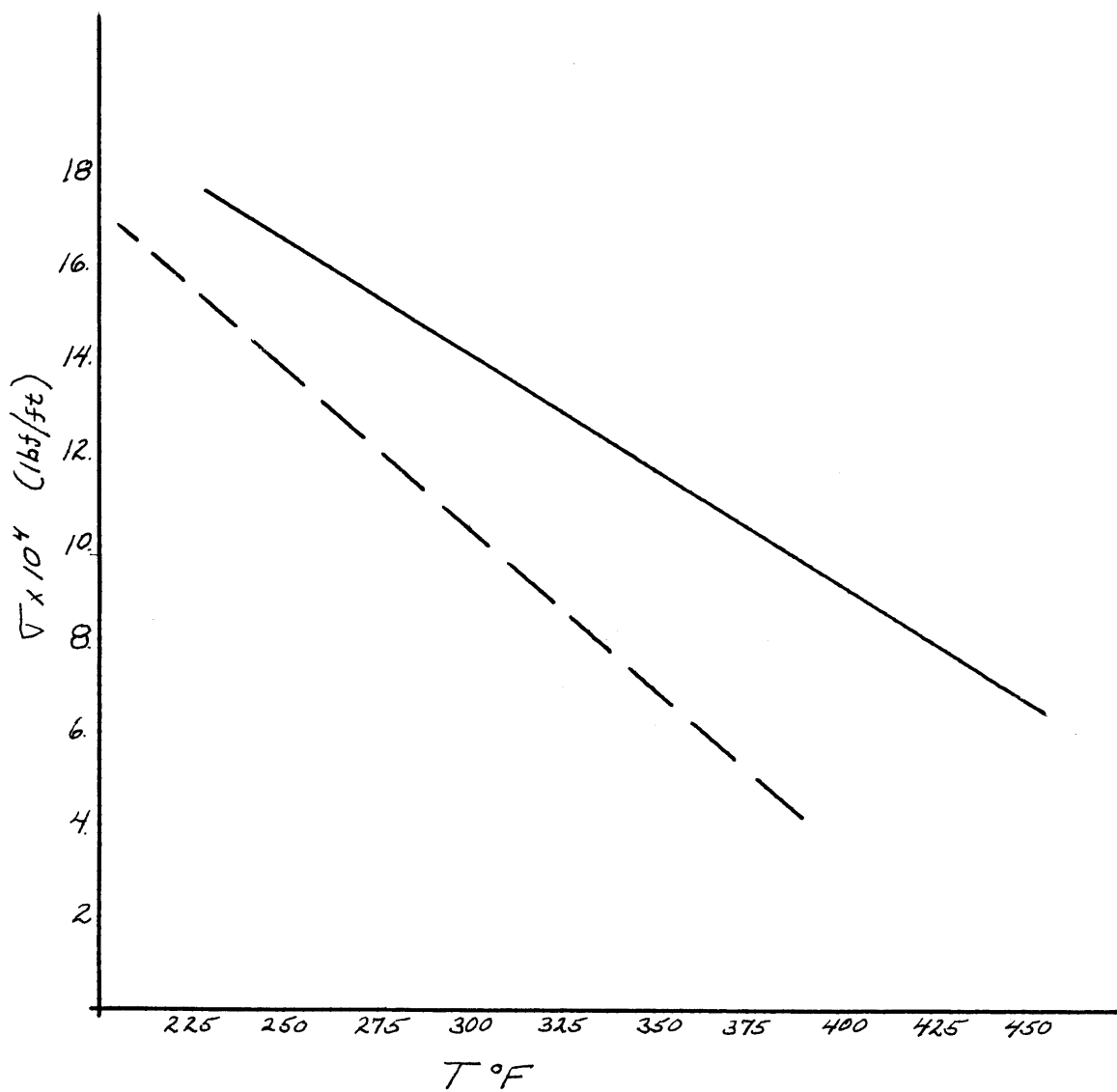


FIG. A.9

HEAT OF VAPORIZATION vs TEMPERATURE

PROPYLENE GLYCOL —————
NITROMETHANE - - - - -

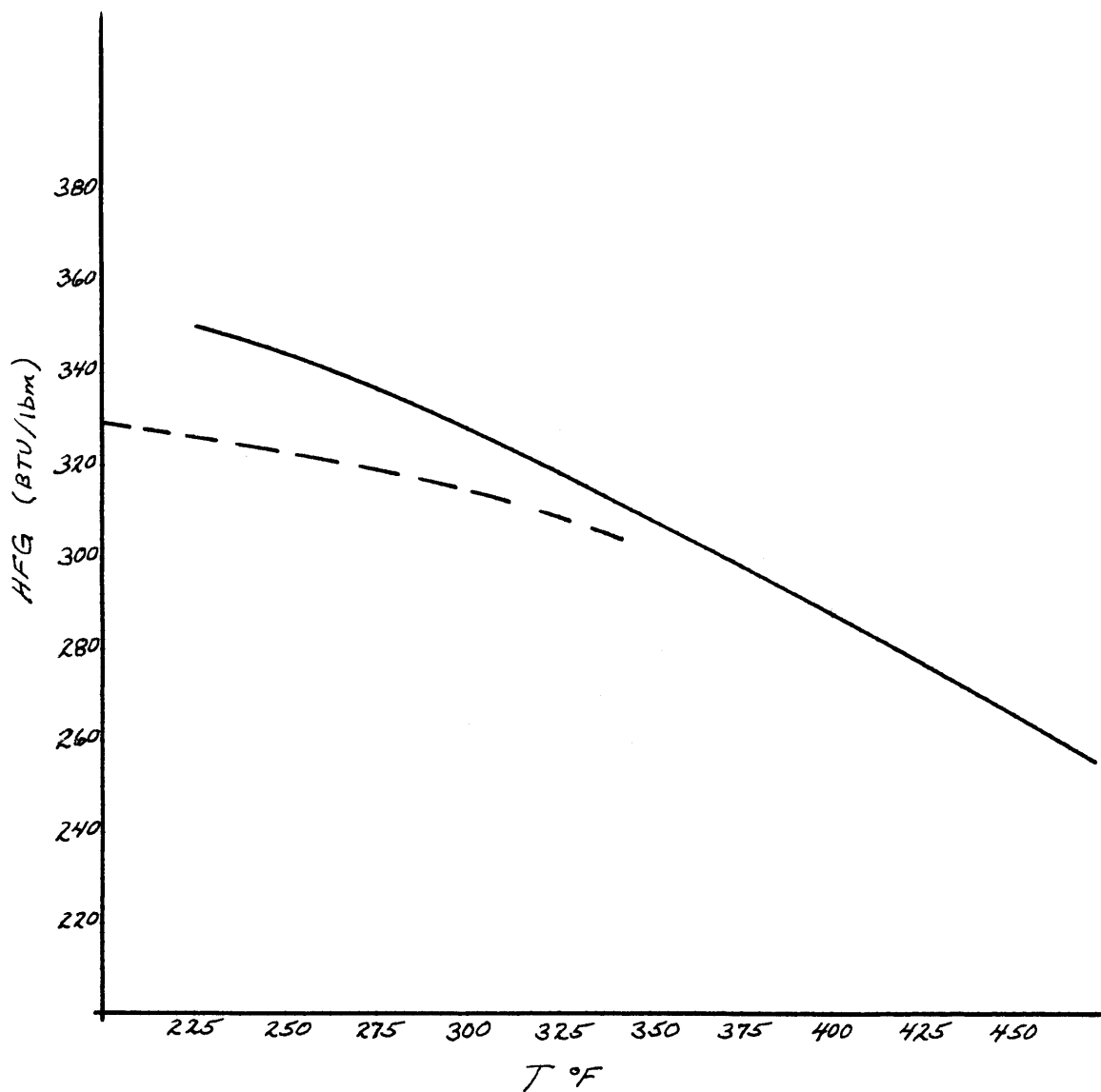


FIG. A.10

A.5 Physical Properties of Nitromethane

- 1.) Vapor pressure (P_v in psia , $T^{\circ}\text{F}$) (22)

$$P_v = 19.1127 - 0.342947(T) + 0.0015267(T)^2$$

$$20^{\circ}\text{C} < T < 268^{\circ}\text{C}$$

- 2.) Liquid density (ρ_l in lbm/ft³ , $T^{\circ}\text{F}$) (29)

$$\rho_l = 74.07513 - 0.0430263(T) - 2.56308 \times 10^{-5}(T)^2$$

$$20^{\circ}\text{C} < T < 268^{\circ}\text{C}$$

- 3.) Vapor density (ρ_v in lbm/ft³ , $T^{\circ}\text{F}$) (29)

$$\rho_v = 0.52092 - 0.008079(T) + 2.8548 \times 10^{-5}(T)^2$$

$$20^{\circ}\text{C} < T < 268^{\circ}\text{C}$$

- 4.) Surface tension (\bar{V} in lbf/ft , $T^{\circ}\text{F}$) (22)

$$\bar{V} = 0.0030398 - 6.6158 \times 10^{-6}(T)$$

$$20^{\circ}\text{C} < T < 268^{\circ}\text{C}$$

- 5.) Heat of vaporization (HFG in Btu/lbm, $T^{\circ}\text{F}$) (22)

$$\text{HFG} = 343.3718 - 0.009790(T) - 2.5489 \times 10^{-4}(T)^2$$

$$25^{\circ}\text{C} < T < 265^{\circ}\text{C}$$

The graphs for property vs temperature are found on FIG.A.6 through FIG.A.10 .

A.6 Discussion of Vapor Density Results

Vapor density data for nitromethane was not readily available from the literature. But some investigators have formulated equations which relate the vapor density with the temperature. These are all based on the Verschaffelt equation (30) which has the general form:

$$d_l - d_g = d_o \left(1 - \frac{T}{T_c} \right)^m \quad (\text{A.2})$$

where; d_l = liquid density

d_g = vapor density

T_c = critical temperature

T = temperature at which the density is to be evaluated.

m, d_o = constants, which differ for different liquids.

Density measurements for a number of liquids have shown (29) these equations to be fairly accurate for all temperatures except those close to the critical temperature.

For the case of nitromethane, the general Verschaffelt equation has been broken down (31) into:

$$\log \frac{d}{d_b} = 5.0 \left(\frac{T}{T_b} - 1.0 \right) \quad (\text{A.3})$$

where T_b is the liquid boiling point in K, and d_b is the vapor density at the boiling point, which is given by:

$$d_b = \frac{0.0122M}{T_b} \quad (\text{A.4})$$

where M is the molecular weight.

Another equation for nitromethane, also derived from the basic Verschaffelt equation, is given (29) by:

$$\log d_g = 4.44 \left(\frac{T}{T_b} - 1.0 \right) + \log \frac{0.0124M}{T_b} \quad (\text{A.5})$$

where the symbols have the same meaning as in the previous equations.

Calculations were made for the vapor density of nitromethane using both equations (A.3 and A.5). The results obtained from these two equations agreed very well with each other.

These results were then used as input for the polynomial regression program so that a polynomial type equation could be obtained.

This same procedure was used with the propylene glycol vapor density data.

These equations for vapor density may be in error by as much as 5%, (29), but they are the only ones available at this time. Therefore, until more experimental measurements of vapor densities are made, these equations are our best approximations.

A.7 Physical Properties of Methyl Alcohol

1.) Vapor pressure (P_v in psia, $T^{\circ}F$) (32)

$$P_v = 98.6548 - 0.018347(T) + 0.00741241(T)^2$$

$$0^{\circ}C < T < 240^{\circ}C$$

2.) Liquid density (ρ_l in lbm/ft³ , $T^{\circ}F$) (32)

$$\rho_l = 49.5607 - 1.26317 \times 10^{-4}(T) - 1.02098 \times 10^{-4}(T)^2$$

$$0^{\circ}C < T < 240^{\circ}C$$

3.) Vapor density (ρ_v in lbm/ft³ , $T^{\circ}F$) (29)

$$\rho_v = 0.88826 - 0.0136(T) + 4.7952 \times 10^{-5}(T)^2$$

$$78^{\circ}F < T < 375^{\circ}F$$

4.) Surface tension (σ in lbf/ft , $T^{\circ}F$) (32)

$$\sigma = 1.7826 \times 10^{-3} - 3.4611 \times 10^{-6}(T)$$

$$0^{\circ}C < T < 150^{\circ}C$$

5.) Heat of vaporization (HFG in Btu/lbm, $T^{\circ}F$) (32)

$$HFG = 527.091 - 0.1779(T) - 0.0011134(T)^2$$

$$0^{\circ}C < T < 240^{\circ}C$$

The graphs for methyl alcohol properties are given in FIG.A.11 through FIG.A.15 .

VAPOR PRESSURE vs TEMPERATURE

METHYL ALCOHOL ———
ETHYL ALCOHOL - - -

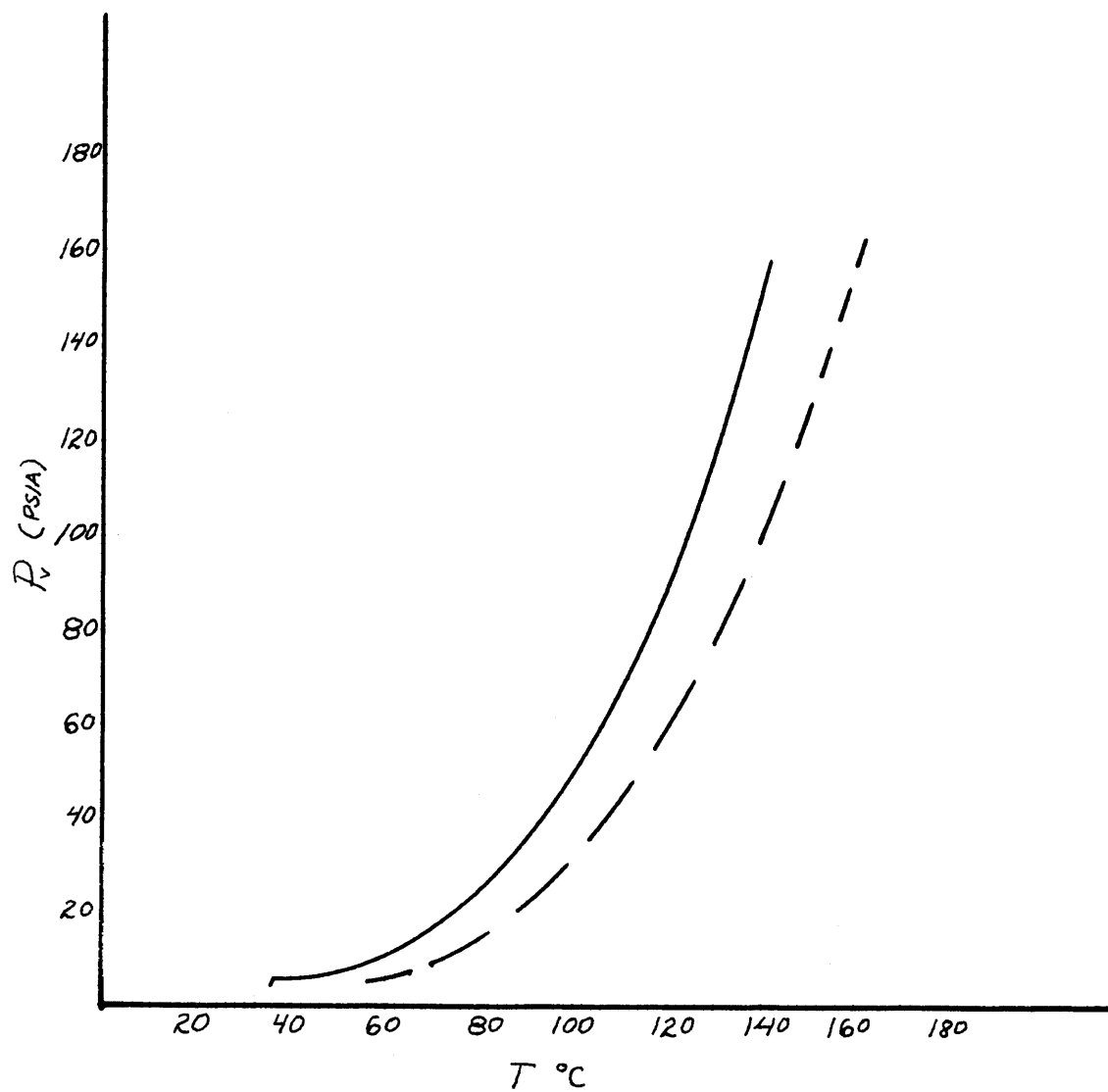


FIG. A. 11

LIQUID DENSITY vs TEMPERATURE

METHYL ALCOHOL _____
ETHYL ALCOHOL - - - - -

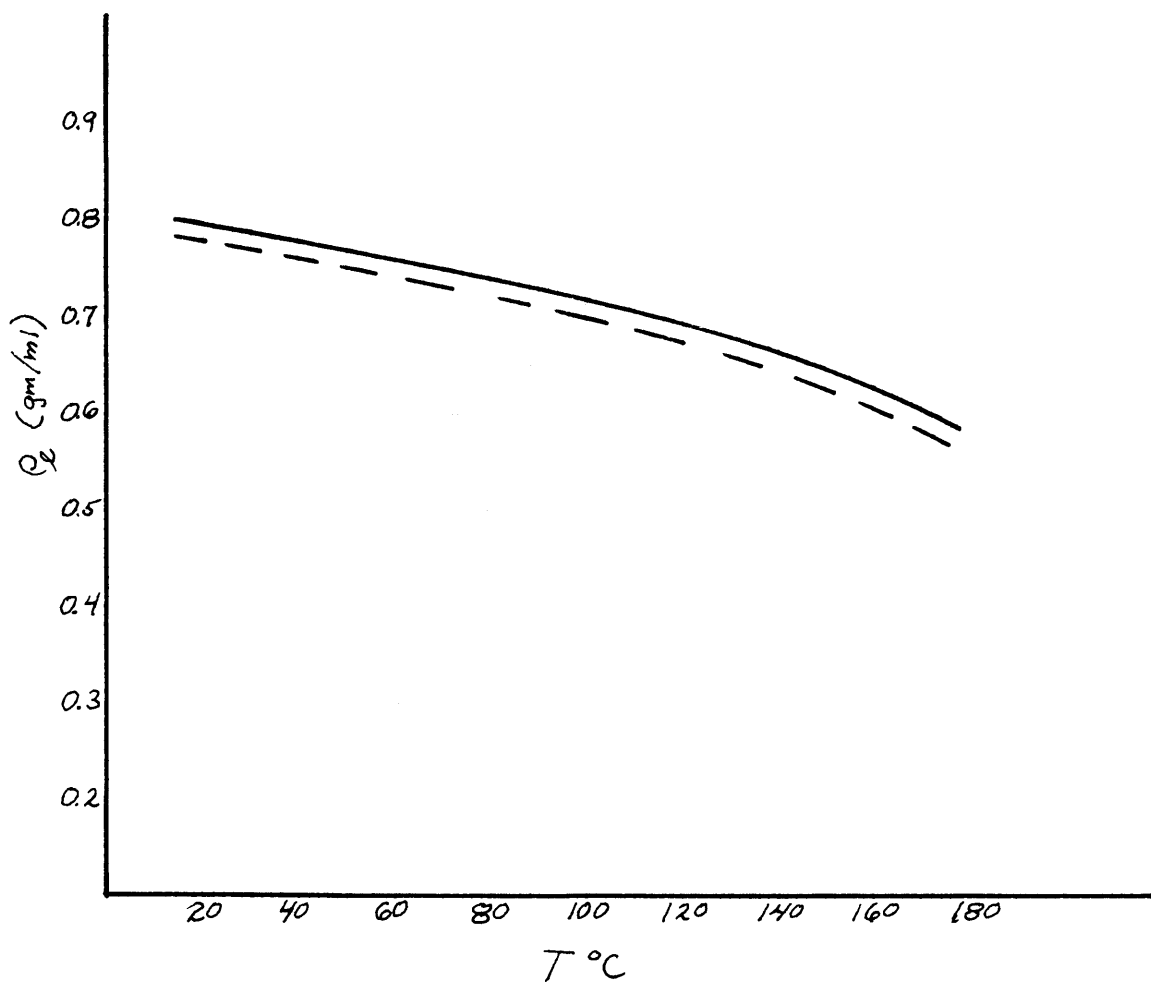


FIG. A. 12

VAPOR DENSITY vs TEMPERATURE

METHYL ALCOHOL ———
ETHYL ALCOHOL - - - -

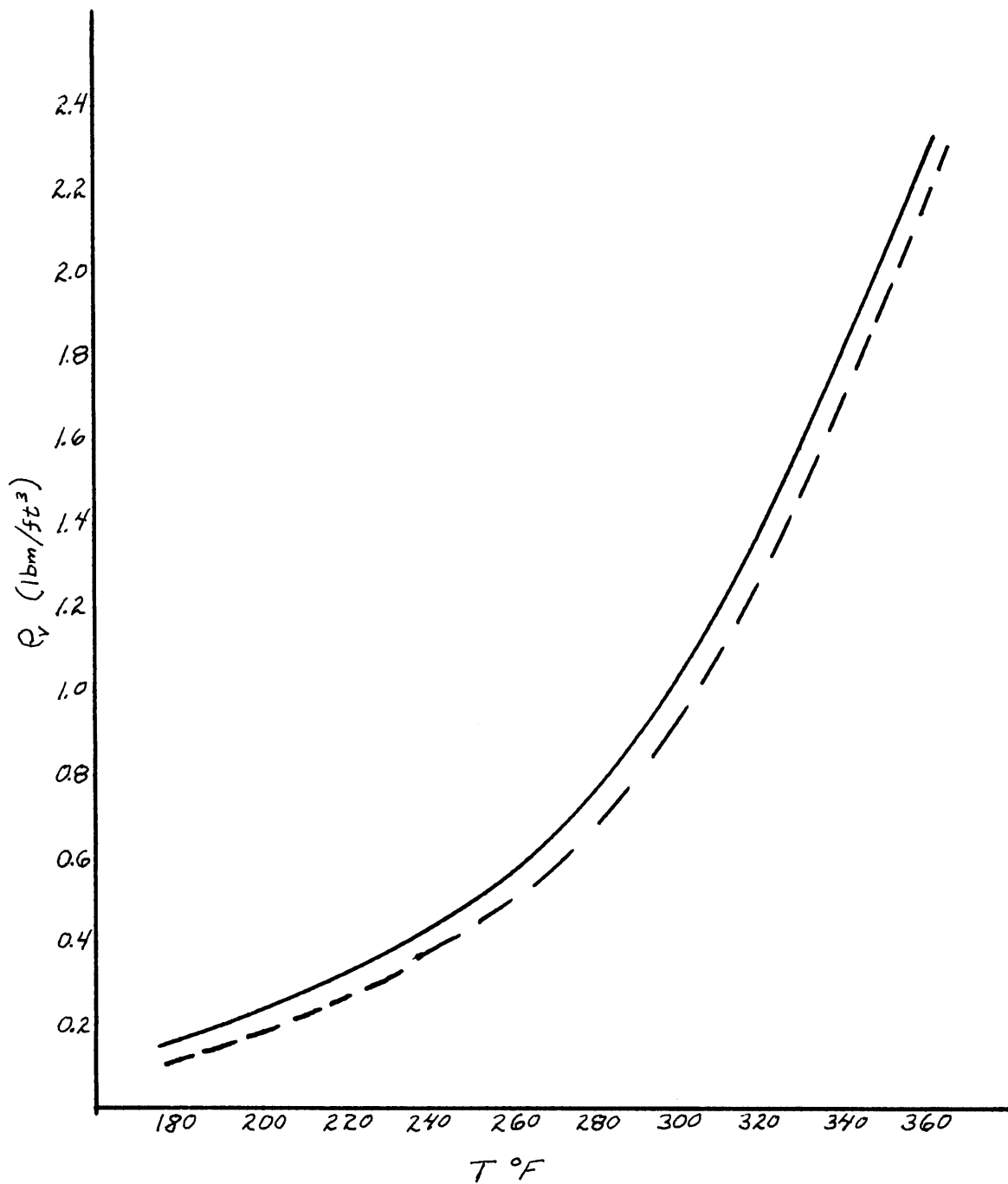


FIG. A.13

SURFACE TENSION vs TEMPERATURE

METHYL ALCOHOL ———
ETHYL ALCOHOL - - - -

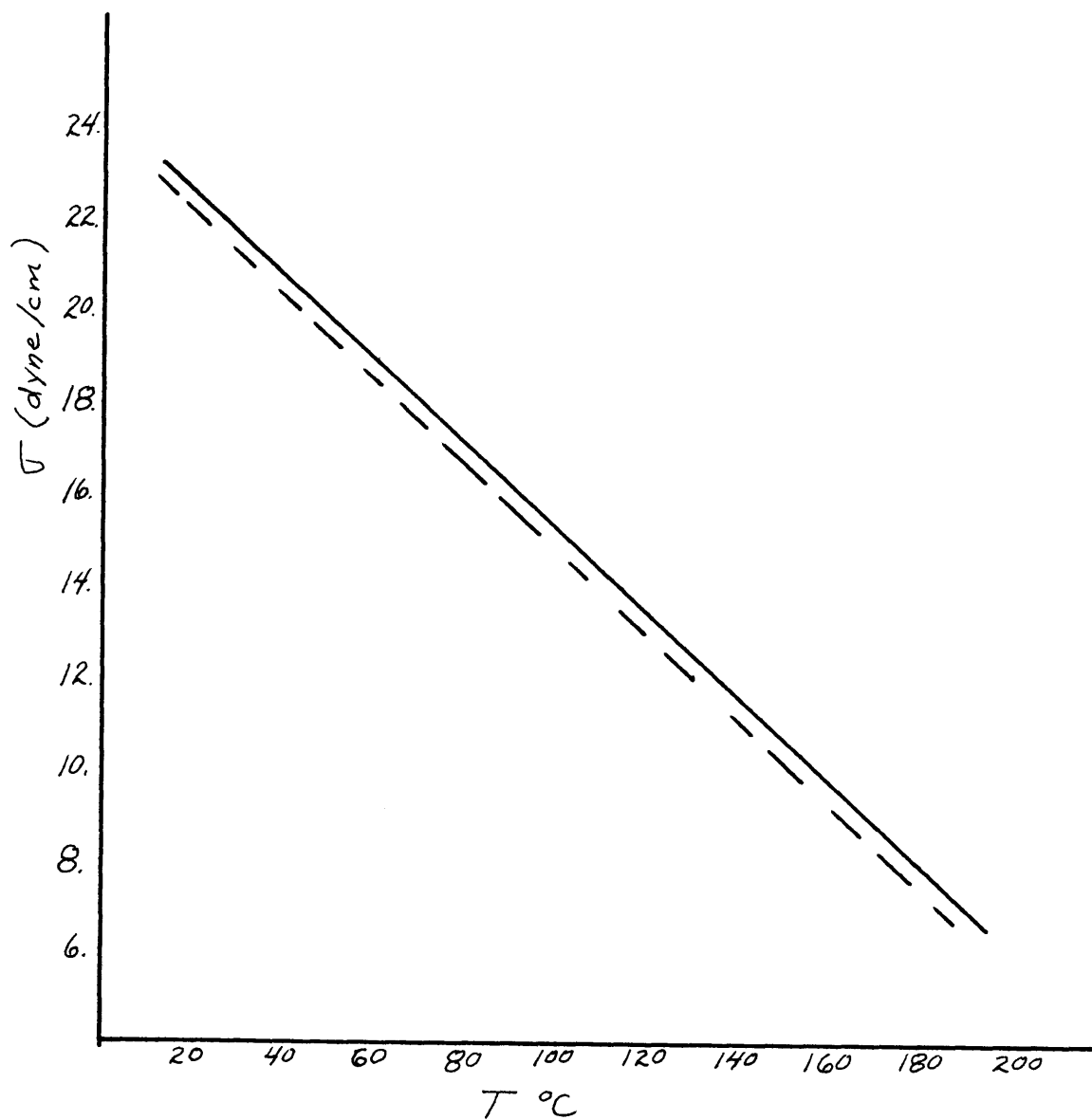


FIG. A.14

HEAT OF VAPORIZATION vs TEMPERATURE

METHYL ALCOHOL ———
ETHYL ALCOHOL - - -

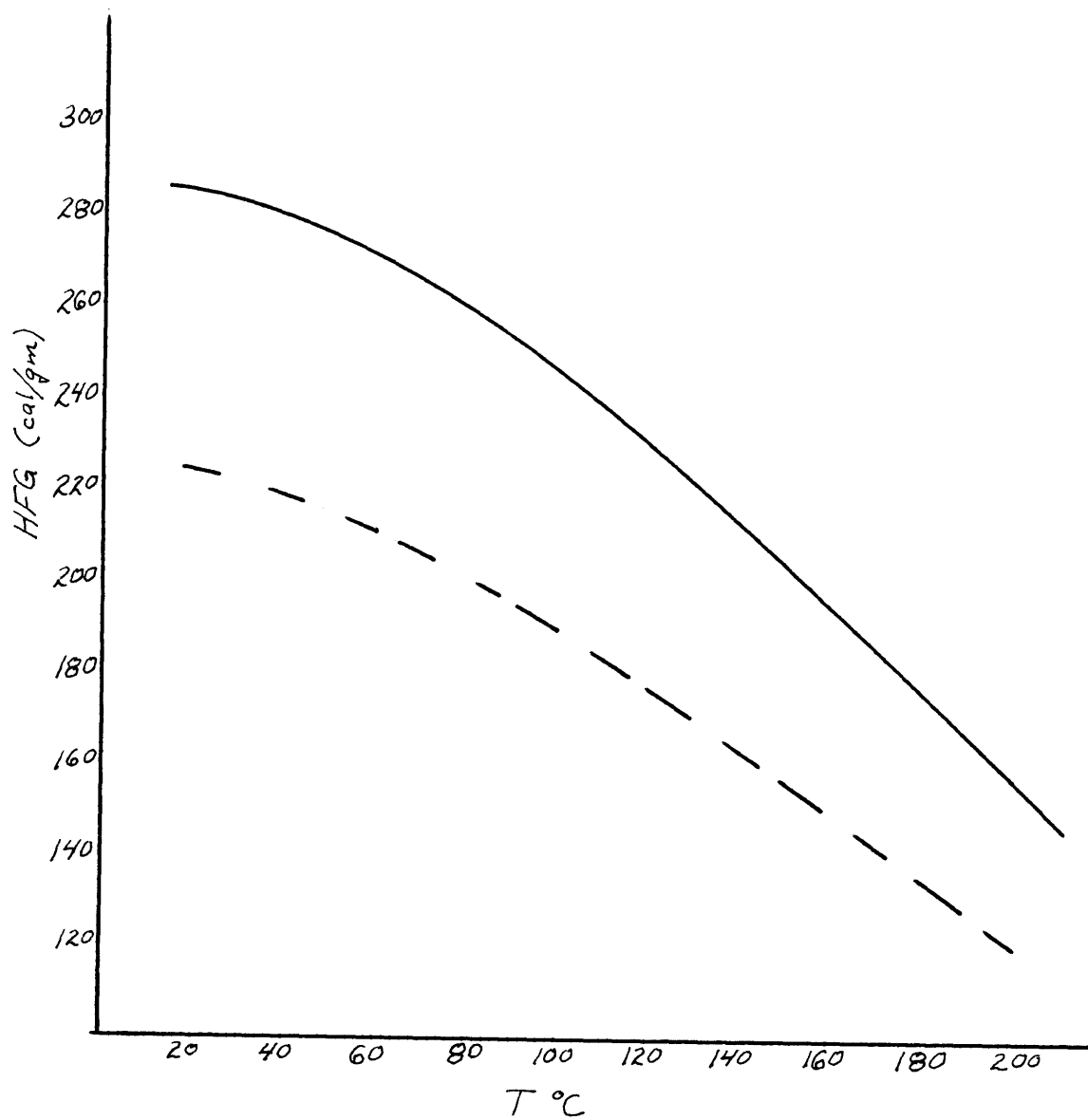


FIG. A.15

A.8 Physical Properties of Ethyl Alcohol

1.) Vapor pressure (P_v in psia, $T^\circ\text{C}$) (32)

$$P_v = 38.862 - 2.02655(T) + 0.018601(T)^2$$

$$0^\circ\text{C} < T < 240^\circ\text{C}$$

2.) Liquid density (ρ_l in gm/cc , $T^\circ\text{C}$) (32)

$$\rho_l = 0.8022 - 5.4322 \times 10^{-4}(T) - 3.3149 \times 10^{-6}(T)^2$$

$$0^\circ\text{C} < T < 240^\circ\text{C}$$

3.) Vapor density (ρ_v in gm/cc , $T^\circ\text{C}$) (29)

$$\rho_v = 8.367 \times 10^{-3} - 3.1762 \times 10^{-4}(T) + 2.541 \times 10^{-6}(T)^2$$

$$68^\circ\text{F} < T < 380^\circ\text{F}$$

4.) Surface tension (σ in dynes/cm , $T^\circ\text{C}$) (32)

$$\sigma = 24.5354 - 0.09173(T)$$

$$0^\circ\text{C} < T < 150^\circ\text{C}$$

5.) Heat of Vaporization (HFG in cal/gm , $T^\circ\text{C}$) (32)

$$\text{HFG} = 223.88 - 0.13821(T) - 2.0431 \times 10^{-3}(T)^2$$

$$0^\circ\text{C} < T < 240^\circ\text{C}$$

The graphs for ethyl alcohol properties are given in FIG.A.11 through FIG.A.15 .

Appendix B

Sample Calculation

Appendix B will give a detailed description of all calculations necessary to calculate the superheat temperature, beginning with the basic equations and concluding with the required inputs for the computer program which performs the actual calculations. The sample calculations will be shown for the case of propylene glycol.

The starting point for all calculations is the energy deposition equation described in chapter 2. This equation is given again below:

$$\frac{1}{N} \frac{dE}{dS} = \frac{4\pi e^4}{m_0 v^2} (Z_1)_{eff}^2 \sum_i v_i Z_i \ln \left[\frac{1.123 m_0 v^3}{(I_i/h) e^2 (Z_1)_{eff}} \right] + \frac{4\pi e^4 (Z_1)^2}{v^2} \sum_i v_i \frac{Z_i}{M_i} \ln \left[\frac{M_1 M_i v^2 (a_{12}^{scr})_i}{(M_1 + M_i) Z_1 Z_i e^2} \right] \quad (B.1)$$

All of the terms in equation (B.1) have been described in chapter 2, and will not be repeated here.

The above equation will first be broken down as far as possible without introducing any specific liquid properties.

The second term on the RHS of equation (B.1) can be neglected for all of the cases considered in this work.

(The reasons have already been outlined in chapter 2)

This leaves only one expression on the RHS. The

substitution is now made for $(Z_1)_{\text{eff}}$:

$$\frac{1}{N} \frac{dE}{ds} = \frac{4\pi e^4}{m_0 v^2} \left[Z_1^{1/3} \frac{\hbar V}{e^2} \right]^2 \sum \nu_i Z_i \ln \left[\frac{1.123 m_0 v^3 \hbar e^2}{I_i e^2 (Z_1)^{1/3} \hbar V} \right] \quad (\text{B.2})$$

Cancelling all common terms

$$\frac{1}{N} \frac{dE}{ds} = 4\pi (Z_1)^{1/3} \frac{\hbar^2}{m_0} \sum \nu_i Z_i \ln \left[\frac{1.123 m_0 2E}{I_i (Z_1)^{1/3} M_1} \right] \quad (\text{B.3})$$

where v has been replaced by the energy equivalent,

from the basic equation

$$E = \frac{1}{2} MV^2 \quad (\text{B.4})$$

The RHS of equation (B.3) is multiplied by $\frac{c^2}{c^2}$, (or 1)

resulting in

$$\frac{1}{N} \frac{dE}{ds} = 4\pi (Z_1)^{1/3} \frac{(\hbar c)^2}{m_0 c^2} \sum \nu_i Z_i \ln \left[\frac{1.123 m_0 2E}{I_i (Z_1)^{1/3} M_1} \right] \quad (\text{B.5})$$

This form gives the constants (such as h, c, m_0) in familiar forms, the values of which can be found in any nuclear physics text. More specifically, we have:

$$\hbar c = 1.9732 \times 10^{-11} \text{ Mev-cm}$$

$$m_0 c^2 = 0.511 \text{ Mev.}$$

$$m_0 = 0.5488 \times 10^{-3} \text{ amu.}$$

The N term is replaced by

$$N = \frac{\rho_l N_{av}}{M_{MEDIUM}} \quad (B.6)$$

and brought to the RHS giving

$$\frac{dE}{dS} = \frac{\rho_l N_{av}}{M_{MEDIUM}} 4\pi (Z_1)^{2/3} \frac{(1.9732 \times 10^{-11})^2}{0.511} \sum_i v_i Z_i \ln \left[\frac{1.232 \times 10^{-3} E}{I_i (Z_1)^{1/3} M_1} \right] \quad (B.7)$$

This is as far as the original equation, (B.1), can be broken down without introducing any specific particle or medium. The case of fission fragments in propylene glycol will now be taken as an example.

The fission fragment properties are as follows

((5) pg 115):

$$A = 97 = M_1$$

$$Z = 38 = Z_1$$

The molecular weight of the medium is

$$M_{medium} = M_{\substack{\text{propylene} \\ \text{glycol}}} = 76.096$$

Substituting the values for M_1 , Z_1 , M_{medium} , and for $N_{av} = 6.023 \times 10^{-23}$, equation (B.7) becomes:

$$\frac{dE}{dS} = (850.0) \rho_l \sum_i v_i Z_i \ln \left[\frac{(3.777 \times 10^{-6}) E}{I_i} \right] \quad (B.8)$$

The summation term is over the atoms in the stopping medium (propylene glycol in this case). The chemical formula for propylene glycol is $C_3H_8O_2$, so the summation sign can be shown as follows: $\sum_{i=C,H,O}$

The values for ν_i , Z_i , and I_i are:

$$\begin{array}{lll} \nu_c = 3 & Z_c = 6 & I_c = 76.4 \text{ ev} \\ \nu_H = 8 & Z_H = 1 & I_H = 15.5 \text{ ev} \\ \nu_o = 2 & Z_o = 8 & I_o = 100.0 \text{ ev} \end{array}$$

Values for the mean ionization potential, I_i , have been obtained from Evans (14).

The values for I_i are given in ev, but the I_i term in equation (B.8) must be in units of Mev (E is given in Mev).

Equation (B.8) thus becomes:

$$\frac{dE}{ds} = \rho_l (850.0) \left[(3)(6) \ln \left(\frac{3.777 \times 10^{-6} E}{76.4 \times 10^{-6}} \right) + (8)(1) \ln \left(\frac{3.777 \times 10^{-6} E}{15.5 \times 10^{-6}} \right) + (2)(8) \ln \left(\frac{3.777 \times 10^{-6} E}{100.0 \times 10^{-6}} \right) \right] \quad (\text{B.9})$$

Equation (B.9) is now reduced to an equation with a single "ln" term:

$$\frac{dE}{dS} = \rho_l (3.57 \times 10^4) \ln(0.0604 E) \quad (\text{B.10})$$

Equation (B.10) is the final form of the energy deposition equation.

dE/dS is in terms of Mev/cm

ρ_l in terms of gm/cc

E in terms of Mev.

The remainder of the calculations provide input parameters to the computer program.

Equation (B.10) is substituted into the integral equation described in chapter 2,

$$\frac{-[E(s_1) - E(s_2)]^2}{a r^*} = \int_{E(s_1)}^{E(s_2)} \left(\frac{dE}{dS} \right) dE \quad (\text{B.11})$$

Performing the integration:

$$\frac{-[E(s_1) - E(s_2)]^2}{a r^*} = \frac{\rho_l (3.57 \times 10^4)}{0.0604} \left[0.0604 E \ln 0.0604 E - 0.0604 E \right]_{E(s_1)}^{E(s_2)} \quad (\text{B.12})$$

Further breakdown of (B.12) and combination of terms leads to:

$$\frac{[E(s_1) - E(s_2)]^2}{E(s_1) \ln E(s_1) - E(s_2) \ln E(s_2) - 3.81(E(s_1) - E(s_2))} = a r^* \rho_l (3.57 \times 10^4) \quad (\text{B.13})$$

The RHS of equation (B.13) is in metric units and is now converted to allow ρ_l and r^* to be input in English units. The final conversion factor is 2.0479, and the RHS must be divided by this. (The LHS is in Mev terms and must remain the same numerical value, no matter what units the RHS has.)

Converting to English units and substituting the relationship,

$$r^* = \frac{2\sigma}{P_v + P_g - P_l} \quad (\text{B.14})$$

the RHS of equation (B.13) becomes:

$$\frac{(3.486 \times 10^4) a \sigma \rho_l}{P_v + P_g - P_l} \quad (\text{B.15})$$

The expression in (B.15) is one of the parameters which is used as an input to the computer program. This parameter is given the name of "COEF".

$$\text{COEF} \equiv \frac{(3.486 \times 10^4) a \sigma \rho_l}{P_v + P_g - P_l} \quad (\text{B.16})$$

COEF is now the RHS of equation (B.13) , which is written as

$$\frac{[E(s_1) - E(s_2)]^2}{E(s_1) \ln E(s_1) - E(s_2) \ln E(s_2) - 3.81(E(s_1) - E(s_2))} = \text{COEF} \quad (\text{B.17})$$

Rearranging terms in equation (B.17)

$$E(s_1)^2 - \text{COEF} \cdot E(s_1) [\ln E(s_1) - 3.81] = E(s_2) \left[2 \cdot E(s_1) + 3.81 \cdot \text{COEF} \right] \\ - E(s_2) \cdot \text{COEF} - \ln E(s_2) \\ - E(s_2)^2$$

(B.18)

The term enclosed in brackets on the RHS is another input to the program, and is labeled "DDD" .

$$\text{DDD} \equiv [2E(s_1) + 3.81 \cdot \text{COEF}] \quad (\text{B.19})$$

The LHS of equation (B.18) can be rewritten in a slightly different form, and is also used as an input to the program. The LHS is labeled "CCC" .

$$\text{CCC} \equiv E(s_1)^2 - \text{COEF} \cdot E(s_1) [\ln 0.0604 E(s_1) - 1.0] \quad (\text{B.20})$$

Equation (B.18) can thus be written as

$$CCC = E(s_2) \left[DDD - COEF \cdot \ln E(s_2) \right] - E(s_2)^2 \quad (B.21)$$

The term inside of the brackets is also an input, and is labeled "BBB" .

$$BBB \equiv DDD - COEF \cdot \ln E(s_2) \quad (B.22)$$

There are thus four inputs to the computer program which were derived from the original energy deposition formula. These were:

- 1.) COEF
- 2.) CCC
- 3.) DDD
- 4.) BBB

These terms will be different for different fluids.

For the case of fast neutrons in the medium, the only difference is that the subscript 1 in equation (B.2) refers to the PKOA. In this case there are actually three possible PKOAs, namely H , C, and O. But, as has been shown by Bell (5), and by El-Nagdy(4)(who went through minimum superheat calculations for each type of atom), the minimum superheat will be obtained with the O-PKOA. Therefore, only the O (Oxygen) PKOA is considered.

There are some more computer inputs which should be discussed. (The computer programs are listed in Appendix C.). One input is the term labeled "EPKA". This is the initial energy of the radiation particle, which has been carried in the equations as $E(s_1)$. The value for $E(s_1)$ will always be known.

The physical properties as a function of temperature are also inputs. These have been given in Appendix A .

There are two final inputs which must be considered. These are computer statement number

0558 (IF(ABS(E-EC)-X.XXX)9858,0658,0658

and the statement

E = Y.YYYY

The important point here is the value of X.XXX in statement 0558. This value sets the convergence criteria. If this convergence criteria is too strict, a COMPLETION CODE error will result. If this is the case, then the convergence criteria must be relaxed (X.XXX must be made larger).

The best method of determining what the value of X.XXX should be, is to choose values for E (beginning with $E(s_1)$ and gradually decreasing in energy) and actually calculating the value of EC.

EC is calculated in statement number 0458:

0458 EC = E - (E*E-BBB*E+CCC)/(2.0*E-BBB)

A simple computer program can be written to calculate EC values for various E values. This will then give an indication of the minimum value for the ABS(E-EC) term used in statement 0558. This minimum value is then used as the value for X.XXX . (For the present work the value of X.XXX varied from 0.0001 to 0.003)

The value chosen for the E term in

$$E = Y.YYY$$

is not too critical, and an approximate value which can be used is : $E = \frac{1}{2}E(s_1)$.

These (from COEF to E) are the factors in the computer program which must be changed for the different fluids. Otherwise, the same basic program may be used for all cases.

Appendix C

Computer Programs

This Appendix contains the three basic computer programs used in this work.

The first one given is the Polynomial Regression Program which gives us the equations for the physical properties as a function of temperature. (Nitromethane is shown as an example.)

The second program listed in this Appendix is the program used to calculate the superheat threshold for the case of fission fragments. (Benzene parameters are used as an example.)

The third program is for calculating the superheat threshold for fast neutrons. (Benzene parameters are used as an example.)

C AND (4) OPTIONALLY PRINT THE TABLE OF RESIDUALS AND A PLOT
C OF Y VALUES AND Y ESTIMATES.
C REMARKS
C THE NUMBER OF OBSERVATIONS, N, MUST BE GREATER THAN M+1,
C WHERE M IS THE HIGHEST DEGREE POLYNOMIAL SPECIFIED.
C IF THERE IS NO REDUCTION IN THE RESIDUAL SUM OF SQUARES
C BETWEEN TWO SUCCESSIVE DEGREES OF THE POLYNOMIALS, THE
C PROGRAM TERMINATES THE PROGRAM BEFORE COMPLETING THE ANALY-
C SIS FOR THE HIGHEST DEGREE POLYNOMIAL SPECIFIED.
C
C SUBROUTINES AND FUNCTION SUBPROGRAMS REQUIRED
C GDATA
C ORDER
C MINV
C MULTR
C PLCT (A SPECIAL PLOT SUBROUTINE PROVIDED FOR THE SAMPLE
C PROGRAM.)
C
C METHOD
C REFER TO B. OSTLE, 'STATISTICS IN RESEARCH', THE ICWA STATE
C COLLEGE PRESS', 1954, CHAPTER 6.
C
C

C THE FOLLOWING DIMENSION MUST BE GREATER THAN OR EQUAL TO THE
C PRODUCT OF $N*(M+1)$, WHERE N IS THE NUMBER OF OBSERVATIONS AND M
C IS THE HIGHEST DEGREE POLYNOMIAL SPECIFIED..
C
C DIMENSION X(1100)
C
C THE FOLLOWING DIMENSION MUST BE GREATER THAN OR EQUAL TO THE
C PRODUCT OF $M*M$..
C
C DIMENSION DI(100)
C
C THE FOLLOWING DIMENSION MUST BE GREATER THAN OR EQUAL TO

POLY0037
POLY0038
POLY0039
POLY0040
POLY0041
POLY0042
POLY0043
POLY0044
POLY0045
POLY0046
POLY0047
POLY0048
POLY0049
POLY0050
POLY0051
POLY0052
POLY0053
POLY0054
POLY0055
POLY0056
POLY0057
POLY0058
POLY0059
POLY0060
POLY0061
POLY0062
POLY0063
POLY0064
POLY0065
POLY0066
POLY0067
POLY0068
POLY0069
POLY0070
POLY0071
POLY0072

POLY0073
POLY0074
POLY0075
POLY0076
POLY0077
POLY0078
POLY0079
POLY0080
POLY0081
POLY0082
POLY0083
POLY0084
POLY0085
POLY0086
POLY0087
POLY0088
POLY0089
POLY0090
POLY0091
POLY0092
POLY0093
POLY0094
POLY0095
POLY0096
POLY0097
POLY0098
POLY0099
POLY0100
POLY0101
POLY0102
POLY0103
POLY0104
POLY0105
POLY0106
POLY0107
POLY0108

(M+2)*(M+1)/2..

DIMENSION D(66)

THE FOLLOWING DIMENSIONS MUST BE GREATER THAN OR EQUAL TO M..

DIMENSION B(10),E(10),SB(10),(10)

THE FOLLOWING DIMENSIONS MUST BE GREATER THAN OR EQUAL TO (M+1)..

DIMENSION XBAR(11),STD(11),COE(11),SUMSQ(11),ISAVE(11)

THE FOLLOWING DIMENSION MUST BE GREATER THAN OR EQUAL TO 10..

DIMENSION ANS(10)

THE FOLLOWING DIMENSION WILL BE USED IF THE PLOT OF OBSERVED DATA

AND ESTIMATES IS DESIRED. THE SIZE OF THE DIMENSION, IN THIS

CASE, MUST BE GREATER THAN OR EQUAL TO N*3. OTHERWISE, THE SIZE

OF DIMENSION MAY BE SET TO 1.

DIMENSION P(300)

IF A DOUBLE PRECISION VERSION OF THIS ROUTINE IS DESIRED, THE
C IN COLUMN 1 SHOULD BE REMOVED FROM THE DOUBLE PRECISION
STATEMENT WHICH FOLLOWS.

DOUBLE PRECISION X,XBAR,STD,D,SUMSQ,DI,E,B,SB,T,ANS,DET,COE

THE C MUST ALSO BE REMOVED FROM DOUBLE PRECISION STATEMENTS
APPEARING IN OTHER ROUTINES USED IN CONJUNCTION WITH THIS

ROUTINE.

C

1 FORMAT(A4,A2,I5,I2,I1)
 2 FORMAT(2F10.0)
 3 FORMAT(27H1POLYNOMIAL REGRESSION.....,A4,A2/)
 4 FORMAT(23HNUMBER OF OBSERVATIONS,I6//)
 5 FORMAT(32HOPOLYNOMIAL REGRESSION OF DEGREE,I3)
 6 FORMAT(12H0 INTERCEPT,E20.7)
 7 FORMAT(26H0 REGRESSION COEFFICIENTS/(6E20.7))
 8 FORMAT(1H0/24X,24HANALYSIS OF VARIANCE FOR,I4,19H DEGREE POLYNOMI
 1AL/)
 9 FORMAT(1H0,5X,19HSOURCE OF VARIATION,7X,9HDEGREE OF,7X,6HSUM OF,9X
 1,4HMEAN,10X,1HF,9X,20HIMPROVEMENT IN TERMS/33X,7HFREEDOM,8X,7HSQUA
 2RES,7X,6HSQUARE,7X,5HVALUE,8X,17HOF SUM OF SQUARES)
 10 FORMAT(20H0 DUE TO REGRESSION,12X,I6,F17.5,F14.5,F13.5,F20.5)
 11 FORMAT(32H DEVIATION ABOUT REGRESSION ,I6,F17.5,F14.5)
 12 FORMAT(8X,5HTOTAL,19X,I6,F17.5//)
 13 FORMAT(17H0 NO IMPROVEMENT)
 14 FORMAT(1H0//27X,18HTABLE OF RESIDUALS//16H OBSERVATION NO.,5X,7HX
 1VALUE,7X,7HY VALUE,7X,10HY ESTIMATE,7X,8HRESIDUAL/)
 15 FORMAT(1H0,3X,I6,F18.5,F14.5,F17.5,F15.5)

C
 C
 C
 C
 C
 C
 C
 C
 C
 C
 C
 C
 C
 C
 C
 C
 C
 C
 C

.....
 READ PROBLEM PARAMETER CARD
 END=1000
 100 READ (5,1) PR,PR1,N,M,NPLOT
 PR....PROBLEM NUMBER (MAY BE ALPHAMERIC)
 PR1...PROBLEM NUMBER (CONTINUED)
 N.....NUMBER OF OBSERVATIONS
 M.....HIGHEST DEGREE POLYNOMIAL SPECIFIED
 NPLOT.OPTION CODE FOR PLOTTING
 0 IF PLOT IS NOT DESIRED.
 1 IF PLOT IS DESIRED.

POLY0109
 POLY0110
 POLY0111
 POLY0112
 POLY0113
 POLY0114
 POLY0115
 POLY0116
 POLY0117
 POLY0118
 POLY0119
 POLY0120
 POLY0121
 POLY0122
 POLY0123
 POLY0124
 POLY0125
 POLY0126
 POLY0127
 POLY0128
 POLY0129
 POLY0130
 POLY0131
 POLY0132
 POLY0133
 POLY0134
 POLY0135
 POLY0136
 POLY0137
 POLY0138
 POLY0139
 POLY0140
 POLY0141
 POLY0142
 POLY0143
 POLY0144

C	PRINT PROBLEM NUMBER AND N.	POLY0145
C		POLY0146
	WRITE (6,3) PR,PR1	POLY0147
	WRITE (6,4) N	POLY0148
C		POLY0149
C	READ INPUT DATA	POLY0150
C		POLY0151
	L=N*M	POLY0152
	DO 110 I=1,N	POLY0153
	J=L+I	POLY0154
C		POLY0155
C	X(I) IS THE INDEPENDENT VARIABLE, AND X(J) IS THE DEPENDENT	POLY0156
C	VARIABLE.	POLY0157
C		POLY0158
	110 READ (5,2) X(I),X(J)	POLY0159
C		POLY0160
	CALL GDATA (N,M,X,XBAR,STD,D,SUMSQ)	POLY0161
C		POLY0162
	MM=M+1	POLY0163
	SUM=0.0	POLY0164
	NT=N-1	POLY0165
C		POLY0166
	DO 200 I=1,M	POLY0167
	ISAVE(I)=I	POLY0168
C		POLY0169
C	FORM SUBSET OF CORRELATION COEFFICIENT MATRIX	POLY0170
C		POLY0171
	CALL ORDER (MM,D,MM,I,ISAVE,DI,E)	POLY0172
C		POLY0173
C	INVERT THE SUBMATRIX OF CORRELATION COEFFICIENTS	POLY0174
C		POLY0175
	CALL MINV (DI,I,DET,E,T)	POLY0176
C		POLY0177
	CALL MULTR (N,I,XBAR,STD,SUMSQ,DI,E,ISAVE,B,SB,T,ANS)	POLY0178
C		POLY0179
C	PRINT THE RESULT OF CALCULATION	POLY0180


```

C
WRITE (6,5) I
IF(ANS(7)) 140,130,130
130 SUMIP=ANS(4)-SUM
IF(SUMIP) 140, 140, 150
140 WRITE (6,13)
GO TO 210
150 WRITE (6,6) ANS(1)
WRITE (6,7) (B(J),J=1,I)
WRITE (6,8) I
WRITE (6,9)
SUM=ANS(4)
WRITE (6,10) I,ANS(4),ANS(6),ANS(10),SUMIP
NI=ANS(8)
WRITE (6,11) NI,ANS(7),ANS(9)
WRITE (6,12) NT,SUMSQ(MM)

C
C
C SAVE COEFFICIENTS FOR CALCULATION OF Y ESTIMATES
C
C
C COE(1)=ANS(1)
DO 160 J=1,I
160 COE(J+1)=B(J)
LA=I

C
200 CONTINUE

C
C TEST WHETHER PLOT IS DESIRED
C
C
210 IF(NPLOT) 100, 100, 220

C
C CALCULATE ESTIMATES
C
220 NP3=N+N
DO 230 I=1,N
NP3=NP3+1
P(NP3)=COE(1)

```

```

POLY0181
POLY0182
POLY0183
POLY0184
POLY0185
POLY0186
POLY0187
POLY0188
POLY0189
POLY0190
POLY0191
POLY0192
POLY0193
POLY0194
POLY0195
POLY0196
POLY0197
POLY0198
POLY0199
POLY0200
POLY0201
POLY0202
POLY0203
POLY0204
POLY0205
POLY0206
POLY0207
POLY0208
POLY0209
POLY0210
POLY0211
POLY0212
POLY0213
POLY0214
POLY0215
POLY0216

```

```

      L=I
      DO 230 J=1,LA
      F(NP3)=P(NP3)+X(L)*CCE(J+1)
230  L=L+N
C
C      CCPY OBSERVED DATA
C
      N2=N
      L=N*M
      DO 240 I=1,N
      F(I)=X(I)
      N2=N2+1
      L=L+1
240  F(N2)=X(L)
C
C      PRINT TABLE OF RESIDUALS
C
      WRITE (6,3) PR,PR1
      WRITE (6,5) LA
      WRITE (6,14)
      NP2=N
      NP3=N+N
      DO 250 I=1,N
      NP2=NP2+1
      NP3=NP3+1
      RESID=P(NP2)-P(NP3)
250  WRITE (6,15) I,P(I),P(NP2),P(NP3),RESID
C
      CALL PLOT (LA,P,N,3,C,1)
      GO TO 100
C
      STOP
1000 CONTINUE
      CALL EXIT
      END
C

```

```

POLY0217
POLY0218
POLY0219
POLY0220
POLY0221
POLY0222
POLY0223
POLY0224
POLY0225
POLY0226
POLY0227
POLY0228
POLY0229
POLY0230
POLY0231
POLY0232
POLY0233
POLY0234
POLY0235
POLY0236
POLY0237
POLY0238
POLY0239
POLY0240
POLY0241
POLY0242
POLY0243
POLY0244
POLY0245
POLY0246
POLY0247
POLY0248
POLY0249
POLY0250
POLY0251
POLY0252

```


DATA BLANK/' '/
DATA ANG(1)/'1'/
DATA ANG(2)/'2'/
DATA ANG(3)/'3'/
DATA ANG(4)/'4'/
DATA ANG(5)/'5'/
DATA ANG(6)/'6'/
DATA ANG(7)/'7'/
DATA ANG(8)/'8'/
DATA ANG(9)/'9'/

1 FORMAT(1H1,60X,7H CHART ,I3,///
2 FORMAT(1H ,F11.4,5X,1(C1A1)
3 FORMAT(1F)
4 FORMAT(10H 123456789)
5 FORMAT(10A1)
7 FORMAT(1H ,16X,101H.
1)
8 FORMAT(1H0,9X,11F10.4)

.....
NLL=NL

IF(NS) 16, 16, 10

 SORT BASE VARIABLE DATA IN ASCENDING CRDER

10 DO 15 I=1,N
 DO 14 J=I,N
 IF(A(I)-A(J)) 14, 14, 11
11 L=I-N
 LL=J-N
 DO 12 K=1,M
 L=L+N
 LL=LL+N

POLY0289
POLY0290
POLY0291
POLY0292
POLY0293
POLY0294
POLY0295
POLY0296
POLY0297
POLY0298
POLY0299
POLY0300
POLY0301
POLY0302
POLY0303
POLY0304
POLY0305
POLY0306
POLY0307
POLY0308
POLY0309
POLY0310
POLY0311
POLY0312
POLY0313
POLY0314
POLY0315
POLY0316
POLY0317
POLY0318
POLY0319
POLY0320
POLY0321
POLY0322
POLY0323
POLY0324

```

      F=A(L)
      A(L)=A(LL)
12  A(LL)=F
14  CONTINUE
15  CONTINUE
C
      TEST NLL
C
16  IF(NLL) 20, 18, 20
18  NLL=50
C
      PRINT TITLE
C
20  WRITE(6,1)NO
C
      DEVELOP BLANK AND DIGITS FOR PRINTING
C
      FIND SCALE FOR BASE VARIABLE
C
      XSCAL=(A(N)-A(1))/(FLCAT(NLL-1))
C
      FIND SCALE FOR CROSS-VARIABLES
C
      M1=N+1
      YMIN=A(M1)
      YMAX=YMIN
      M2=M*N
      DO 40 J=M1,M2
      IF(A(J)-YMIN) 28,26,26
26  IF(A(J)-YMAX) 40,40,30
28  YMIN=A(J)
      GO TO 40
30  YMAX=A(J)
40  CONTINUE
      YSCAL=(YMAX-YMIN)/100.0

```

```

POLY0325
POLY0326
POLY0327
POLY0328
POLY0329
POLY0330
POLY0331
POLY0332
POLY0333
POLY0334
POLY0335
POLY0336
POLY0337
POLY0338
POLY0339
POLY0340
POLY0341
POLY0342
POLY0343
POLY0344
POLY0345
POLY0346
POLY0347
POLY0348
POLY0349
POLY0350
POLY0351
POLY0352
POLY0353
POLY0354
POLY0355
POLY0356
POLY0357
POLY0358
POLY0359
POLY0360

```

```

C
C      FIND BASE VARIABLE PRINT POSITION
C
      XB=A(1)
      L=1
      MY=M-1
      I=1
45  F=I-1
      XPR=XB+F*XSCAL
      IF(A(L)-XPR) 50,50,70
C
C      FIND CROSS-VARIABLES
C
50  DO 55 IX=1,101
55  CUT(IX)=BLANK
      DO 60 J=1,MY
      LL=L+J*N
      JP=((A(LL)-YMIN)/YSCAL)+1.0
      CUT(JP)=ANG(J)
60  CONTINUE
C
C      PRINT LINE AND CLEAR, OR SKIP
C
      WRITE(6,2)XPR,(CUT(IZ),IZ=1,101)
      L=L+1
      GO TO 80
70  WRITE(6,3)
80  I=I+1
      IF(I-NLL) 45, 84, 86
84  XPR=A(N)
      GO TO 50
C
C      PRINT CROSS-VARIABLES NUMBERS
C
86  WRITE(6,7)
      YPR(1)=YMIN

```

```

POLY0361
POLY0362
POLY0363
POLY0364
POLY0365
POLY0366
POLY0367
POLY0368
POLY0369
POLY0370
POLY0371
POLY0372
POLY0373
POLY0374
POLY0375
POLY0376
POLY0377
POLY0378
POLY0379
POLY0380
POLY0381
POLY0382
POLY0383
POLY0384
POLY0385
POLY0386
POLY0387
POLY0388
POLY0389
POLY0390
POLY0391
POLY0392
POLY0393
POLY0394
POLY0395
POLY0396

```

```
DO 90 KN=1,9
90 YPR(KN+1)=YPR(KN)+YSCAL*10.0
   YPR(11)=YMAX
   WRITE(6,8)(YPR(IP),IF=1,11)
   RETURN
END
```

```
POLY0397
POLY0398
POLY0399
POLY0400
POLY0401
POLY0402
```

C
C
C
C
C
C
C
C
C
C
C
C
C
C
C
C
C
C
C
C
C
C
C
C
C

```
*****
*
*                               *
*          FISSIGN FRAGMENTS IN BENZENE          *
*
*
*          ENERGY BALANCE METHCD          *
*
*
*****
```

```
IMPLICIT REAL*8 (A-H,C-Z)
EXP(X)=DEXP(X)
ALOG(X)=DLOG(X)
SQRT(X)=DSQRT(X)
ABS(X)=DABS(X)
```

C

```
DIMENSION PLIQ(30),TSAT(30)
DIMENSION A(30)
500 FORMAT(F10.4)
501 FORMAT(I3/(10X,2F10.2))
503 FORMAT(1H1,30X,' THE SUPERHEAT LIMIT FOR BENZENE EXPOSED
1 TO FISSIGN FRAGMENTS '/////))
504 FORMAT(1H0,119H A PKC GT EPKA DELTI ALPHA PRESS SAT ENER A
1VG ENER J XNI REL SIZE GAS VAPCR DEL T DEL T SUP
```

FFBZ0001
FFBZ0002
FFBZ0003
FFBZ0004
FFBZ0005
FFBZ0006
FFBZ0007
FFBZ0008
FFBZ0009
FFBZ0010
FFBZ0011
FFBZ0012
FFBZ0013
FFBZ0014
FFBZ0015
FFBZ0016
FFBZ0017
FFBZ0018
FFBZ0019
FFBZ0020
FFBZ0021
FFBZ0022
FFBZ0023
FFBZ0024
FFBZ0025
FFBZ0026
FFBZ0027
FFBZ0028
FFBZ0029
FFBZ0030
FFBZ0031
FFBZ0032
FFBZ0033
FFBZ0034
FFBZ0035
FFBZ0036


```

1 )
505 FORMAT(1H ,119H          RATE      TIME      LIQUID TEMP  LEVEL C
1EP RATE          INIT EMBR  PRESS    PRESS    EQA48    E.B.M.  TEMP
1 )
506 FORMAT(1H0,119H          NC/SEC      SEC          LBF/FT2 DEG F    MEV  M
1EV/CM          LBF/FT2 LBF/FT2  DEG F    DEG F    DEG F
1 )
508 FORMAT(1H ,F5.2,D6.3 ,D8.1,F6.3,F8.1,F8.3,F9.5,D10.3,I5,F5.1,F10.8
1, F7.1,F8.1,EX,F8.3,F8.3)
600 FORMAT(1H0,29HTHE VALLE OF THE CONSTANT IS ,F10.4//)
999 FORMAT(I3/(F10.3))
601 FORMAT(8H EPKA = ,F10.4//)

```

C
C
C
C

EPKA IS THE INITIAL ENERGY OF THE FISSION FRAGMENT

EPKA = 95.0

```

1 READ(5,501)N,(PLIQ(L),TSAT(L),L=1,N)
READ(5,999)K,(A(M),M=1,K)
3 WRITE(6,503)
4 WRITE(6,504)
5 WRITE(6,505)
6 WRITE(6,506)
1000 READ(5,500)CCNST
WRITE(6,600)CCNST
WRITE(6,601)EPKA
DO 110 M=1,K,1
8 DO 109 L=1,N,1
10 DELTF=10.0
15 TF=TSAT(L)+DELTf
23 CONTINUE

```

C
C
C

PHYSICAL PROPERTIES OF BENZENE

```

25 PVA = 85.143 - 0.9599*TF + 0.003178*TF*TF
26 PVPSF = PVA*144.0

```

FFBZ0037
FFBZ0038
FFBZ0039
FFBZ0040
FFBZ0041
FFBZ0042
FFBZ0043
FFBZ0044
FFBZ0045
FFBZ0046
FFBZ0047
FFBZ0048
FFBZ0049
FFBZ0050
FFBZ0051
FFBZ0052
FFBZ0053
FFBZ0054
FFBZ0055
FFBZ0056
FFBZ0057
FFBZ0058
FFBZ0059
FFBZ0060
FFBZ0061
FFBZ0062
FFBZ0063
FFBZ0064
FFBZ0065
FFBZ0066
FFBZ0067
FFBZ0068
FFBZ0069
FFBZ0070
FFBZ0071
FFBZ0072

27	SIGMA = 2.268E-3 - 4.610E-6*TF	FFBZ0073
46	RCWL = 1.0/(0.01831 + 0.15524E-5*TF + 0.3444E-7*TF*TF)	FFBZ0074
55	ROWV = 1.0/(26.8282 - 0.1614*TF + 0.24878E-3*TF*TF)	FFBZ0075
56	FG = 196.119 - 0.12169*TF - 0.1734E-3*TF*TF	FFBZ0076
57	BA=(PVPSF-PLIQ(L))/PVPSF	FFBZ0077
C		FFBZ0078
	E = 10.0	FFBZ0079
C		FFBZ0080
	ROWL=CONST*RCWL	FFBZ0081
C		FFBZ0082
C		FFBZ0083
C	BENZENE PARAMETERS FOR FISSION FRAGMENTS	FFBZ0084
C		FFBZ0085
C		FFBZ0086
C		FFBZ0087
C		FFBZ0088
C158	CDEF = (3.4212E04)*RCWL*A(M)*SIGMA/(BA*PVPSF)	FFBZ0089
C258	CCC = EPKA*EFKA - CDEF*EPKA*(ALCG(0.0622*EPKA)-1.0)	FFBZ0090
3258	DDD = 2.0*EPKA + 3.777*CDEF	FFBZ0091
C358	BBB = DDD - CDEF*ALCG(E)	FFBZ0092
C		FFBZ0093
C458	EC=E-(E*E-BBB*E+CCC)/(2.0*E-BBB)	FFBZ0094
0558	IF((ABS(E-EC)-0.0010).LT.0.0) GO TO 9858	FFBZ0095
	E = (E + EC)*0.5	FFBZ0096
	IF (E.LE.0.C) E = 1.C	FFBZ0097
C758	GO TO 0358	FFBZ0098
9858	IF((EC-10.00).LT.0.0) GO TO 96	FFBZ0099
	IF((EC-EPKA).GE.0.0) GO TO 93	FFBZ0100
	DEDS = (EPKA-E)*BA*PVPSF/(60.96*A(M)*SIGMA)	FFBZ0101
	RCRIT=2.0*SIGMA/(BA*PVPSF)	FFBZ0102
62	GATE=3.700221E-19*A(M)*(TF+459.69)*DEDS/SIGMA**2	FFBZ0103
	ART=(2.0*GATE*(PVPSF-PLIQ(L))-1.0)**2-4.C*GATE**2*(PVPSF-PLIQ(L))*	FFBZ0104
	1*2	FFBZ0105
	IF(ART.LT.0.C) GO TO 93	FFBZ0106
63	PGPSF=(1.0-2.0*GATE*(PVPSF-PLIQ(L))-SQRT(ART))/(2.0*GATE)	FFBZ0107
64	E=(PVPSF+PGPSF-PLIQ(L))/PVPSF	FFBZ0108

```

0164 IF((B-BA).LT.0.00001) GO TO 464
      BA = B
0364 GO TO 0158
464 GO TO 103
103 EQA53=0.8010E-12*(M)*DEDS-RCRIT*RCRIT*RCWV*HFG*778.26-RCRIT*SIGMA
104 IF(EQA53-0.0)9696,106,9393
9696 IF(ABS(EQA53).LE.1.0E-16) GO TO 106
      GO TO 96
9393 IF(ABS(EQA53).LE.1.0E-16) GO TO 106
      GO TO 93
93 TF=TF-DELTF
94 DELTF=0.1*DELTF
95 IF(DELTF.LT.0.009) GO TO 106
96 TF=TF+DELTF
97 GO TO 23
106 DELT3=TF-TSAT(L)
      PKO2RT=0.0
      XI=0.0
      DELTI=0.0
      ALPHA=0.0
      J=0
      XN1=0.0
107 WRITE(6,508)A(M),PKO2RT,DELTI,ALPHA,PLIQ(L),TSAT(L),E ,DEDS ,J,
      1XNI,XI,PGPSF,PVPSF,DELT3,TF
109 CONTINUE
7 WRITE(6,900)
900 FORMAT(/ /45X,22H DIFFERENT VALUE OF A ,//)
110 CONTINUE
      GO TO 1000
      END

```

```

FFBZ0109
FFBZ0110
FFBZ0111
FFBZ0112
FFBZ0113
FFBZ0114
FFBZ0115
FFBZ0116
FFBZ0117
FFBZ0118
FFBZ0119
FFBZ0120
FFBZ0121
FFBZ0122
FFBZ0123
FFBZ0124
FFBZ0125
FFBZ0126
FFBZ0127
FFBZ0128
FFBZ0129
FFBZ0130
FFBZ0131
FFBZ0132
FFBZ0133
FFBZ0134
FFBZ0135
FFBZ0136
FFBZ0137
FFBZ0138

```

C
C
C
C
C
C
C
C
C
C
C
C
C
C
C
C
C
C

*
* FAST NEUTRONS IN BENZENE *
*
* ENERGY BALANCE METHOD *
*

IMPLICIT REAL*8 (A-H,C-Z)
EXP(X)=DEXP(X)
ALOG(X)=DLOG(X)
SQRT(X)=DSQRT(X)
ABS(X)=DABS(X)

C

DIMENSION PLIQ(30),TSAT(30)
DIMENSION A(30)
500 FORMAT(F10.4)
501 FORMAT(I3/(10X,2F10.2))
503 FORMAT(1H1,30X,' THE SUPERHEAT LIMIT FOR BENZENE EXPOSED
1 TO FAST NEUTRONS '/////)
504 FORMAT(1H0,119H A PKO GT EPKA DELTI ALPHA PRESS SAT ENER A
1VG ENER J XNI REL SIZE GAS VAPCR DEL T DEL T SUP
1)
505 FORMAT(1H ,119H RATE TIME LIQUID TEMP LEVEL D
1EP RATE INIT EMBR PRESS PRESS EQA48 E.B.M. TEMP
1)
506 FORMAT(1H0,119H NG/SEC SEC LBF/FT2 DEG F MEV M
1EV/CM LBF/FT2 LBF/FT2 DEG F DEG F DEG F

FNBZ0001
FNBZ0002
FNBZ0003
FNBZ0004
FNBZ0005
FNBZ0006
FNBZ0007
FNBZ0008
FNBZ0009
FNBZ0010
FNBZ0011
FNBZ0012
FNBZ0013
FNBZ0014
FNBZ0015
FNBZ0016
FNBZ0017
FNBZ0018
FNBZ0019
FNBZ0020
FNBZ0021
FNBZ0022
FNBZ0023
FNBZ0024
FNBZ0025
FNBZ0026
FNBZ0027
FNBZ0028
FNBZ0029
FNBZ0030
FNBZ0031
FNBZ0032
FNBZ0033
FNBZ0034
FNBZ0035
FNBZ0036

1)	FNBZ0037
508 FORMAT(1H ,F5.2,D6.3 ,D8.1,F6.3,F8.1,F8.3,F9.5,D10.3,I5,F5.1,F10.8	FNBZ0038
1, F7.1,F8.1,8X,F8.3,F8.3)	FNBZ0039
600 FORMAT(1H0,25HTHE VALLE OF THE CCNSTANT IS ,F10.4//)	FNBZ0040
999 FORMAT(I3/(F10.3))	FNBZ0041
601 FORMAT(8H EPKA = ,F10.4///)	FNBZ0042
C	FNBZ0043
C EPKA IS THE ENERGY OF THE PKOA	FNBZ0044
C	FNBZ0045
C EPKA = 2.12	FNBZ0046
C	FNBZ0047
1 READ(5,501)N,(PLIQ(L),TSAT(L),L=1,N)	FNBZ0048
READ(5,999)K,(A(M),M=1,K)	FNBZ0049
3 WRITE(6,503)	FNBZ0050
4 WRITE(6,504)	FNBZ0051
5 WRITE(6,505)	FNBZ0052
6 WRITE(6,506)	FNBZ0053
1000 READ(5,500)CCNST	FNBZ0054
WRITE(6,600)CCNST	FNBZ0055
WRITE(6,601)EPKA	FNBZ0056
DO 110 M=1,K,1	FNBZ0057
8 DO 109 L=1,N,1	FNBZ0058
10 DELTF=10.0	FNBZ0059
15 TF=TSAT(L)+DELTf	FNBZ0060
23 CONTINUE	FNBZ0061
C	FNBZ0062
C PHYSICAL PROPERTIES OF BENZENE	FNBZ0063
C	FNBZ0064
25 PVA = 85.143 - 0.9595*TF + 0.003178*TF*TF	FNBZ0065
26 PVPSF = PVA*144.0	FNBZ0066
27 SIGMA = 2.268E-3 - 4.610E-6*TF	FNBZ0067
46 ROWL = 1.0/(0.01831 + 0.15524E-5*TF + 0.3444E-7*TF*TF)	FNBZ0068
55 ROWV = 1.0/(26.8282 - 0.1614*TF + 0.24878E-3*TF*TF)	FNBZ0069
56 HFG = 196.119 - 0.12169*TF - 0.1734E-3*TF*TF	FNBZ0070
57 BA=(PVPSF-PLIQ(L))/PVPSF	FNBZ0071
C	FNBZ0072

```

      E = 1.50
C
      ROWL=CONST*RCWL
C
C
0158 COEF = (1.00E04*ROWL*A(M)*SIGMA)/(BA*PVPSF)
0258 CCC = EPKA*EPKA - COEF*EPKA*(ALOG(0.9450*EPKA)-1.0)
3258 DDD = 1.0565*COEF + 2.0*EPKA
0358 BBB = DDD - COEF*ALOG(E)
C
0458 EC=E-(E*E-BBB*E+CCC)/(2.0*E-BBB)
0558 IF((ABS(E-EC)-0.0030).LT.0.0) GO TO 9858
      E = ( E + EC ) * 0.5
      IF ( E.LE.0.0) E = 1.0
0758 GO TO 0358
9858 IF((EC-10.00).LT.0.0) GO TO 96
      IF((EC-EPKA).GE.0.0) GO TO 93
      DEDS = (EPKA-E)*BA*PVPSF/(60.96*A(M)*SIGMA)
      RCRIT=2.0*SIGMA/(BA*PVPSF)
62 GATE=3.700221E-19*A(M)*(TF+459.69)*DEDS/SIGMA**2
      ART=(2.0*GATE*(PVPSF-PLIQ(L))-1.0)**2-4.0*GATE**2*(PVPSF-PLIQ(L))*
1*2
      IF(ART.LT.0.0) GO TO 93
63 PGPSF =(1.0-2.0*GATE*(PVPSF -PLIQ(L))-SQRT(ART))/(2.0*GATE)
64 B=(PVPSF +PGPSF -PLIQ(L))/PVPSF
0164 IF((B-BA).LT.0.00001) GO TO 464
      BA = B
0364 GO TO 0158
464 GO TO 103
103 EQA53=0.8010E-12*A(M)*DEDS-RCRIT*RCRIT*RCWV*HFG*778.26-RCRIT*SIGMA
104 IF(EQA53-0.0)9696,106,9393
9696 IF(ABS(EQA53).LE.1.0E-16) GO TO 106
      GO TO 96
9393 IF(ABS(EQA53).LE.1.0E-16) GO TO 106
      GO TO 93
93 TF=TF-DELTF

```

```

FNBZ0073
FNBZ0074
FNBZ0075
FNBZ0076
FNBZ0077
FNBZ0078
FNBZ0079
FNBZ0080
FNBZ0081
FNBZ0082
FNBZ0083
FNBZ0084
FNBZ0085
FNBZ0086
FNBZ0087
FNBZ0088
FNBZ0089
FNBZ0090
FNBZ0091
FNBZ0092
FNBZ0093
FNBZ0094
FNBZ0095
FNBZ0096
FNBZ0097
FNBZ0098
FNBZ0099
FNBZ0100
FNBZ0101
FNBZ0102
FNBZ0103
FNBZ0104
FNBZ0105
FNBZ0106
FNBZ0107
FNBZ0108

```

```
94 DELTF=0.1*DELTF
95 IF(DELTF.LT.0.009) GO TO 106
96 TF=TF+DELTF
97 GO TC 23
106 DELT3=TF-TSAT(L)
    PKO2RT=0.0
    XI=0.0
    DELTI=0.0
    ALPHA=0.0
    J=0
    XN1=0.0
107 WRITE(6,508)A(M),PKO2RT,DELT I,ALPHA,PLIQ(L),TSAT(L),E ,DEDS ,J,
    IXNI,XI,PGPSF,PVPSF,DELT3,TF
109 CONTINUE
    7 WRITE(6,900)
900 FORMAT(//45X,22H DIFFERENT VALUE OF A ,//)
110 CONTINUE
    GO TC 1000
    END
```

```
FNBZ0109
FNBZ0110
FNBZ0111
FNBZ0112
FNBZ0113
FNBZ0114
FNBZ0115
FNBZ0116
FNBZ0117
FNBZ0118
FNBZ0119
FNBZ0120
FNBZ0121
FNBZ0122
FNBZ0123
FNBZ0124
FNBZ0125
FNBZ0126
FNBZ0127
```

Appendix D

References

1. Glaser, D.A. Phys. Rev 87 665(1952)
2. Becker, A.G. "Effect of Nuclear Radiation on the Superheated Liquid State." Thesis, Wayne State University, Detroit, 1963
3. Deitrich, L.W. "A Study of Fission-Fragment-Induced Nucleation of Bubbles in Superheated Water." Technical Report No. SU-326-P13-14 Stanford Univ. 1969
4. M.M. El-Nagdy, "An Experimental Study of the Influence of Nuclear Radiation on Boiling in Superheated Liquids." Thesis, University of Manchester, England.
5. Bell, C.R. "Radiation Induced Nucleation of the Vapor Phase." Thesis, M.I.T., Cambridge, Mass. 1970
6. Tso, Chih-Ping "Some Aspects of Radiation-Induced Nucleation in Water." Thesis, M.I.T. 1970
7. Glaser, D.A. Nuovo Cimento II Supp.2, 361(1954)
8. Seitz, F. Phys. Fluids 1 2(1958)
9. Glaser, D.A. "The Bubble Chamber"
Encyclopedia of Physics Vol XLV S. Flugge ed. (1958)
10. Peyrou, C. H. "Bubble Chamber Principles",
Bubble and Spark Chambers , R.P.Shutt, ed.(1967)
11. Norman, A. and Spiegler, P. Nuclear Science
And Engineering : 16 213-217 (1963)

12. Deitrich, L.W. Nuclear Science and Engineering
45 218-232 (1971)
13. Segre, E. Experimental Nuclear Physics Vol I
John Wiley and Sons. (1960)
14. Evans, R.D. The Atomic Nucleus
McGraw-Hill (1955)
15. Glasstone, S. and Sesonske, A. Nuclear Reactor
Engineering D. Van Nostrand Inc. (1963)
16. Claxton, K.T. "The Influence of Radiation on the
Inception of Boiling Liquid Sodium"
U.K.A.E.A., Harwell, England
17. Mellan, I. Compatibility and Solubility
Noys Data Corp. 1968
18. Timmermans, J. "Physico-chemical Constants of
Pure Organic Compounds" Elsevier Pub. Co. (1965)
19. International Critical Tables Vol. III, IV
20. Marsden and Mann , Solvents Guide
Interscience Publishers, 1963.
21. CRC Handbook of Chemistry and Physics 50th ed.
22. Riddick, J.A. and Bunger, W.B. Organic Solvents
Wiley-Interscience 1970
23. Young, C. and Coons, K.W. Surface Active Agents
Chemical Publishing Co. ,Inc. (1945)

24. Burdon, R.S. Surface Tension and the Spreading of Liquids Cambridge Univ. Press (1949)
25. Willows, R.S. and Hatschek, E. Surface Tension and Surface Energy R. Blakistons Sons & Co. 1923
26. Bikerman, J.J. Surface Chemistry Academic Press Inc, 1958
27. Buehler, C.H. J. CHEM PHYS 42, 1207(1938)
28. Papazian, H.A. Jour. of the Amer. Chem. Soc. 93:22 Nov. 1971
29. Costello, J.M. and Bowden, S.T. Recueil des Travaux Chimiques des Pays-Bas 77(1958) 28
30. Verschaffelt, J.E. Comm. Leiden 28, 12(1896)
31. Sugden, Reed, Wilkins Journal of the Chemical Society (London) Vol CXXVII Part II 1925 (1525)
32. Gallant, R.W. Physical Properties of Hydrocarbons Gulf Publishing Co. 1968
33. Connolly, T.J., et al "A Study of Radiation Induced Nucleation in Superheated Liquids " Technical Report No. SU-326-P13-6
34. Adam, N.K. Physical Chemistry (pg.230) Oxford Press, 1956
35. Lord Rayleigh Philosophical Magazine Aug. 1892